POLITECNICO
MILANO 1863

School of Industrial and Information Engineering
Department of Aerospace Science and Technology

Master of Science in
Aeronautical Engineering

Overall Analysis of Hydrogen, Kerosene and Methane in LRE Technology

Advisor:
Luciano Galfetti

Candidate:
Venkatesh Pakalapati
(ID: 914947)

July 23, 2021

Academic Year **2020-21**

Abstract

The current mantra in the field of rocket propulsion is "THE FUTURE IS GREEN". Liquid oxygen and methane are often regarded as new promising green propellant components. This thesis aims to do a comparative analysis of methane, kerosene, and hydrogen as rocket fuel combined with liquid oxygen using NASA CEA code. The propulsive parameters examined were vacuum specific impulse, combustion temperature, molar mass, combustion products, coefficient of thrust and characteristic velocity at different O/F ratios, chamber pressures and expansion ratios. In addition to this, propellant mass and tank volume estimation are done for each propellant pair based on Ariane 5 model case. Initially, the optimum O/F ratio for each propellant pair was found. Then, from comparing performance parameters, LOX/LH_2 showed the highest efficiency from vacuum specific impulse and characteristic velocity point of view. LOX/Rp-1 showed the highest values at optimum O/F ratios and various chamber pressures from a combustion temperature perspective. Compared to kerosene, methane showed higher vacuum specific impulse and more environmentally friendly combustion products. At last, mass and volume comparison for core and booster stages showed a huge advantage in tank volume size for methane over hydrogen. Overall, the study showed promising results for LOX/LCH_4 propellant pair.

Abstract (Italian version)

L'attuale mantra nel campo della propulsione a razzo è "IL FUTURO È VERDE". L'ossigeno liquido e il metano sono spesso considerati nuovi promettenti componenti di propellente verde. Questa tesi mira a fare un'analisi comparativa di metano, cherosene e idrogeno come combustibile per endoreattori combinato con ossigeno liquido utilizzando il codice CEA della NASA. I parametri propulsivi esaminati sono impulso specifico nel vuoto, temperatura di combustione, massa molare, prodotti di combustione, coefficiente di spinta e velocità caratteristica a diversi rapporti O/F, pressioni della camera e rapporti di espansione. Oltre a ciò, la stima della massa del propellente e del volume del serbatoio viene eseguita per ciascuna coppia di propellente basata sul caso del modello Ariane 5. Inizialmente, è stato trovato il rapporto O/F ottimale per ciascuna coppia di propellenti. Quindi, dal confronto dei parametri di prestazione, LOX/LH_2 ha mostrato la massima efficienza dal punto di vista dell'impulso specifico nel vuoto e della velocità caratteristica. LOX/Rp-1 ha mostrato valori più alti con rapporti O/F ottimali e varie pressioni della camera e temperatura di combustione. Rispetto al cherosene, il metano ha mostrato un impulso specifico nel vuoto più elevato e prodotti di combustione più rispettosi dell'ambiente. Infine, il confronto di massa e volume per gli stadi del nucleo e del booster ha mostrato un enorme vantaggio nella dimensione del volume del serbatoio per il metano rispetto all'idrogeno. Nel complesso, lo studio ha mostrato risultati promettenti per la coppia di propellenti LOX/LCH_4.

Acknowledgements

First and foremost, I would like to express my gratitude to my thesis advisor, Professor Luciano Galfetti of the Department of Aerospace Science and Technology at Politecnico di Milano to provide the opportunity and guidance to complete my work. *"Overall Analysis of Hydrogen, Kerosene and Methane in LRE Technology".*
I am also grateful to all my colleagues/friends who are with me during these years of study with valuable encouragement and constructive criticism. Last but not least, I would like to thank my wonderful parents for providing me with constant support and continuous encouragement throughout my years of study and through the process of researching and writing this thesis. This accomplishment would not have been possible without them.

- Venkatesh Pakalapati

Contents

List of Figures

List of Tables

Acronyms

$C_{12}\ H_{24}$	Rp-1
H_2	Hydrogen
$H_2\ O$	Water
$H_2\ O_2$	Hydrogen Peroxide
$N_2\ O_2$	Dinitrogen tetroxide
O_2	Oxygen
$Zr\ O_2$	Zirconium dioxide
ADN	Ammonium dinitramide
Al	Aluminum
AP	Ammonium perchlorate
CH_4	Methane
CO_2	Carbon dioxide
CEA	Chemical Equilibrium Analysis
CO	Carbon monoxide
FRG	Closed fuel rich gas generator
HAN	Hydroxylammonium nitrate
HNF	Hydrazinium nitroformate
HTPB	Hydroxyl-terminated polybutadiene
LNG	Liquified natural gas
LOX/**L**H_2	Liquid oxygen and liquid hydrogen
LOX/**LC**H_4	Liquid oxygen and liquid methane
LOX/**RP-1**	Liquid oxygen and kerosene
MCC	Main combustion chamber
MMH	Monomethylhydrazine
NASA	National Aeronautics and Space Administration
O/**F**	Oxidizer to Fuel ratio
ORG	Closed oxidizer rich gas generator
RCS	Reaction control system

SSTO	Single stage to orbit
TEHF	Toxic and Environmental Hazard Figure
UDMH	Unsymmetric Dimethylhydrazine

Nomenclature

Nondimensional Quantities

η_g	Global efficiency
γ	Specific heat ratio (C_p/C_v)
C_t	Coefficient of thrust

Physical Quantities

$\dot{m}_f$	Mass flow rate of fuel
$\dot{m}_o$	Mass flow rate of oxidizer
$\dot{m}_p$	Mass flow rate of propellant
ε	Expansion ratio (A_e/A_t)
ρ_f	Density of oxidizer
ρ_o	Density of fuel
A_e	Nozzle exit area
A_t	Throat area
C^*	Characteristic velocity
C^*_{th}	Theoretical characteristic velocity
C_p	Specific heat at constant pressure
C_v	Specific heat at constant volume
g_0	Acceleration due to gravity
I_{spv}	Vacuum specific impulse
I_{sp}	Specific impulse
I_{tot}	Total specific impulse

M	Molar mass
N_s	Specific speed
P_a	Ambient pressure
P_c	Combustion chamber pressure
P_e	Exit pressure
P_o	Total pressure
S	Suction speed
T	Thrust
t_b	Burnout time
T_f	Flame temperature
T_{gg}	Gas generator temperature
V_e	Exit velocity
V_f	Volume of fuel
V_o	Volume of oxidizer

1 Chapter

Introduction

1.1 Motivation

LOX/Methane is currently regarded worldwide as a propellant combination for future rocket-propelled vehicles. There has been occasional interest in this propellant since the early 1960s in the United States. However, no severe development activity or flight vehicle has used this relatively inexpensive and easily handled cryogenic fuel [1]. Instead, most rocket engine development efforts have focused on using more traditional fuels such as hydrogen, kerosene and earth storable without any severe development or application of methane to propulsion systems. However, in the last two decades, a major concern about rocket launches has been air pollution. As a result, research efforts in the rocket propulsion field are directed towards propellant combinations with minimal environmental impact and high-performance levels, also known as green propellants. For such purposes, LOX/Methane engines have been considered as a new clean fuel alternative for space missions. Methane is a pure hydrocarbon as kerosene and a cryogenic fuel compared to hydrogen. Methane can be easily extracted from natural gas (LNG). It is non-toxic and non-corrosive.

In order to prepare future launch systems, ArianeGroup had been investing since few years in research and technology of LOX/Methane engines through a demonstrator program including the design and manufacturing of a 400KN class thrust chamber, a Gas Generator, and a TurboPump (done in cooperation with IHI Corporation of Japan).[2]

Extensive experience of LOX/LH2 rocket engines was acquired in Europe through the development and utilization of HM-7, Vulcain and Vinici engines, and advantages and problems with this propellant combination are well understood. In contrast, no recent practical experience exists for hydrocarbons propellants in Europe. Vigorous research has been done to replace Ariane 5 solid boosters with Liquid boosters since liquid boosters could be the first step towards reusability for ARIANE 5. Propellant combinations that were considered are LOX/LH2, LOX/KEROSENE and LOX/METHANE.[3]

In this view, the present thesis consists of executing a detailed theoretical study, aiming to understand the propulsive parameters of METHANE, KEROSENE and HYDROGEN. Computational simulations using the chemical equilibrium software CEA-NASA were carried out to analyse and compare the performance of propellant pairs and diverse thermodynamic conditions in the combustion chamber. Finally, the results were used as a basis for a preliminary study of mass and volume estimations for educational purposes.

1.2 Objectives

Here are the primary objectives of this thesis:

• Firstly, to understand the criteria for green propellants and their applications fields along with technological issues.

• To study the particularities of methane as rocket fuel and compare its combustion chamber compatibility, cooling capacity, choice of engine cycles and turbopumps with Kerosene engine.

• Using NASA CEA analysis and taking Ariane 5 launcher as reference case finding out different ideal performance parameters of LOX/LH2, LOX/KEROSENE, LOX/METHANE engines. Parameters like Optimal mixture ratio, combustion temperature, vacuum specific impulse, coefficient of thrust, characteristic velocity.

• Optimizing the performance of different engines by analyzing their variations at different mixture ratios, chamber pressures and expansion ratios.

• To estimate propellant mass and volumes for each engine case and compare it with Ariane 5 core and booster stages.

1.3 Plan of Presentation

The workflow of the thesis is organized as listed below:

• Chapter 2 deals with the historical background of the different propellant combinations and development needs for applying high thrust and low thrust devices.

• Chapter 3 is dedicated to understanding the properties of methane as rocket fuel and different engine cycles by extensive literature survey.

• Chapter 4 presents the trade-off between LOX/Methane and LOX/Kerosene of their performances, combustion chamber materials, cooling circuits, engine cycles and turbopumps from the research papers.

• Chapter 5, a comparative study of different propellant parameters like vacuum specific impulse, combustion temperature, molar mass, combustion products, characteristic velocity and coefficient of thrust at different mixture ratios, chamber pressures and expansion ratios, has been done for hydrogen, kerosene and methane cases using NASA CEA code and preliminary study of propellant mass and volume estimations for each engine and compare it with core and booster stages of Ariane 5.

• Chapter 6 presents the conclusions of the case study and the future work that can be done.

2 Chapter

Green Propellants Propulsion Concepts

2.1 Historical Background

A green propellant propelled the first rocket ever to reach outer space with liquid oxygen and alcohol. One of the main reasons for using this as a fuel is its ready availability and cooling ability because of its high water content, which reduces the flame temperature and thermal stress. However, even though petroleum-based fuels produce more power than alcohol, they left too much silt and combustion byproducts that could clog the engine values.

From the early 1950s, the USA worked on improving this petroleum-based rocket fuel which would not leave a high amount of residue and keep the engine cool. This led to discovering high performance and highly used rocket fuel RP-1 (e.g., Atlas, Titan 1, Thor etc.).

During the Cold war, scientists are assigned to find a propellant combination that can be used for large tactical missiles which needed to be kept in submarines and land-based silos for many months and years and to be able to launch within a matter of seconds when need. This requirement led to the use of hypergolic propellant combinations like N_2O_4-MMH and N_2O_4-UDMH.

Hydrogen based fuels are the cleanest rocket fuels in use. They mainly produce water as a byproduct because of its high specific impulse LOX/ LH_2 was first used in Centaur, an upper stage for Atlas Rocket. Even though hydrogen has low density, leading to larger tank volumes, a slight increase in specific impulse in upper stages can be benefited mainly by an increase in the payload mass. Nowadays, LOX/LH_2 are also used for the core stage, like in Ariane 5.

LOX/LCH_4 is also one of the environmentally friendly propellant combinations that have been studied since the early 1960s. However, no serious development for a flight vehicle was done in those days due to its lower density than other hydrocarbon fuels like RP-1. Since then, the space industry has changed a lot. The idea of travelling to Mars has made the scientist reconsider the LOX/LCH_4 as a rocket fuel since it can be produced on the surface of Mars. Some of the rocket engines using methane as fuel are SpaceX's Raptor, Blue origins BE-4 engine. In recent years lot of companies have successfully demonstrated

the LOX/LCH_4 propulsion system.

As the world is moving more and more towards the green propellant for future rocket and satellite propulsion systems, here are some of the examples of non-toxic propellants that are developed so far are listed below table 2.1.

ENGINE	CYCLE	PROPELLANTS	THRUST(KN)	I_{spv} (s)	P_c(bar)
VULCAIN 2	Gas-Generator	LOX-LH_2	1350	433	115
SSME/RS-25	Staged Combustion	LOX-LH_2	2278	453	189
LE-7A	Staged Combustion	LOX-LH_2	1098	440	120
RD-0120	Staged Combustion	LOX-LH_2	1961	454	218
RS-68	Gas-Generator	LOX-LH_2	3370	409	97
F-1	Gas-Generator	LOX-RP1	7776	304	67.7
RD-180	Staged Combustion	LOX-RP1	4152	338	257
RS-27	Gas-Generator	LOX-RP1	1023	295	48
MA-5A	Gas-Generator	LOX-RP1	1910	265	49.5
NK 33	Staged Combustion	LOX-RP1	1687	331	145
RAPTOR	Full-Flow Staged Combustion	LOX-LCH_4	2200	380	330
RD-185	Staged Combustion	LOX-LCH_4	167	351	147
RD-167	Staged Combustion	LOX-LCH_4	179	378	147
TM-65	Gas-Generator	LOX-ALCOHOL	85	230	120
GAMMA-8	Expander (closed)	H_2O_2-RP1	235	265	47.4

Table 2.1: *Green Propellent Rocket engines*

2.2 High Thrust Propulsion

Lower and Upper launcher stages require "High Thrust" propulsion systems to overcome the earth's gravitational pull. Therefore, high performance is required from the non-toxic propellant combination to achieve a high amount of thrust to replace the current core and booster stages. Some of the propellant options that achieve such performance levels and still be environmentally friendly are various hydrocarbons in combination with Liquid oxygen and hydrogen peroxide. Here are some of those propellant combinations and their TEHF levels from [4] in the below table 2.2.

OXIDIZER	FUEL	TEHF	STORABILITY
O_2	Hydrogen	0	Semi-Cryogenic
O_2	Methane	0	Semi-Cryogenic
O_2	Propane	0	Semi-Cryogenic
O_2	Ethanol (96%)	0.15	Semi-Cryogenic
O_2	Kerosene	0.19	Semi-Cryogenic
H_2O_2 (95%)	Kerosene	4.58	Earth storable
H_2O_2 (95%)	Propane	4.61	Earth storable
H_2O_2 (95%)	Methane	4.66	Earth storable

Table 2.2: *Green Propellent TEHF Levels*

From previous studies[4] LOX-Methane, LOX-Kerosene and LOX-Propane seem to be good choices, but still, much improvement can be made in the technological areas. Here are few issues that can be investigated:

- cooling characteristics, coking, material compatibility, film cooling and thermal barrier coatings.
- Material and coatings in the oxygen-rich environment

• Oxygen-rich gas generator injection and injection of burner gas for staged combustion and sooting.

2.3 Low Thrust Propulsion

For orbital transfers, manoeuvres and reaction control of stages require Low Thrust engines. The criteria for choosing the right green propellant choice for such engines depends on various performance parameters. For Low Thrust applications, the specific impulse is not the only criteria for choosing the propellant combination. Volume, cost, storability, and hardware complexity should be taken into consideration.

Some of the interesting non-toxic monopropellant choices from [4] are H_2O_2, HAN-water blends, ADN-water blends, and HNF-water blends. These advanced monopropellants can be a good choice for Low Thrust engines because of their system simplicity and good performance levels compared to bipropellants, especially in the required volume. In addition, the composition of these propellants can be modified to improve the specific impulse.

Liquid bipropellants used for Low Thrust application are hydrocarbons in combination with liquid oxygen or hydrogen peroxide. This propellant choice gives us the advantage of using the same propellant for both lower and RCS stages so that the ground complexity of fuel storage and fuel loading reduces. Moreover, cost reduction in handling the propellants is due to their very low toxic content. Overall, life cycle costs can be reduced in terms of hardware and ground operations.

3 Chapter

Kerosene and Methane for rocket fuels

3.1 Methane as rocket fuel

By the year 2030, NASA is planning to launch its first manned mission to Mars. Space agencies all around the world are planning to reach and colonize Mars in there next hundred years are so. One of the major hurdles of reaching deep space is the availability of rocket fuel to make the round trip. Methane is the best option to solve this problem. We ship up a small amount of hydrogen of about eight tons and a fuel production plant that would take carbon dioxide from the Martian atmosphere. Using the Sabatier process and combining it with hydrogen, we get methane and liquid oxygen of about a hundred tons of propellant out of eight tons of Hydrogen, which would be enough to launch our spacecraft into space. Liquid Hydrogen can also be produced and used for these kinds of missions. However, it could potentially leave carbon residue inside the engines that needed to be cleaned before take-off, something not possible to accomplish on the Mars atmosphere. Apart from being In-situ resource utilization on Mars LOX/LCH_4 can also be used as an alternative for LOX/RP-1 because of its higher performance and more eco-friendly and cost-effectiveness.

Methane is the simplest hydrocarbon, and it is a carbon atom with four hydrogen atoms around with covalent bonds(fig. 3.1).On the other hand, Kerosene is not a fix-composition hydrocarbon but is like RP-1 a blend of many different hydrocarbons components. Also, 87 identifiable hydrocarbons are found in RP-1, so the engine's performance depends on the kerosene composition batch. So, it is much easier to refine methane to a much simpler molecule. When it is burnt, it has fewer partial combustion products that can form into polymers, which makes designing a methane engine a lot easier because we do not have to worry about coking happening in the wrong area and setting down deposits of carbon which might gum up the engines or injectors. Because methane has more hydrogen atoms than carbon compared to other complex hydrocarbons, it produces twice as much water than carbon dioxide as other fuels; therefore, the exhaust products are lighter, giving us a slightly higher specific impulse.

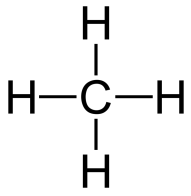

Figure 3.1: *Methane molecular structure*

Chemical reaction of methane and oxygen: $CH_4 + 2O_2 \rightarrow CO_2 + 2H_2O$

Methane has exceptional heat capacity properties that provide better chamber cooling than kerosene, so the same amount of heat flux can be taken off by a twice lower methane flow rate, which means an additional increase in specific impulse. These higher performance characteristics can increase the payload mass by about 20,30% for the same amount of initial vehicle mass as kerosene. According to [5], several experiments established the absence of carbon black formation in fuel-rich gas generator, that means any engine cycle can be used.

Moreover, methane is soft cryogenic that is not corrosive and less toxic, making it easier to store and handle. It has a boiling point of 111.51K, and liquid oxygen has a boiling point of 90.19 k, making it possible to store both fuel and oxidizer at similar temperatures. So, a common bulkhead can be used, which reduces the structural weight and insulation requirements.The temperature of liquefied methane is close to that of liquid oxygen as an oxidizer, and the required volume of loaded liquefied methane is comparable with that of oxygen. Accordingly, the design and manufacturing of equipment such as propellant tanks or valves can be standardized between liquefied methane and liquid oxygen, including the aspect of handling process of propellant, thus making it possible to reduce development cost and production cost [6]. Furthermore, it is less likely to vaporize and capable of being stored for longer space missions. Methane as liquefied natural gas is available for 100-120 years, and its cost is three times less than kerosene.

Here below are standard thermodynamic properties comparison of Methane with Hydrogen and RP1 in table 3.1:

Properties	**HYDROGEN**	**RP-1**	**METHANE**
Chemical formula	H_2	$C_{12}H_{24}$	CH_4
Molecular Weight(g/mol)	2	172	16
Tank temperature(k)	20	298	112
Optimum mixture ratio (O/F)	≈6	≈2.5	≈3
Fuel density (kg/m^3)	70	820	423
Bulk density (kg/m^3)	358	1026	801
Flame temperature (K)	3610	3803	3589
Vacuum sp.impulse(s)	455.9	354.6	368.3
Max theoretical sp.impulse (s)	532	370	459

Table 3.1: *Standard values of different fuels*

Different Chemical, physical, and thermal properties of Methane are listed in table 3.2:

PROPERTY	VALUE	UNIT
Autoignition temperature	810	K
Boiling point	111.51	K
Critical density	162.7	kg/m^3
Critical pressure	45.99	bar
Critical Volume	0.00615	m^3/kg
Density, Liquid	422.6	kg/m^3
Gibbs free energy of formation	-3179	K
Latent heat of vaporization	511	kJ/kg
Specific heat, C_p	2.232	kJ/kg K
Specific heat, C_v	1.709	kJ/kg K
Heat of combustion	-55528	kJ/kg
Enthalpy of formation	-4675	kJ/kg
Melting point	90.55	K
Molecular weight	16.042	g/mol
Solubility in water	0.022	mg/mol
Sound velocity	446	m/s
Specific heat ratio (C_p/C_v)	1.31	
Specific volume	1.52	m^3/kg
Standard molar entropy	11.59	kJ/kg K
Thermal conductivity	0.0339	W/m*C
Triple point pressure	0.117	bar
Triple point temperature	90.69	K
Viscosity, Dynamic	0.01107	cP
Viscosity, Kinematic	17.08	cSt

Table 3.2: *Methane Properties*

In recent years, many space organizations have begun using methane for high thrust applications. For example, SpaceX's Raptor engine and Blue origins BE-4 engine. Here is the comparison of general features of these engines with Rp-1 and Hydrogen engines in table 3.3.

	RD-180	**RS-25**	**Raptor**	**BE-4**
Cycle	Closed (Lox rich)	Closed (fuel rich)	Closed (Full flow)	Closed (Lox rich)
Fuel Type	Rp-1	Hydrogen	Methane	Methane
Total Thrust	3.83 MN	1.86 MN	2.00 MN	2.40 MN
Thrust: Weight	78:01:00	73:01:00	107:01:00	80:01:00
Specific Impulse (sea level)(s)	311	366	330	310
Specific Impulse Vacuum (s)	338	452	350	340
Chamber pressure (bar)	257	206	270	135
Price (Million dollars)	25	50	2	8
Reusability	No	19 flights	50 flights	25 flights

Table 3.3: *Current hydrocarbon fuel engines comparison*

3.2 Comparison of Engine cycles

For higher performance in liquid bipropellant engines, turbopumps are used to feed the combustion chamber. These pumps drive power from the turbines using excess thermal energy in the propellants. The way in which the hot gas is provided to drive the turbines is the way to distinguish from different cycles. There are OPEN cycles and CLOSED cycles[7]. Open cycles: The working fluid which operates the turbine is discharged off-board or in the divergent of the nozzle. This enables pre-combustion and turbine expansion at lower pressure. Closed cycles: All the working fluid from the turbine is injected into the engine combustion chamber to make the most efficient use of its remaining energy. In the closed cycles, the turbine exhaust gas is fed into the injector of the thrust chamber. It is expanded through the total pressure ratio of the main thrust chamber nozzle, thus giving a little more performance than the open cycles, where these exhaust gases expand only through a relatively small pressure ratio. The most common engine cycles are the gas generator, expanded cycle, staged combustion cycle, tap off cycle.

Gas generator cycle fig. 3.2 was used in the F1 engine and is also in use in the Delta II, Atlas and Titan rockets. In this cycle, a small fraction of the pressurized oxidizer and fuel is diverted to a medium-temperature burner (Gas Generator), typically 2% to 7%, which produces typically very fuel-rich gas to drive the turbine or turbines.[8] These are designed with a large pressure ratio, and their exhaust is either dumped overboard, or injected at some point into the main nozzle to provide some extra thrust. Nevertheless, this cycle is inherently somewhat lossy in that the turbine gas is not fully utilized in the main combustor. On the other hand, the power control is relatively straightforward, and there is little interaction of the feed system with the rest of the rocket. Thus, any propellant combination can be used, all power levels are suitable, and any desired pressure level can be obtained. However, the specific impulse loss increases with pressure (1.5-4 s per 100 atm).

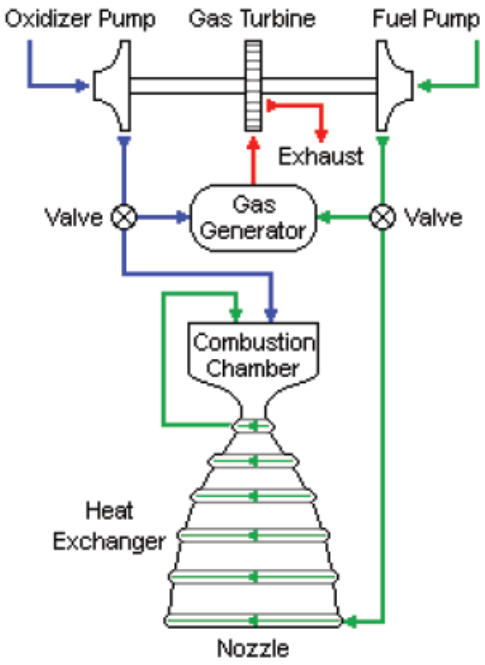

Figure 3.2: *Gas Generator engine cycle*

For engines utilizing hydrogen as fuel, the gas generator can be eliminated. Instead, the fuel is routed from the exit manifold of the nozzle cooling circuit to the turbine inlet. It is possible because hydrogen is supercritical at the pump exit, and it simply expands smoothly into an ordinary gas as it picks up heat. The resulting "Expander Cycle" fig. 3.3 is efficient and straightforward (the fuel is fully utilized in the thrust chamber). This cycle is used in the RL-10 engine and in the start-up sequence of the Japanese LE-5 engine (which then transitions to gas-generator operation). The principal limitation of this cycle is the small amount of heat available from regenerative cooling, which limits applicability to chamber pressures under approximately 70 atm.

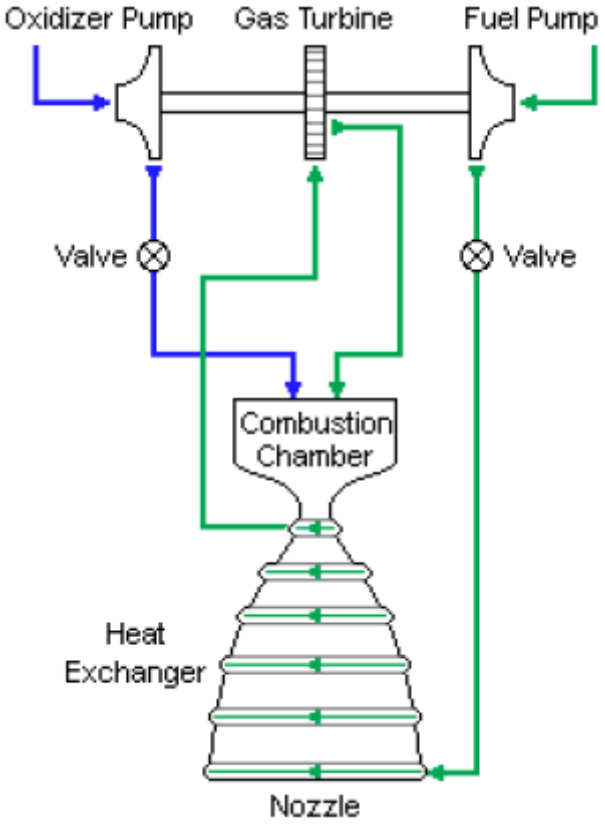

Figure 3.3: *Expander engine cycle*

For rockets with high chamber pressure, as well as high efficiency, is desired, the staged combustion cycle fig. 3.4 is the preferred choice. One could think of this as a modified expander cycle.[8] A small amount of oxidizer is added to the fuel after the cooling circuit, thus increasing the available enthalpy for the turbine drive. As in the expander cycle, all the propellant is entirely used in the combustion chamber. Unlike the expander, though, any oxidizer-fuel combination can be used. Two prominent examples of this cycle are the Space Shuttle Main Engine (SSME) and the Russian RD-170 booster engine. In the SSME, the pre-burners are incorporated into separate fuel and oxidizer turbopump assemblies and process most of the fuel (LH_2) with a small fraction of the oxidizer (LOX), producing a light "vitiated hydrogen" turbine driving gas. In the RD-170, the pre-burners process all the oxidizer (LOX) and a fraction of the fuel (kerosene) to produce a fuel-lean gas that drives the single central turbine. In both cases, the turbine exhaust is ducted to the main combustor injectors, together with the remaining LOX (SSME) or kerosene (RD-170). The choice of fuel-rich pre burners is precluded by carbon deposits on turbine

blades and other surfaces when hydrocarbon fuel is involved. The staged combustion cycle provides the highest levels of rocket performance but at the cost of significantly increased complexity. This is both because of the many ducts and valves involved and because of the very high pump exit pressures. A secondary potential difficulty, which is shared by the expander cycle, is that the turbines are unchoked and there is a possibility of low-frequency instability developing.

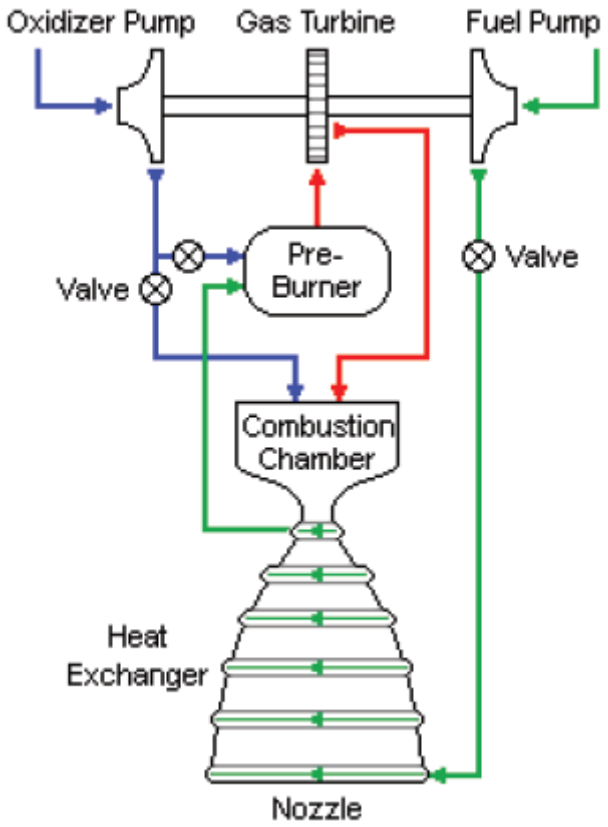

Figure 3.4: *Staged combustion engine cycle*

The combustion tap-off cycle is also known as the "topping cycle" or "chamber bleed cycle." It is an open liquid bipropellant cycle, usually liquid hydrogen and liquid oxygen, that combines the fuel and oxidizer in the main combustion chamber. Gases from the edges of the combustion chamber are used to power the engine's turbine and are expelled as exhaust. fig. 3.5 below shows a picture representation of the cycle [9].

The combustion tap-off cycle is rather unconventional for rocket engines as it has only been put into practice with two engines. It was conceived to evolve the J2 rocket into J2S (simplified, from gas-generator to tap-off). Part of hot gas is picked up from the combustion chamber sides and expanded through a turbine before discharge. The unique aspect of this cycle is that it allows for the engine to go into "idle mode" with a much lower thrust than maximum. Furthermore, the wide range of thrust options allows this cycle to be throttled, which is very appealing for rockets designed to carry people.

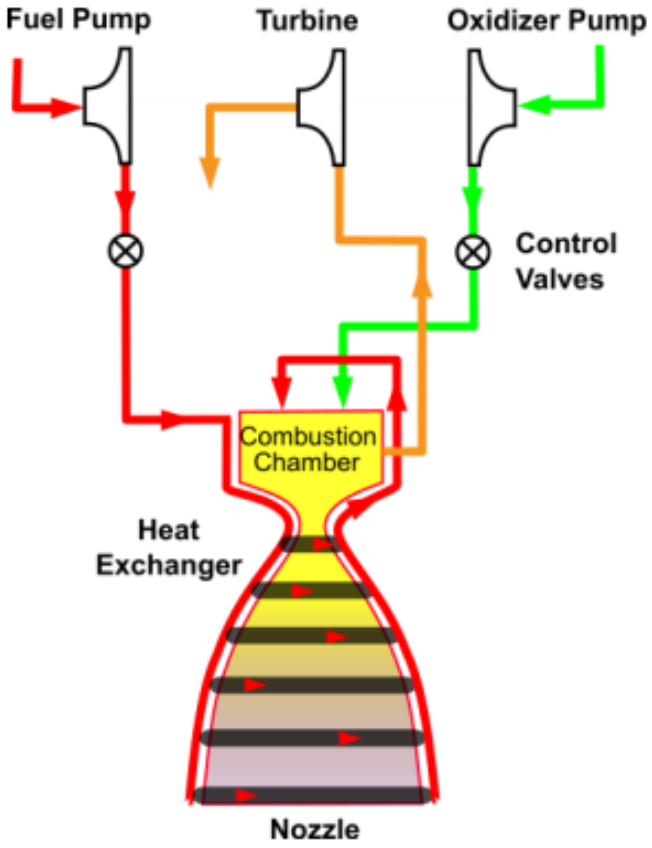

Figure 3.5: *Tap-Off engine cycle*

Here are some of the comparison on various features of different cycles [9] in table 3.4:

CYCLE	APPLICATION	SPECIFICATIONS
Pressure Feed	Upper stage, Space propulsion	Low Pressure 2 Mpa Low Thrust 40 KN
Gas Generator	Booster, Core, Upper stage	Medium Pressure 15 Mpa Large Thrust 60 KN – 7 MN
Expander	Upper stage	Low-Medium Pressure 3-7 Mpa Small Thrust Range 80-200 KN
Staged Combustion	Booster, Core, Upper stage	High Pressure 13-26 Mpa Large Thrust Range 80 KN-8MN
Full Flow Staged Combustion	Booster, Core	High Pressure 30MPa Large Thrust Range up to 10MN

Table 3.4: *Different engine cycles specifications and application*

Advantages and disadvantages of different engine cycles [9] are listed in table 3.5:

	Staged Combustion Single Chamber Tri-Propellant	**Staged Combustion Dual preburner**	**Single Preburner Staged combustion**	**Gas Generator**	**Expander**	**Tap Off**
Advantages	Highest integrated performance available (closed cycle).Maximizes propellant bulk density and tsp.	High performance (closed cycle). Very attractive for reusable applications Easier MR and thrust level throttling characteristics	High performance (closed cycle).Simpler than multi preburner options to left. Very attractive for reusable applications	Simple cycle, low production costs, earlier to develop	High reliability, benign failure modes (contained), simple cycle	Simple cycle with fewer parts, lower production costs, easier maintainability
Disadvantages	Most difficult to develop. Will be very expensive. Production cost makes reusable applications mandatory. Vehicle must be very performance dawn such as SST O.	More difficult to develop than single preburner. Tends to be very expensive. Failure modes tend to be more invoked. Production cost makes reusable applications almost mandatory	More difficult to develop. Tends to be more expensive. Failure modes tend to be more involved	Lower performance because of open cycle. Performance level makes this unattractive for most reusable applications	Limited to LOX/LH2 propellants only.Limited performance because of heat transfer limitations	Hot gas duct that taps off from the MCC and mixes diluent fuel to regulate gas temperature Lower performance (Open cycle).
Potential applications	Reusable SSTO	Reusable SSTO	Booster or upper stage, reusable or expendable rockets (May depend on propellant choices)	Booster or upper stage, expendable rockets	Booster or upper stage, reusable or expendable rockets	Booster or upper stage, reusable or expendable rockets

Table 3.5: *Advantages and disadvantages of different engine cycles*

According to [5] research was done on three different engine cycles ORG(closed oxidizer rich gas generator), FRG (closed fuel rich gas generator), Open cycle gas generator with thrust approximately 200 tons and same chamber geometry(all with hydrogen as fuel). The study was done to calculate maximum chamber pressure and other parameters for each cycle. Maximum allowable temperatures for oxidizer gas generator were kept at 900K and fuel rich gas generator at 1000K and the propellant component pressure at entrance of chamber cooling to $<500\text{kg}/cm^2$. And the turbine pressure ratio was set less than 2. Results from this study showed that closed oxidizer rich gas generator gives the best rocket performance characteristics in comparison with other cycles. Values of different parameters achieved are listed in the table 3.6 below:

Parameter	**ORG**	**FRG**	**Open cycle**
Engine Thrust (tons)	207.8	200	215.2
Chamber Vacuum specific Impulse (s)	357.4	348.2	352.7
Engine Vacuum specific impulse (s)	357.4	348.2	340
Temperature of Gas generator (k)	890	1000	1100
Pressure at entrance of chamber cooling (kg/cmˆ2)	420	503	400
Chamber pressure(kg/cmˆ2)	270	165	250
Turbine pressure ratio (kg/cmˆ2)	1.92	1.84	50
Engine specific mass (kg/t)	16.3	16	14

Table 3.6: *Main performance characteristics of different cycles*

4 Chapter

LOX/Methane and LOX/Kerosene engine trade-off

4.1 Theoretical performance comparison

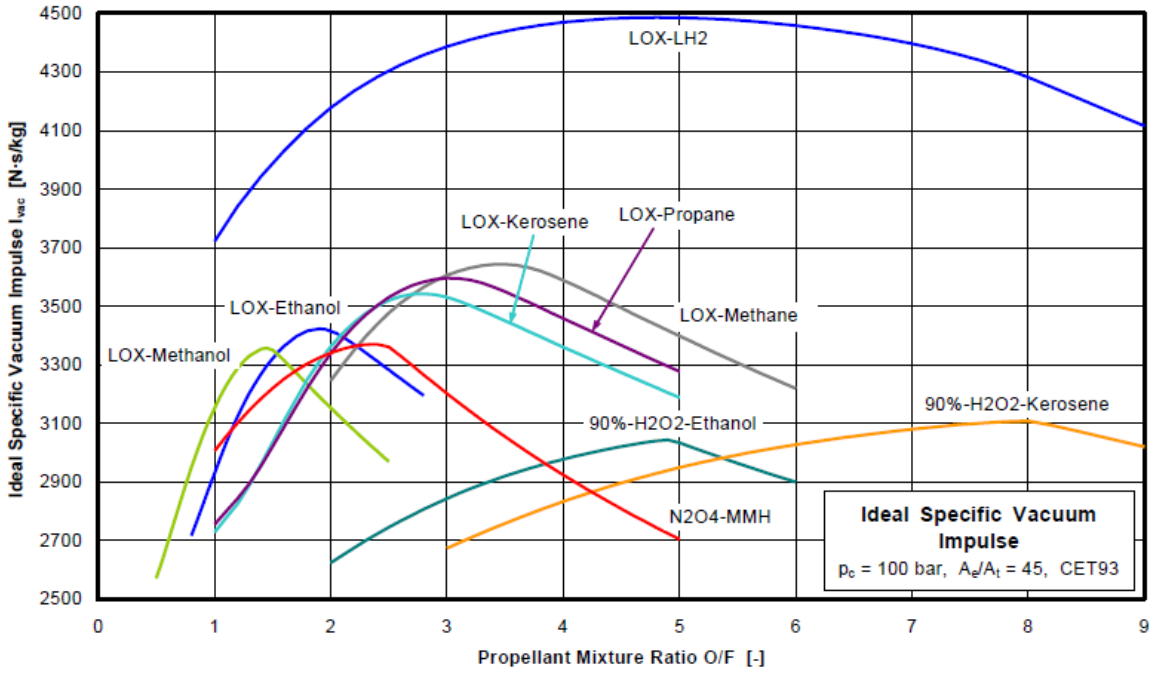

Figure 4.1: *Theoretical vacuum specific impulse of various non toxic propellants*

The theoretical performance in terms of vacuum specific impulse was predicated for various non-toxic propellants shown in fig. 4.1 The prediction was performed for a chamber pressure of 100 bar and an expansion ratio of 45 using the NASA CEA code. Of all the LOX-hydrocarbon combinations methane, propane and kerosene show the best performances. From the graph, it is clear that methane shows a slightly higher vacuum specific impulse than kerosene. However, due to its low bulk density of 423 kg/m^3 methane engine will have a larger tank volume compared to a kerosene engine having a bulk density of 820 kg/m^3 which is not ideal for stage optimization.

4.2 Combustion chamber material compatibility

According to [10], an experimental investigation was done on various hydrocarbons like Kerosene and Methane under conditions that simulate high pressure, rocket engine cooling system to determine the carbon deposition rates in heated cooper and nickel-plated copper tubes. Here are some of the findings from this research:

1. Due to trace elements of sulphur impurities in the fuels, corrosion was found on the copper tube surface. By plating nickel inside the copper tubes reduced the deposit formation and eliminated the corrosion in most cases. However, when Nickel plating is subjected to cryogenic natural gas at 160 K cracking happened. For natural gas in copper tubes, operation above wall temperatures of 700 K produced a significant reduction in deposit formation.

2. Increase in fuel velocity for RP-1 in copper tubes at wall temperatures of $<$650 K resulted in a decrease in the rate of carbon deposition. However, when the wall temperatures are $>$650 K carbon deposition increases for copper and nickel tubes.

3. Fuel velocity had no effect on carbon deposition for Methane.

4. For both, the Fuels formation of deposit did not always coincide with the rise in wall temperatures. Total deposit thermal resistance ranged from 0.001 to 1 K.cm^2/W. For RP-1, peak thermal resistance build-up rates were found to decrease rapidly as fuel velocity increased.

5. At wall temperatures between 500 and 650 K, Methane has the lowest carbon deposition in copper tubes of less than 80 μg/cm^2-hr. If the wall temperatures decrease, the carbon deposition rate can increase to the values of Rp-1.

6. At wall temperature between 560 and 750 K, RP-1 has deposition rates of 200 to 320 μg/cm^2-hr in copper tubes.

From these findings, we can say that Methane is an attractive fuel with regards to thermal stability. Nickel coating inside copper cooling tubes can reduce carbon deposition and tube corrosion. In addition, some of the impurities which are detrimental to thermal stability can be eliminated by cryogenic cooling.

4.3 Cooling Capacity

From [11] a study was performed to find the regenerative cooling limits (maximum chamber pressure) for Kerosene and Methane engines. Maximum chamber pressure limits were first determined for Kerosene and Methane without carbon layer. Later seven different thermal barriers (carbon layer, ceramic coating, graphite liner, film cooling, transpiration cooling, zoned combustion and a combination of any of the above two) were established to find the chamber pressure cooling limits.

Significant findings from the un-enhanced case:

1. For Lox/RP-1 design, cooling limits are at very low chamber pressures because of limiting RP-1 coolant decomposition temperature at $T_{wc} <= 589$K. LOX/RP-1 cooling limit chamber pressure decreases with a decrease in thrust.

2. For LOX/LCH_4 cooling limit chamber pressure decreases with an increase in thrust. Furthermore, these chamber pressure limits slightly favour a gas generator engine cycle.

Findings from the enhanced case:

1. Best option of all the seven different thermal barriers was the combined thermal barriers. The combination of ZrO_2 ceramic coating and film cooling has the highest cooling capacity for LOX/LCH_4. In the case of LOX/RP-1 ZrO_2 ceramic coating and carbon layer combination proven to be the best option.

2. All the fluid barriers (Film cooling, Transpiration cooling, Zoned combustion) have performance loss of 3%.

3. The second best option for LOX/LCH_4 is transpiration cooling, and for LOX/RP-1, it's the carbon layer barrier.

4. For LOX/LCH_4 ZrO_2 coating provides a notable increase in chamber pressure P_c whereas carbon layer does not affect.

5. For LOX/RP-1 carbon layer thermal barrier provides a significant increase of P_c whereas ZrO_2 has minimal effect.

6. Transpiration cooling is not applicable for LOX/RP-1 because of coking temperature limits.

7. Zoned combustion has negligible effects on both fuels.

8. From a fabrication and installation standpoint, graphite liner is not applicable for high heat flux designs.

So, the highest chamber pressures that can be attained is for LOX/LCH_4. LOX/RP-1 gives the lowest cooling limits because of its low decomposition temperature. Moreover, a Gas generator engine system provides a slightly higher chamber pressure than a staged combustion cycle engine, assuming the same energy release efficiency obtained for either cycle.

In another research, [12] the regenerative cooling circuit of a gas generator engine cycle, all the main chamber fuel is used to cool the chamber walls. During this process, methane is in a supercritical state at the cooling circuit exit, and because of its lower density and viscosity, lower pressure losses are estimated. So a simple regenerative cooling circuit, as shown in the below fig. 4.2 can be used for a Methane engine. Whereas for kerosene which stays in a liquid state at the exit, this circuit becomes too long considering the high velocities required to keep the cooling channel temperature below the coking limit. A different (parallel)cooling circuit, as shown in the fig. 4.3, is used to reduce the length and keep the pressure losses in check. However, still, the pressure losses from the kerosene circuit are three times more than methane. Moreover, higher manifolds to reduce the length can lead to more mass penalties.

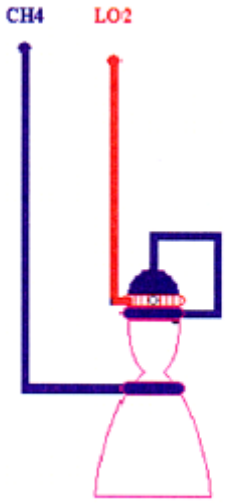

Figure 4.2: *Methane Cooling circuit*

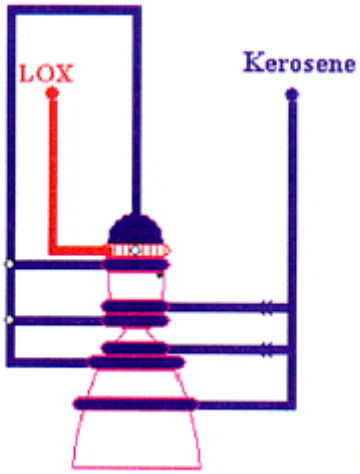

Figure 4.3: *Kerosene Cooling circuit*

Both the studies show us that methane is a better option than kerosene from a thrust chamber cooling perspective.

4.4 Staged Combustion and Gas Generator cycles

For High thrust applications of LOX/Hydrocarbons fuels, major engine cycles that needed to be considered are Staged combustion fig. 4.4, Full flow fig. 4.5 and Gas Generator cycles fig. 4.6. For better understanding, a schematic of these cycles are shown below:

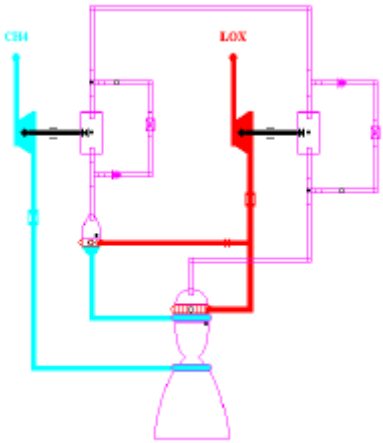

Figure 4.4: *Staged combustion cycle*

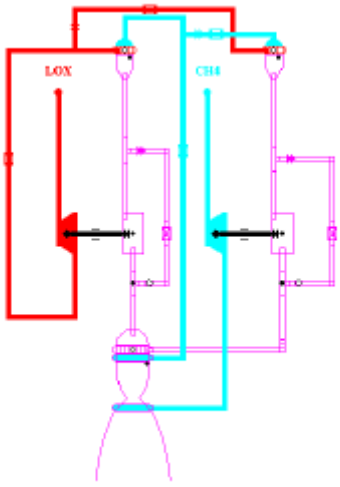

Figure 4.5: *Full flow combustion cycle*

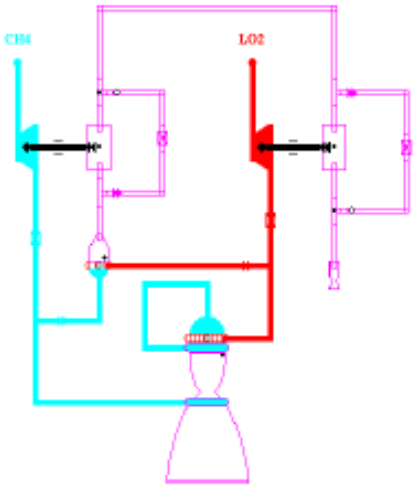

Figure 4.6: *Gas Generator cycle*

In a gas generator cycle, mass flow is diverted to drive the turbopumps. This flow is not burned and expanded in the combustion chamber, so the gas generator cycle is less efficient. However, it offers a significant advantage in moderate turbopump discharge pressures and a simple start sequence. The main parameter for the gas generator cycle is the turbine inlet temperature which must be less than 900K (and 700 K for reusable engines).On the other hand, a staged combustion cycle gives a higher specific impulse efficiency.

Analysis was done to compare different cycles for the case of LOX-LCH_4 by [13] :

	GAS GENERATOR		**STAGED COMBUSTION**		
	Full rich	Lox Rich	Fuel Rich	Lox Rich	Full Flow
Specific Impulses (s)	350	328	358	358	358
Power for turbopumps (MW)	37	41	45	36	36

Table 4.1: *Gas Generator vs staged combustion*

Lox Rich gas generator cycle has the least performance out of all. Full flow cycle has the lowest turbopumps power compared to fuel-rich and LOX rich staged combustion despite its complexity. Fuel rich gas generator looks to be the best choice despite its low specific impulse of about 8 s for this particular case of (Thrust = 400 tons, Pc = 100 bar, $\varepsilon = 45$, Tgg = 900K) because of its simplicity and lower power for turbopumps.

Comparison of the specific impulse of LOX/LCH_4 gas generator cycle for different chamber pressures at various mixture ratios fig. 4.7 shows that despite the increase in chamber pressure, the specific impulse values drop after a certain point because of a huge increase in turbopump power required which leads to a higher gas generator mass flow rates. This increase in turbopump power from 15 Mw at 50bar to 70 Mw at 200 bar chamber pressure is clearly shown in fig. 4.8 which compares staged and gas generators specific impulses for different pressures.

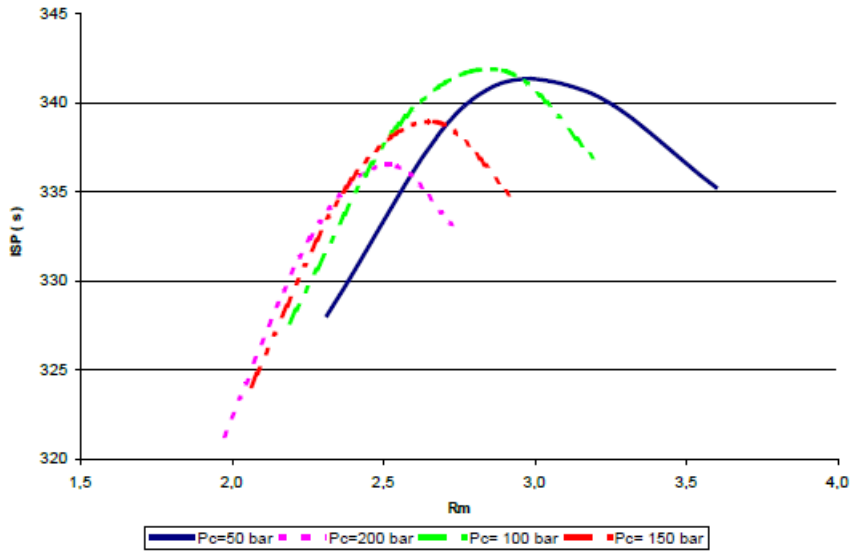

Figure 4.7: *ISP vs Pc Vs MR*

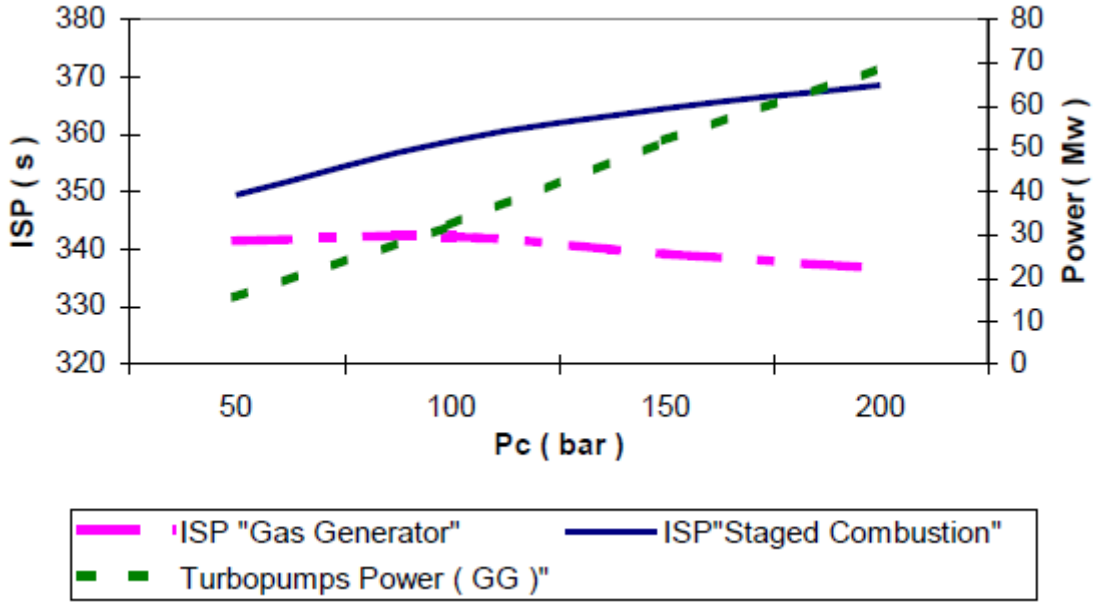

Figure 4.8: *Staged vs Gas Generator cycle performance*

4.5 About Turbines and Pumps

A turbopump in a rocket engine consists of a pump that delivers fuel or oxidizer to the thrust chamber, where the propellants are brought to react and increase in temperature. Here the propellants are pressurized using pumps, which in turn are driven by turbines. The turbines derive their power from the expansion of hot gases. Several different turbopump arrangements can be made. Two of the most common are :

1. One Turbine with two propellant pumps on the same shaft.fig. 4.9

2. Two smaller separate turbopumps, one where a turbine drives an oxidizer pump and another turbine drive a fuel pump.fig. 4.10

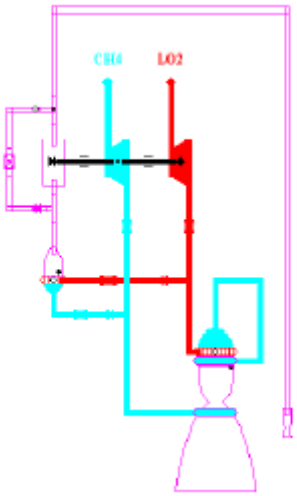

Figure 4.9: *Single Shaft Turbopump*

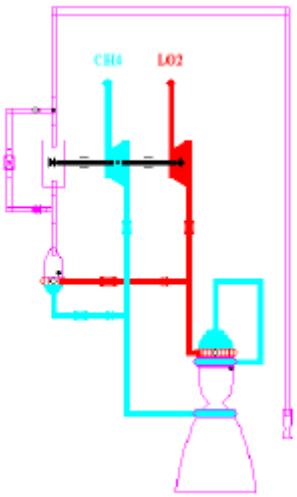

Figure 4.10: *Dual Shaft Turbopump*

The selection of a specific turbopump arrangement can be complex. It depends on various parameters like engine cycle, propellant physical properties, the nominal flows and pumps discharge pressures and many other factors. The turbopump design requires the careful balancing of the propellant flows, the shaft speeds and the power between the essential pumps and turbines and the pressure distribution of the propellant along its flow paths. For Lox/Hydrocarbons engines, it is proven that a single shaft/direct drive is the best solution by [14]. For these kinds of turbopumps, the condition to be fulfilled is that the specific speed of oxidizer pump is equal to the specific speed of fuel pumps.

From [13], an acceptable value of 2.2 for specific speeds(N_s) was found, but for specific suction speed(S), this figure of ratio is unacceptable, and as a result, a direct drive pump for LOX/LCH_4 engine requires a booster pump to feed the LOX turbopump. However,

instead of adding a complex booster pump, a two separate turbine arrangement makes a better choice for methane engines.

Coming to the choice of turbine, a turbine must provide adequate shaft power for driving the propellant pumps at the desired shaft speed and torque. Single-stage impulse and the Curtis turbines are the most prominent choices. From [12] a single stage impulse turbine which is highly supersonic, is a better choice.

5 Chapter

A different propellant system for Ariane 5

Ariane 5 is a heavy launcher by ESA (European space agency). It consists of two solid boosters and two liquid stages. Each of the two solid boosters uses P241 engines and are 31.6 meters tall and 3.05 meters in diameter. Each booster produces a thrust of 7080 KN during 140s of burn time .68% AP 18% Al 14% HTPB is the propellant combination. Various specifications of the booster are listed in table 5.1

Parameters	**Values**
Propellent combination	68% Ap – 18%Al – 14% HTPB
Chamber pressure (bar)	64
Expansion ratio (A_e/A_t)	30
Thrust vacuum (KN)	7080
Burn time (s)	140
Vacuum specific impulse (s)	275
Density of propellant combination(kg/m^3)	1690

Table 5.1: *P241 booster specifications*

A Vulcain-2 cryogenic engine [15] is used for the core stage of the Ariane 5 launcher. It uses LOX/LH_2 propellant combination. It is 3.6 m tall and 2.15 m in width at the nozzle exit. It provides a vacuum thrust of 1350 KN at lift-off for a burn time of 540s. Turbopumps, driven by gases from a gas generator fed from small bleeding of propellants, feed the main combustion chamber, operating at 115 bar pressure and 3500 K temperature, with a Specific impulse of 433s. The oxygen turbopump rotates at 12600 rpm, and with a power of 5100 KW, hydrogen turbopump rotates at 35500 rpm with a power of 14100 KW. Vulcain-2 features regenerative cooling through a tube wall design in the nozzle and gas film cooling for the lower part of the nozzle, where exhaust gas from the turbopumps is injected. Various specifications of this engine are listed in table 5.2:

Parameters	Values
Propellant combination	LOX/LH_2
Vacuum thrust (KN)	1350
Specific impulse (s)	433
Chamber pressure (bar)	115
Mixture ratio	6.1
Expansion ratio (A_e/A_t)	58.5
Burn time (s)	540
Exit diameter (d_e)(m)	2.15

Table 5.2: *Vulcain-2 specifications*

These parameters are used as a reference in the thesis for trying different propellant combinations like LOX/RP-1 and LOX/LCH_4 for core stage comparison and also mass and volume comparison for liquid booster combinations of (LOX/LH_2, LOX/RP-1 and LOX/LCH_4) to the solid booster.

5.1 The Mathematical Model Implemented

The thrust is the force produced by a rocket propulsion system acting upon a vehicle. It is represented by the eq. (5.1).

$$T = \dot{m}_p v_e + A_e \left(p_e - p_a\right) \tag{5.1}$$

The first term in the above equation is the momentum thrust represented by the product of the propellant mass flow rate and its exhaust velocity relative to the vehicle. The second term represents the pressure thrust consisting of the product of the cross-sectional area at the nozzle exit A_e and the difference between the exhaust gas pressure at the exit and the ambient fluid pressure. When the ambient atmospheric pressure is equal to the exhaust pressure, the pressure term is zero. For any nozzle, this occurs only at one attitude, and this referred to as the rocket nozzle with an optimum nozzle expansion ratio (A_e/A_t) the thrust equation becomes:

$$T = \dot{m}_p v_e \tag{5.2}$$

In the vacuum space the ambient fluid pressure $P_a = 0$ and the thrust is :

$$T = \dot{m}_p v_e + A_e p_e. \tag{5.3}$$

The Total Impulse (I_t) is the thrust force integrated over the burning time t_b. It is proportional to the total energy released by all the propellants in the propellant system.

$$I_{tot} = \int_{t_p}^{t_b} T dt \tag{5.4}$$

For constant thrust and very short start and stop transients which we are going to assume for this thesis eq. (5.4) reduces to

$$I_{tot} = Tt_b \tag{5.5}$$

The specific impulse is thrust per unit propellant weight flow rate. It is an important figure of merit in the performance of a rocket propulsion system. For a constant thrust and propellant mass flow rate $\dot{m}_p$:

$$I_{sp} = \frac{T}{\dot{m}_p g_0} = \frac{c}{g_0} \tag{5.6}$$

Here c is the exhaust velocity, and it is the average equivalent velocity at which propellant is ejected from the vehicle. It is given in meters per second . Since c and I_{sp} differ only by an arbitrary constant, either can be used as a measure of rocket performance. In this thesis, c is generally used while presenting the various performance graphs.

The specific impulse can also be defined in terms of thermodynamic properties as:

$$I_{sp} = \sqrt{2 \cdot \frac{\gamma}{\gamma - 1} \cdot \frac{T_f}{M} \cdot R \cdot \left[1 - \left(\frac{p_e}{p_c}\right)^{\frac{\gamma-1}{\gamma}}\right]} \tag{5.7}$$

The characteristic velocity C^* is a parameter of merit of a combustion chamber. It is only a function of propellant characteristics and combustion chamber properties, independent of the nozzle.

$$C^* = p_c A_t / \dot{m}_p \tag{5.8}$$

C^* theoretical is given by:

$$C^*_{\text{th}} = \sqrt{\frac{\frac{R}{M} T_c}{\gamma \left[\frac{2}{\gamma+1}\right]^{\frac{\gamma+1}{\gamma-1}}}} \tag{5.9}$$

The coefficient of thrust C_t is a parameter of merit of the nozzle. It is represented by:

$$C_t = \frac{T}{p_c A_t} \tag{5.10}$$

For an ideal expansion including static contribution C_t

$$C_t = \sqrt{\frac{2\gamma^2}{\gamma - 1}\left(\frac{2}{\gamma+1}\right)^{\frac{\gamma+1}{\gamma-1}}\left[1 - \left(\frac{P_e}{P_0}\right)^{\frac{\gamma-1}{\gamma}}\right]} + \left(\frac{P_e - P_a}{P_0}\right)\frac{A_e}{A_t} \tag{5.11}$$

Specific impulse can also represented in terms of C_* and C_t as below:

$$I_{sp} = \frac{T}{\dot{m}_p g_0} = \frac{C_T C^*}{g_0} \tag{5.12}$$

Expansion ratio is the ratio between nozzle exit area to nozzle throat area :

$$\varepsilon = \frac{A_e}{A_t} = \frac{\sqrt{\gamma\left(\frac{2}{\gamma+1}\right)^{\frac{\gamma+1}{\gamma-1}}}}{\left(\frac{P_e}{P_0}\right)^{\frac{1}{y}}\sqrt{\frac{2\gamma}{\gamma-1}\left[1 - \left(\frac{P_e}{P_0}\right)^{\frac{\gamma-1}{\gamma}}\right]}} \tag{5.13}$$

The mixture ratio is defined as the ratio of the mass flow rate of the oxidizer to that of the fuel. The stoichiometric ratio of a propellant combination, the ratio at which the fuel will be completely oxidized, is typically higher than that of the actual mixture ratio used in the propulsion system of a rocket.

$$O/F = \frac{\dot{m}_o}{\dot{m}_f} \tag{5.14}$$

From the thrust and specific impulse definitions the propellant mass flow rate can be written as:

$$\dot{m}_p = T/(I_{sp})^*(g_0) \tag{5.15}$$

$$\dot{m}_p = P_c A_t / C^* \tag{5.16}$$

In liquid rocket engines, the propellant mass flow rate can be written as the sum of the mass of fuel flow rate and mass of oxidizer flow rate:

$$\dot{m}_p = \dot{m}_f + \dot{m}_o \tag{5.17}$$

Mass flow rates of fuel and oxidizers in terms of mixture ratio are:

$$\dot{\mathrm{m}}_\mathrm{f} = ((\mathrm{O/F})/(1 + \mathrm{O/F}))\dot{\mathrm{m}}_\mathrm{p} \tag{5.18}$$

$$\dot{\mathrm{m}}_\mathrm{o} = (1/(1 + \mathrm{O/F}))\dot{\mathrm{m}}_\mathrm{p} \tag{5.19}$$

Mass of fuel and oxidizers (an additional sum of 5% will be added for safe ignition):

$$\mathrm{M_f} = \dot{\mathrm{m}}_\mathrm{f} \mathrm{t_b} \tag{5.20}$$

$$\mathrm{M_o} = \dot{\mathrm{m}}_\mathrm{o} \mathrm{t_b} \tag{5.21}$$

Volumes of fuel and oxidizers:

$$\mathrm{V_f} = \mathrm{M_f} \rho_\mathrm{f} \tag{5.22}$$

$$\mathrm{V_o} = \mathrm{M_o} \rho_\mathrm{o} \tag{5.23}$$

The volume of fuel and oxidizers tanks are not equal to the volume of fuel and oxidizer because the change in temperature decreases the density and increases the volumes, so considering this, an extra 10% will be added to the volume of fuel and oxidizers to get the tank volumes.

5.2 LOX/LH_2 ENGINE

The present Vulcain-2 engine uses LOX/LH_2 as its propellant combination. LOX/LH_2 propellant combination is considered as a reference for comparison with kerosene and methane engines due to the existing state of art Vulcain-2 engine. NASA CEA analysis is done for LOX/LH_2 combination to find different theoretical performance values taking Vulcain-2 engine chamber pressure and nozzle expansion ratio as the starting values.

5.2.1 O/F ratio

The chemical reaction for gaseous hydrogen and oxygen is presented in the eq. (5.24). The stoichiometric O/F ratio is equal to 8. However, the best operative mixture ratio for high-performance rocket engines ranges between 4.5 to 6. In order to begin the study of the performance of this engine, it is necessary to choose the O/F ratio that the engine will operate at. The O/F ratio for the design chamber conditions was determined by a nested analysis in the NASA computer program CEA (Chemical Equilibrium with Applications). During the analysis, shifting equilibrium condition was chosen for the entire thesis.

$$H_2 + \frac{1}{2}O_2 \rightarrow H_2O \tag{5.24}$$

The conditions given for the analysis are in table 5.3

Parameter	Value
Chamber pressure (bar)	115
Expansion ratio (A_e/A_t)	58.5
Fuel	Hydrogen (LH2)
Oxidizer	Oxygen (LOX)
Fuel temperature (K)	20
Oxidizer temperature (K)	90
O/F range	2,3,4,5,6,7,8,9

Table 5.3: *Parameters considered for CEA analysis*

Variation of vacuum specific impulse for different O/F ratios

The values of vacuum specific impulse is plotted for different mixture ratios:

O/F	Vacuum specific impulse (m/s)
2	4199.8
3	4415.2
4	4504.5
5	4526.9
6	4506.1
7	4450.5
8	4341.7
9	4170.3

Table 5.4: *Vacuum specific impulse values for different O/F ratios*

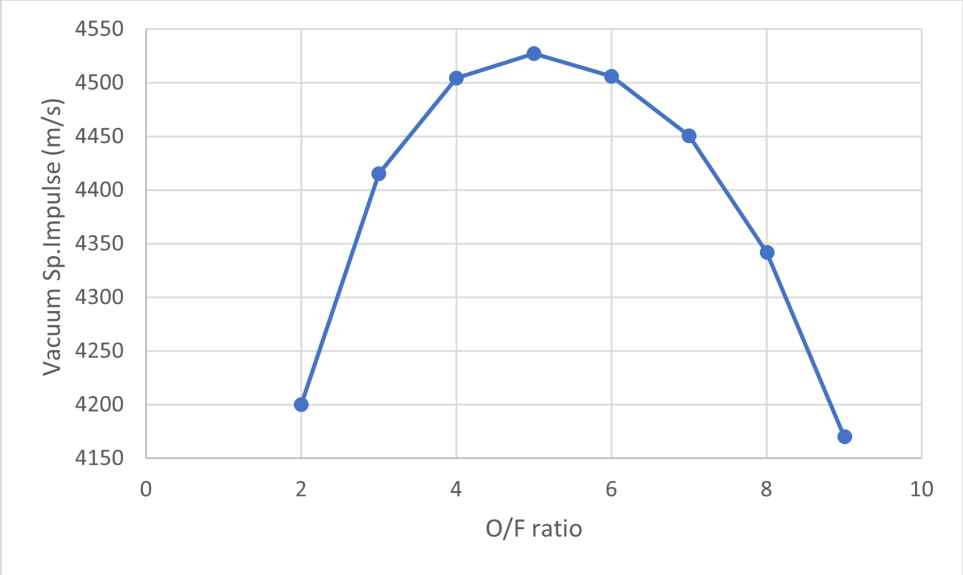

Figure 5.1: *Variation of vacuum specific impulse for different O/F ratios*

The above fig. 5.1 depicts that the maximum vacuum specific impulse is achieved around 4 to 6. Unlike other propellants, the optimum mixture ratio for liquid oxygen and liquid hydrogen does not necessarily produce the maximum specific impulse. Because of the extremely low density of liquid hydrogen, the propellant volume decreases significantly at higher mixture ratios. Maximum vacuum specific impulse typically occurs at a mixture ratio of 5. However, by increasing the mixture ratio to, say, 6.1(from the reference engine), the storage volume is reduced significantly. It results in smaller propellant tanks, lower vehicle mass, and less drag, which generally offsets the loss in performance that comes with using the higher mixture ratio.

Variation of vacuum specific impulse for different chamber pressures at different O/F ratios

Analysis was done to determine the effect of mixture ratio on vacuum specific impulse at different chamber pressures (20 bar, 40 bar, 60bar, 80 bar, 100 bar, 120 bar, 150 bar, 200 bar) by keeping the expansion ratio constant at 58.5

Vacuum specific impulse (m/s)								
O/F	**P_c 20 bar**	**P_c 40 bar**	**P_c 60 bar**	**P_c 80 bar**	**P_c 100 bar**	**P_c 120 bar**	**P_c 150 bar**	**P_c 200 bar**
2	4199.4	4199.4	4199.5	4199.6	4199.7	4199.9	4200.1	4200.5
3	4415	4415.1	4415.2	4415.2	4415.2	4415.2	4415.3	4415.3
4	4502	4503.2	4503.8	4504.1	4504.4	4504.6	4504.8	4505
5	4518.2	4522.2	4524.2	4525.4	4526.3	4527	4527.8	4528.8
6	4486.8	4495.4	4499.8	4502.7	4504.8	4506.5	4508.4	4510.7
7	4415.7	4430.8	4438.9	4444.2	4448.1	4451.2	4454.9	4459.3
8	4291.2	4312.5	4324.2	4332.1	4338.1	4342.8	4348.4	4355.4
9	4130	4147.3	4156.6	4162.8	4167.5	4171.2	4175.5	4180.8

Table 5.5: *Vacuum specific impulse values for different chamber pressures at different O/F ratios*

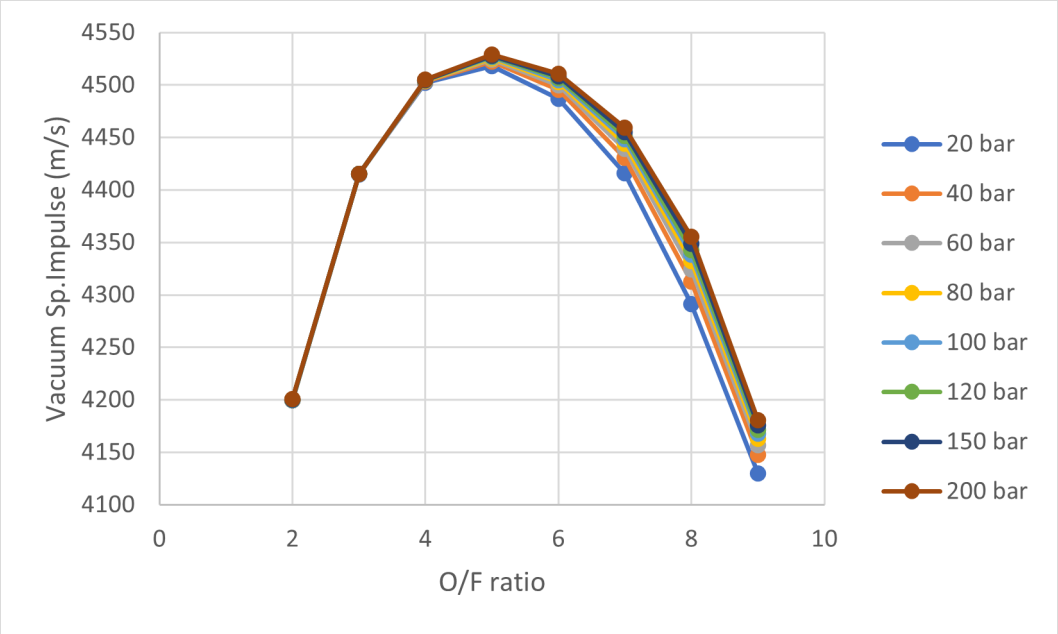

Figure 5.2: *Variation of vacuum specific impulse for different chamber pressures at different O/F ratios*

The above fig. 5.2 shows that vacuum specific impulse increases with increases in chamber pressure, but the effect of chamber pressure on vacuum specific impulse seemed very minimum. Therefore, further analysis was done in the later sections to better understand chamber pressure effect on vacuum specific impulse.

Variation of vacuum specific impulse for different expansion ratios at different O/F ratios

Vacuum specific impulse (m/s)							
O/F	**ε 20**	**ε 50**	**ε 75**	**ε 100**	**ε 125**	**ε 150**	**ε 200**
2	4074.2	4184.5	4223.4	4249.6	4269.3	4284.9	4309.1
3	4263.3	4397	4441.8	4469.3	4488.6	4503.1	4523.9
4	4326.1	4482.8	4536.3	4569.5	4592.8	4610.4	4635.9
5	4323.8	4501.7	4564	4603	4630.7	4651.8	4682.3
6	4280.5	4477.7	4548.3	4593.2	4625.2	4649.8	4685.7
7	4202.2	4418.8	4497.8	4548.5	4585	4613.2	4654.6
8	4076.6	4307	4394	4450.7	4491.9	4523.9	4571.5
9	3923.8	4138.5	4218.1	4269.6	4306.8	4335.7	4378.3

Table 5.6: *Vacuum specific impulse values for different expansion ratios at different O/F ratios*

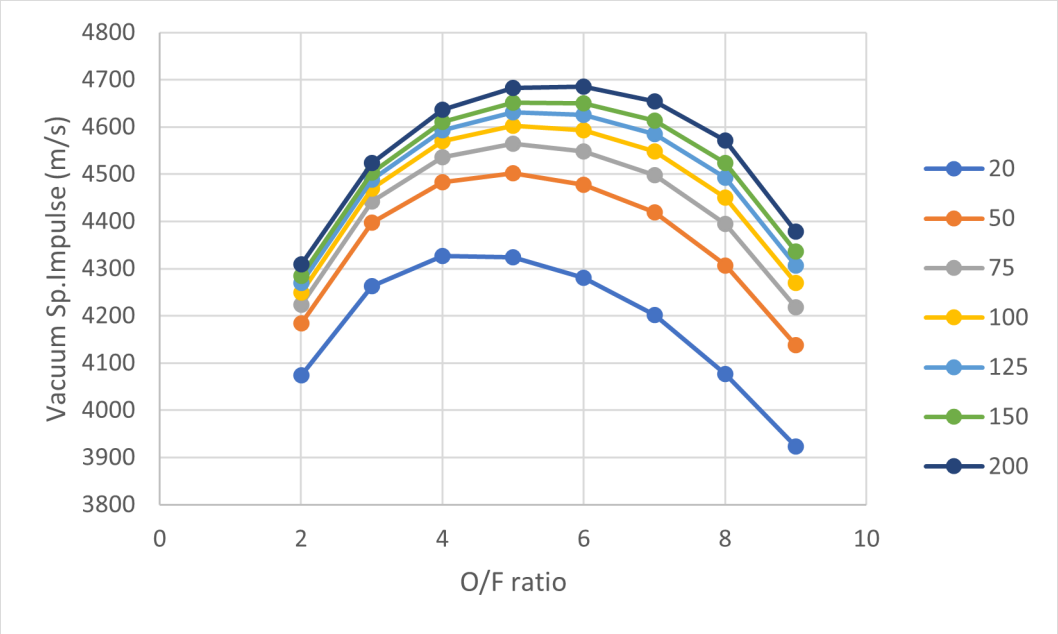

Figure 5.3: *Variation of vacuum specific impulse for different expansion ratios at different O/F ratios*

To understand how expansion ratio affects the vacuum specific impulse vs mixture ratio, analysis was done at different expansion ratios (20,50,75,100,125,150,200) by keeping chamber pressure constant at 115 bar. Above fig. 5.3 shows us that the higher the expansion ratio higher the vacuum specific impulse. The practical limits on the expansion ratio act as a barrier for the maximum specific impulse that can be achieved.

Variation of combustion temperature and molar mass for different O/F ratios

Vacuum specific impulse is not the sole criteria for determining the exact mixture ratio for a propellant combination. Variation of several other parameters like combustion temperature and molar mass should be considered. Analysis was performed with the same initial parameters as in the vacuum specific impulse. (P_c=115 bar, esp = 58.5)

O/F	Combustion temperature (K)
2	1797.7
3	2453.4
4	2961.1
5	3318
6	3538.7
7	3642.8
8	3661.1
9	3631

Table 5.7: *Combustion temperature values for different O/F ratios*

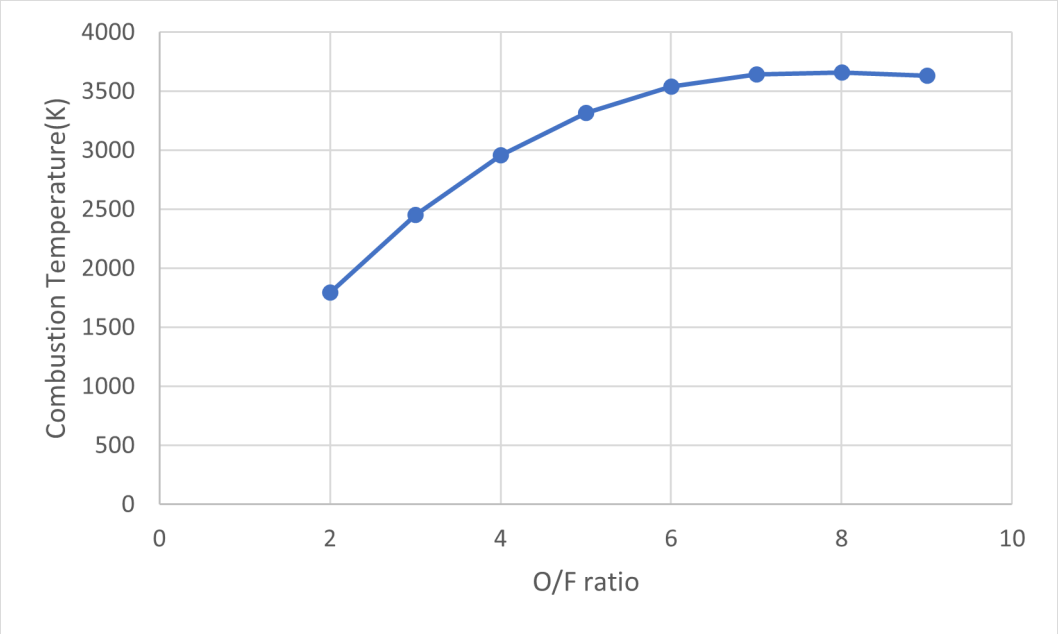

Figure 5.4: *Variation of combustion temperature for different O/F ratios*

From the fig. 5.4 the combustion temperature keeps on increasing as the mixture ratio increases because of fuel-rich conditions. Maximum flame temperature generally achieved around the stoichiometric ratio (which is 8 for LOX/LH_2) typically in a fuel-rich condition. Since the maximum amount of heat release occurs at the stoichiometric condition and by adding more fuel than the stoichiometric ratio causes the formation of partly oxidized products, which release less energy than the products of complete combustion, the maximum combustion temperature does not increase to the left of the peak, even though the fuel content is increased. Moreover, the increase in combustion temperature after the mixture ratio of 6 is insignificant if we compare it with the increase in combustion temperature, let's say from 4 to 6 mixture ratio, which is almost 500K.

	Molar mass (kg/kmol)		
O/F	**Chamber**	**Throat**	**Exit**
2	6.048	6.048	6.101
3	8.057	8.061	8.064
4	8.057	8.061	8.064
5	8.057	8.061	8.064
6	13.533	13.671	14.111
7	14.998	15.182	16.126
8	16.245	16.451	18.007
9	17.308	17.519	18.876

Table 5.8: *Molar mass values for different O/F ratios*

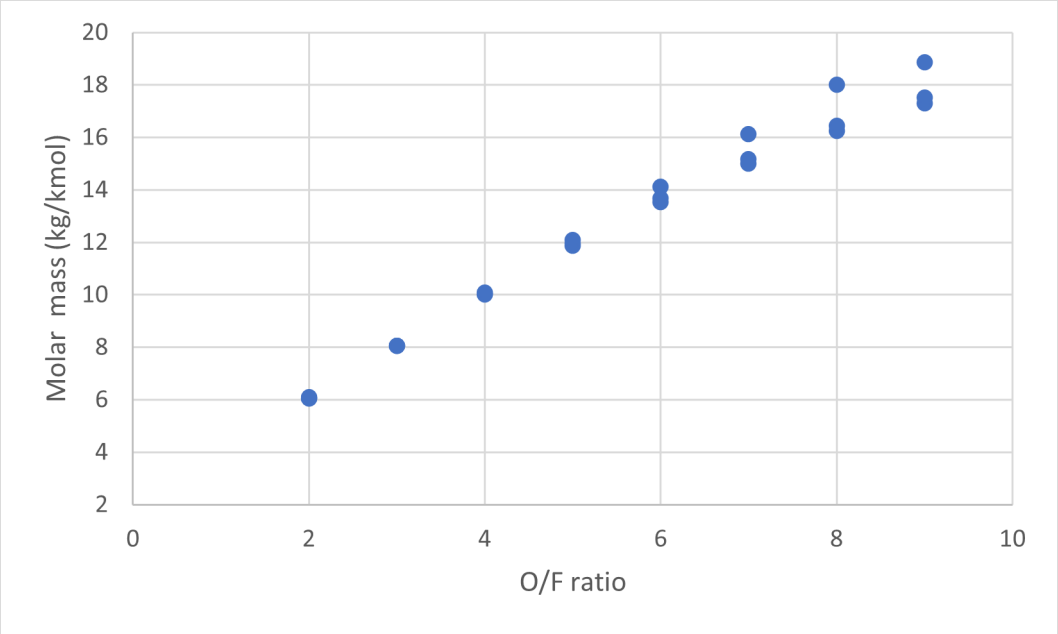

Figure 5.5: *Variation of molar mass for different O/F ratios*

From the fig. 5.5 the molar mass increases with an increase in mixture ratio, and also we can see different molar mass at the same mixture ratio because the molar mass varies from the chamber to exit conditions because we have chosen to shift equilibrium conditions in our CEA analysis which means during the expansion process from throat to the nozzle exit the recombination reactions are considered, so the molar mass increases from the combustion chamber to nozzle exit at the same mixture ratio.

By considering the effect of various parameters on mixture ratio, the choice of 6.1 as mixture ratio seemed reasonable for further analysis on LOX/LH_2 engine.

5.2.2 Chamber pressure

The conditions taken for the analysis are given in table 5.9:

Parameter	**Value**
Chamber pressure (bar)	20,40,60,80,100,120,140,160,180,200,220,240,260,280,300
Expansion ratio (A_e/A_t)	58.5
Fuel	Hydrogen (LH2)
Oxidizer	Oxygen (LOX)
Fuel temperature (K)	20
Oxidizer temperature (K)	90
O/F ratio	6.1

Table 5.9: *Parameters considered for CEA analysis*

Vacuum specific impulse variation with chamber pressure

Chamber pressure P_c (bar)	**Vacuum sp.impulse (m/s)**
20	4481.5
40	4490.6
60	4495.4
80	4498.5
100	4500.7
120	4502.5
140	4503.9
160	4505.1
180	4506.1
200	4507.0
220	4507.8
240	4508.4
260	4509.1
280	4509.6
300	4510.1

Table 5.10: *Vacuum specific impulse values for different chamber pressures*

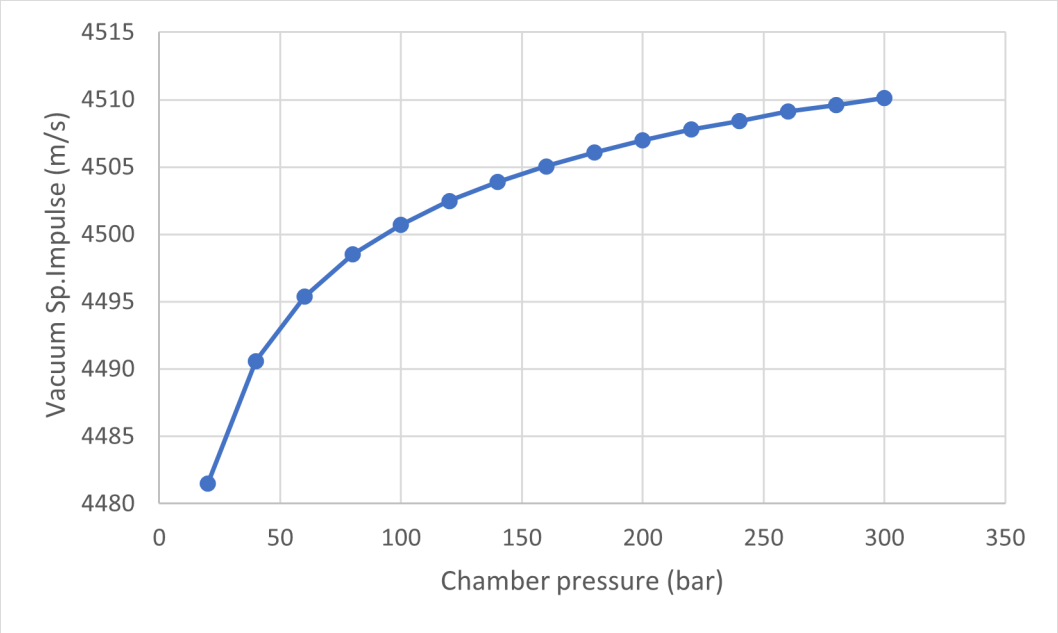

Figure 5.6: *Variation of vacuum specific impulse for different Chamber Pressures*

As mentioned previously, to clearly understand the chamber pressure effect on vacuum specific impulse analysis was done, which shows in fig. 5.6 the increase in vacuum specific impulse of was only about 20 for variation of chamber pressure of about 280 bar. It is because the specific impulse depends mainly on the O/F ratio, combustion temperature and molar mass.

Combustion temperature variation with chamber pressure

Chamber pressure P_c (bar)	Combustion temperature (K)
20	3352.0
40	3434.1
60	3481.1
80	3513.7
100	3538.6
120	3558.6
140	3575.2
160	3589.4
180	3601.8
200	3612.7
220	3622.5
240	3631.3
260	3639.3
280	3646.7
300	3653.5

Table 5.11: *Combustion temperature values for different chamber pressures*

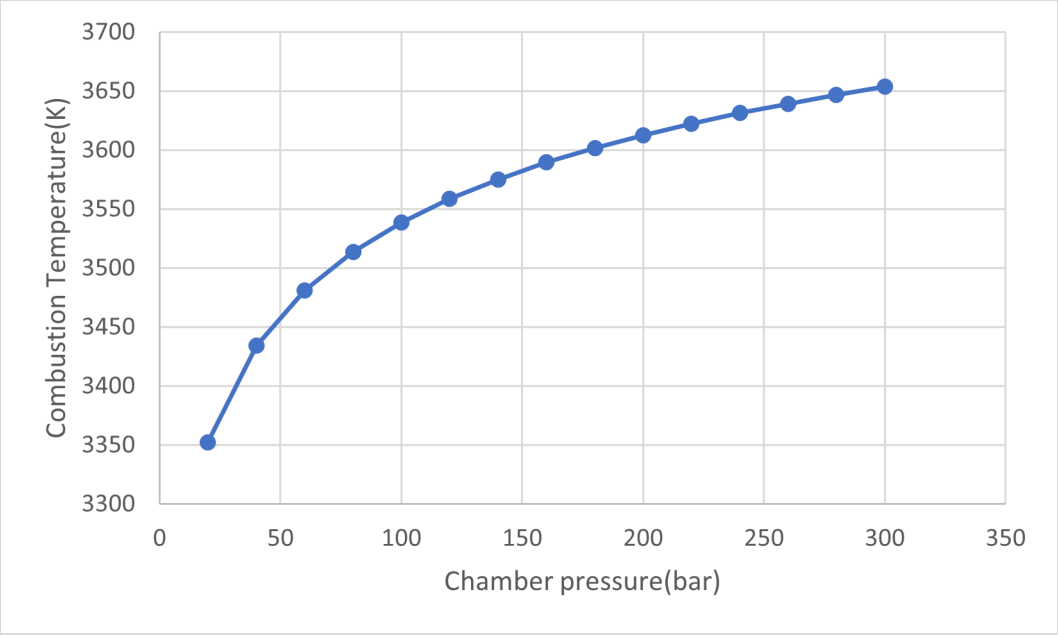

Figure 5.7: *Variation of combustion temperature for different chamber pressures*

Combustion temperature variation with chamber pressure follows the same trend as that of vacuum specific impulse. It increases with increased chamber pressure because the combustion products behave like an ideal fluid at such high temperatures. It is a characteristic feature of an ideal gas to increase the temperature with an increase in pressure.

Coefficient of thrust variation with chamber pressure

Chamber pressure P_c (bar)	Coefficient of thrust
20	1.8920
40	1.8848
60	1.8808
80	1.8780
100	1.8760
120	1.8743
140	1.8730
160	1.8718
180	1.8709
200	1.8700
220	1.8692
240	1.8685
260	1.8679
280	1.8673
300	1.8668

Table 5.12: *Coefficient of thrust values for different chamber pressures*

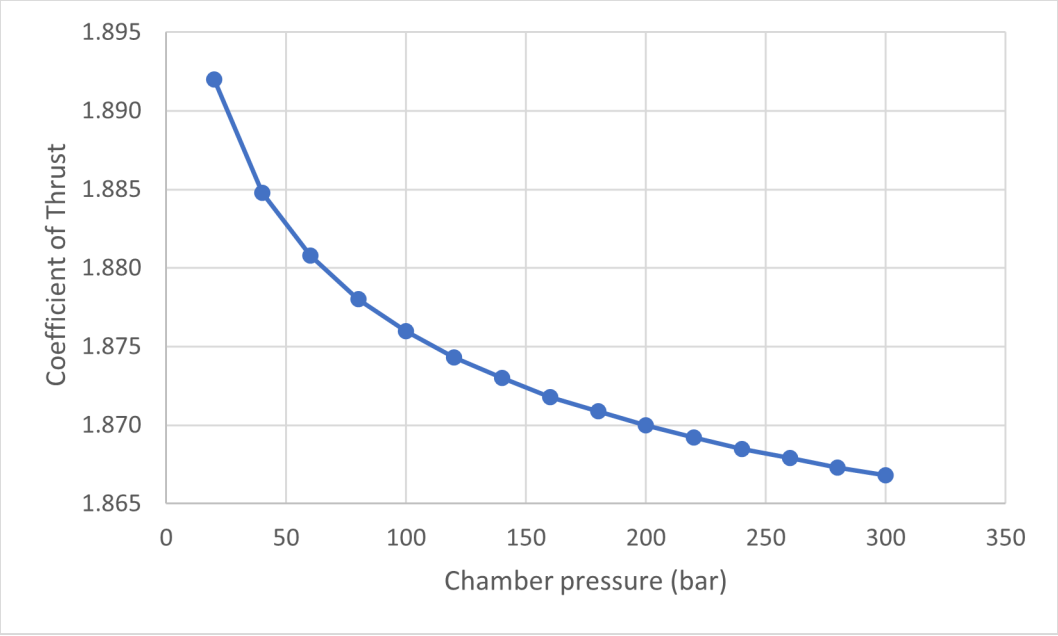

Figure 5.8: *Variation of coefficient of thrust for different chamber pressures*

From the fig. 5.8, we can see that coefficient of thrust curve has an inverse trend to chamber pressure increases because from eq. (5.11) the coefficient of thrust is inversely proportional to chamber pressure and curve see a sharp drop at lower pressures and at higher pressures the effect is less.

Characteristic velocity variation with chamber pressure

Chamber pressure P_c(bar)	**Characteristic velocity C* (m/s)**
20	2270.9
40	2285.9
60	2294.1
80	2299.6
100	2303.7
120	2307
140	2309.6
160	2311.9
180	2313.8
200	2315.5
220	2317
240	2318.3
260	2319.5
280	2320.6
300	2321.6

Table 5.13: *Characteristic velocity values for different chamber pressures*

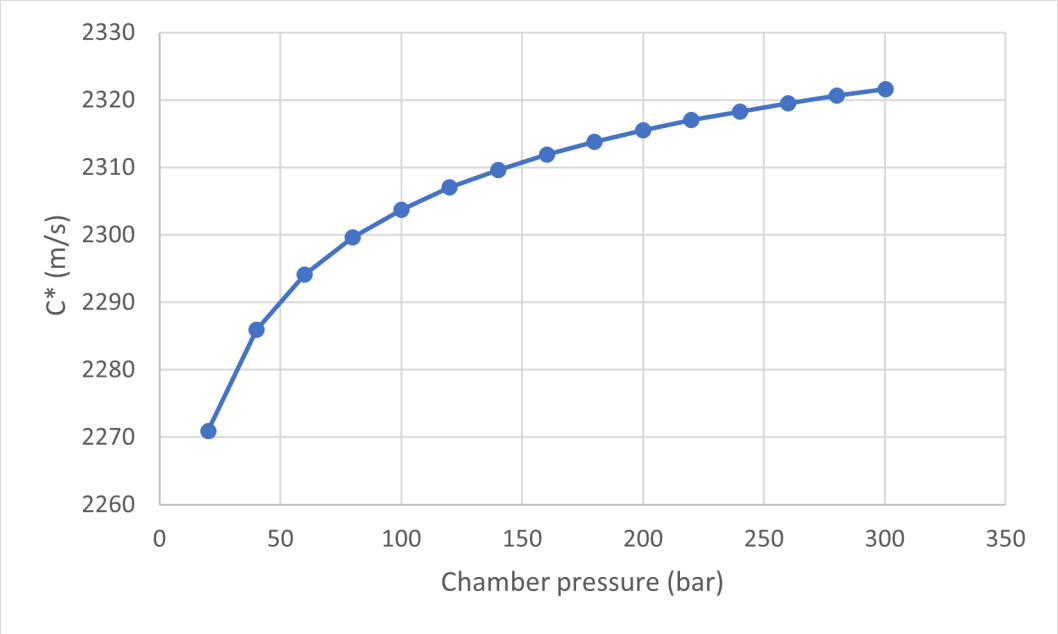

Figure 5.9: *Variation of Characteristic velocity for different chamber pressures*

From the fig. 5.9, C* varies just about 50m/s for chamber pressure variation of about 280 bar. We can deduce that the characteristic velocity obtained values are a weak form of the pressure value. It mainly depends on the thermodynamic properties of the propellant, and it is a function of the propellant considered.

5.2.3 Expansion ratio (A_e/A_t)

The conditions taken for the analysis are tabulated in table 5.14:

Parameter	Value
Chamber pressure (bar)	115
Expansion ratio (A_e/A_t)	10,20,30,40,50,60,70,80,90,100,120,140,160
Fuel	Hydrogen (LH2)
Oxidizer	Oxygen (LOX)
Fuel temperature (K)	20
Oxidizer temperature (K)	90
O/F mixture ratio	6.1

Table 5.14: *Parameters considered for CEA analysis*

Vacuum specific impulse variation with expansion ratio

Vacuum specific impulse dependence on expansion ratio is like that of chamber pressure. As shown in fig. 5.10 keeps increases with an increase in expansion ratio. Practical limits on expansion ratio limit the maximum performance that can be achieved. Here the possibility of shocks in the nozzle due to over-expansion is not taken into account.

Expansion ratio	Vacuum specific impulse (m/s)
10	4079.50
20	4274.20
30	4369.50
40	4430.00
50	4473.40
60	4506.60
70	4533.30
80	4555.30
90	4574.10
100	4590.20
120	4617.00
140	4638.40
160	4656.10

Table 5.15: *Vacuum specific impulse values for different expansion ratios*

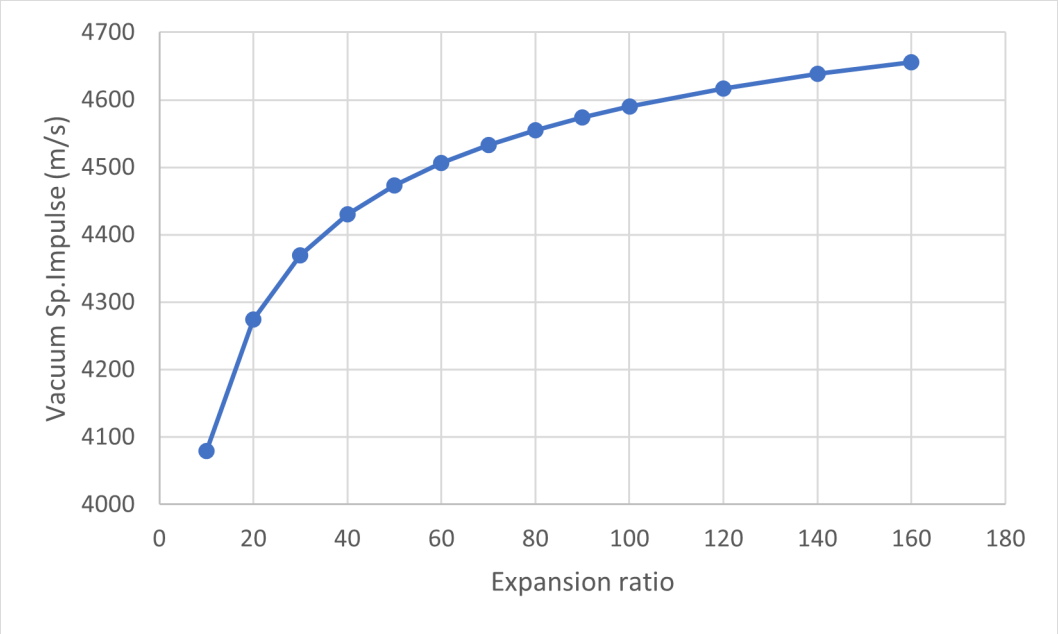

Figure 5.10: *Variation of vacuum specific impulse for different expansion ratios*

Coefficient of thrust variation with expansion ratio

As we can see in the fig. 5.11, the coefficient of thrust increases with an increase in expansion ratio because from the eq. (5.11), it depends on only expansion ratio and gamma value, and it is directly proportional to expansion ratio.

Expansion ratio	**Coefficient of thrust**
10	1.6326
20	1.7448
30	1.7992
40	1.8337
50	1.8584
60	1.8773
70	1.8925
80	1.905
90	1.9157
100	1.9249
120	1.9402
140	1.9524
160	1.9626

Table 5.16: *Coefficient of thrust values for different expansion ratios*

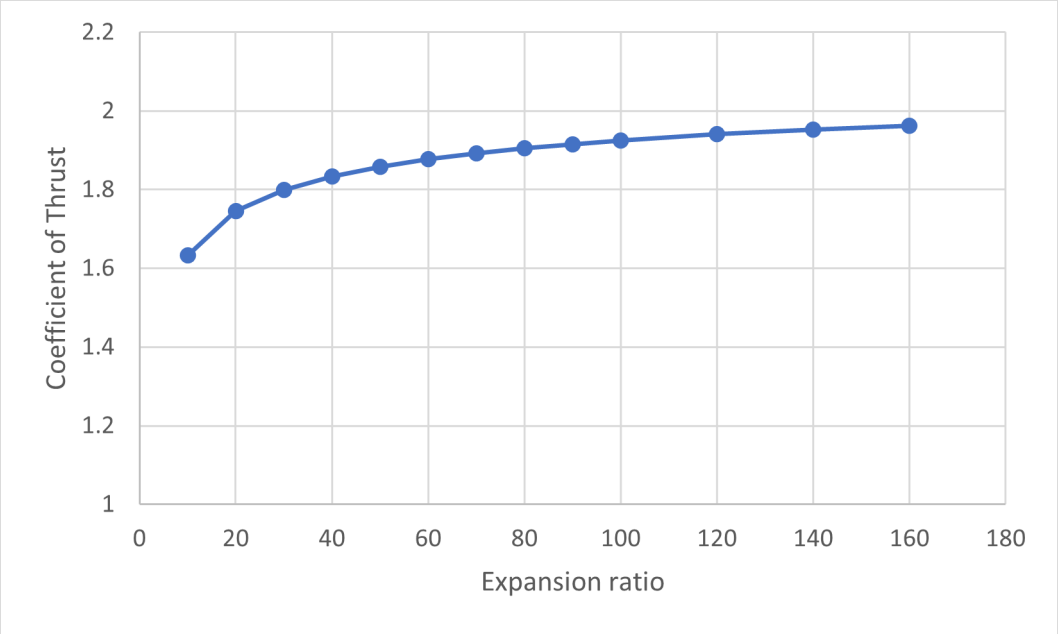

Figure 5.11: *Variation of Coefficient of thrust for different expansion ratios*

Characteristic velocity variation with expansion ratio

On the other hand, in the fig. 5.12, characteristic velocity is constant for variation in expansion ratio because characteristic velocity is a parameter of merit of the combustion chamber. So, it does not get affected by the change in expansion ratio.

Expansion ratio	**Characteristic velocity C* (m/s)**
10	2306.20
20	2306.20
30	2306.20
40	2306.20
50	2306.20
60	2306.20
70	2306.20
80	2306.20
90	2306.20
100	2306.20
120	2306.20
140	2306.20
160	2306.20

Table 5.17: *Characteristic velocity values for different expansion ratios*

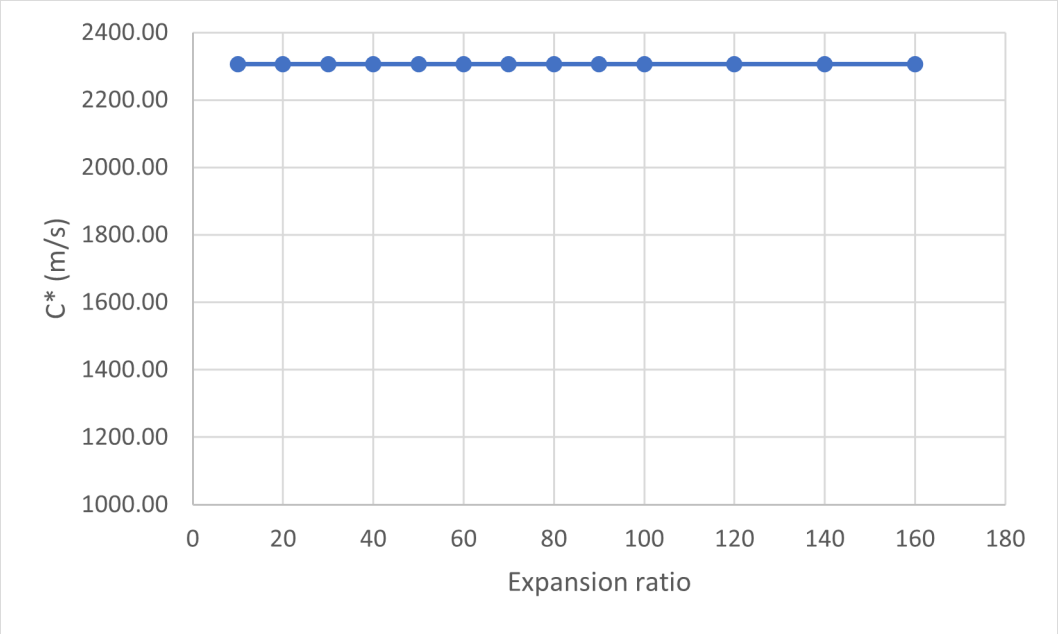

Figure 5.12: *Variation of characteristic velocity for different expansion ratios*

5.2.4 Combustion products

LOX/LH_2 propellant combination is perhaps the cleanest burning fuel. When we burn hydrogen with oxygen, we get water vapour. The conditions taken for the analysis are tabulated in table 5.18

Parameter	**Value**
Chamber pressure (P_c) (bar)	115
Expansion ratio (A_e/A_t)	58.5
Fuel	Hydrogen (LH2)
Oxidizer	Oxygen (LOX)
Fuel temperature (K)	20
Oxidizer temperature (K)	90
O/F mixture ratio	6.1

Table 5.18: *Parameters considered for CEA analysis*

From the diagram, we can see that the products are mostly H_2O and a small amount of H_2^* icons. However, apart from these products, there will be a trace amount of nitrogen oxides (NO_x) while the vehicle is in the lower atmosphere, otherwise known as the troposphere, as an after-burning effect of the hot flame coming in contact with the air. All rocket engines will do this to a certain degree when in our troposphere, which is primarily composed of nitrogen.

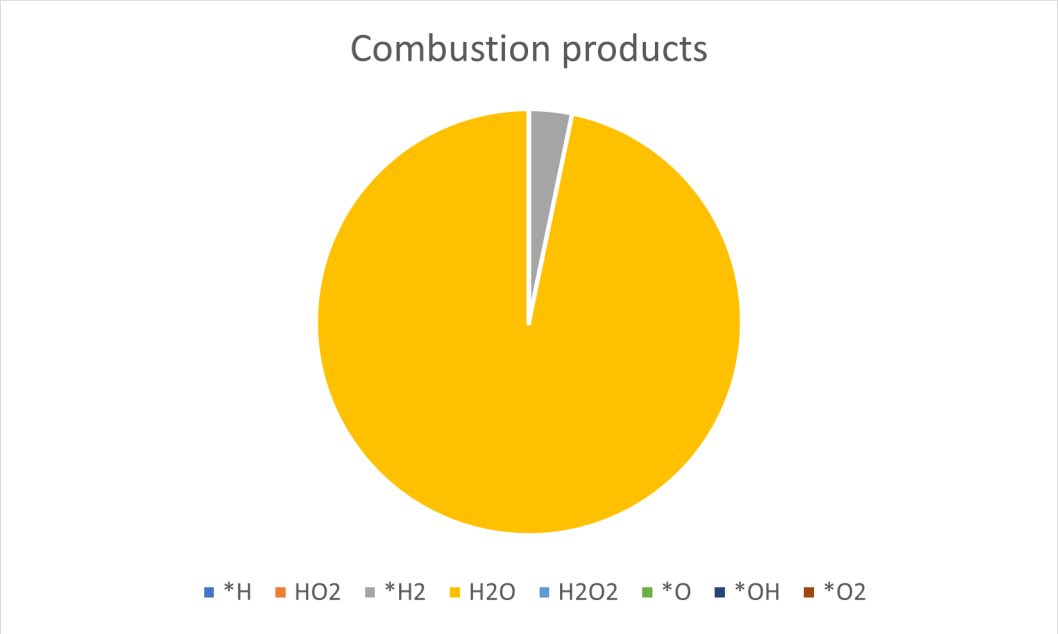

Figure 5.13: *Combustion products of LOX/LH_2*

5.2.5 Masses and volumes

Mass and volumes for core stage LOX/LH_2 engine

Core stage Ariane 5 produces a total impulse of 729000 KN-s, assuming constant thrust and very short start and stop time transients. This value is used as the starting point to calculate mass and volumes for all the different propellant combinations considered in this thesis for core stage engines. At this point, we have the required information from CEA analysis and reference engine data listed in table 5.19 to calculate the thrust(t) and burnout time (t_b) and area of the throat (A_t).

Parameters	Specification values
Vacuum specific impulse (s)	458.9
Expansion ratio (A_e/A_t)	58.5
Exit diameter (d_e) (m)	2.15
O/F ratio	6.1
Coefficient of thrust (C_t)	1.8747
Chamber pressure (P_c) (bar)	115
Density of fuel (kg/m^3)	70
Density of oxidizer (kg/m^3)	1140

Table 5.19: *Input values from CEA analysis*

Methodology

1. To find the throat area (A_t), we use the eq. (5.13).

2. Using area of throat (A_t), chamber pressure (P_c) and coefficient of thrust (C_t) from the eq. (5.10) we get the thrust (t).

3. From the thrust(T) we got and the assumed total impulse at the beginning and using the eq. (5.5) we get our burn time (t_b).

4. Now, the total mass flow of the propellant can be calculated by solving eq. (5.15) and using acquired Ispv and thrust obtained.

5. By using total propellant mass flow rate and mixture ratio, we get the oxidizer and fuel mass flow rates from eq. (5.18) and eq. (5.19)

6. Multiplying these mass flow rates with the obtained burn time (t_b) and adding 5% extra for safety purposes, we get the masses of oxidizer and fuel.

7. Dividing these mass with respective densities, we get volumes of oxidizer and fuel. An extra 10% is added to these volumes to get the volumes of the tanks.

Masses and volumes obtained by using the above methodology are listed in table 5.20:

Parameter	**Values**
Mass of oxidizer(LOX) (kgs)	146089
Mass of fuel (kgs)	23949
Total mass of propellant (kgs)	170038
Volume of oxidizer (m^3)	128
Volume of fuel (m^3)	342
Volume of oxidizer tank (m^3)	141
Volume of fuel tank (m^3)	376
Total volume of tanks (m^3)	517

Table 5.20: *Core mass and volumes of LOX/LH$_2$*

Mass and volumes for booster stage LOX/LH_2 engine

Booster stage Ariane 5 produces a total impulse of 991200 KN-s, assuming constant thrust and very short start and stop time transients. This value is used as the starting point to calculate mass and volumes for all the different propellant combinations done in the next sections for booster stage engines.

Using the same parameters in the table 5.19 and by the same methodology, we get the mass and volumes for the booster stage. To compare these values with actual Ariane 5 booster values in the next sections, mass and volumes of oxidizer and fuel both are added, and just the total masses and volumes are listed in the table 5.21

Parameter	**Values**
Total mass of propellant (kgs)	231195
Total volume of tanks (m^3)	703

Table 5.21: *Booster mass and volumes of LOX/LH$_2$*

5.3 LOX/RP-1 ENGINE

Much experience with LOX/Kerosene engines available in the USA, in Russia and also former experience in Europe, leading up to some well-known operational engines like the F-1 engine in the Saturn V and the Rd-170/RD-180/RD-191 engine family in Russia. LOX/Kerosene propellant combination has the advantage of ambient storability and high density. However, its cooling capabilities are inferior to methane for conventional thrust chamber design. A countermeasure is to reduce the heat flux by introducing film-cooling or applying a thermal barrier coating to the liner hot gas side as mentioned in the section 4.2. This section aims to understand how LOX/Kerosene propellant combination works as a replacement of LOX/LH_2. Different performance parameters and their variations are studied. NASA CEA analysis is performed as before with the same initial parameters of LOX/LH_2 engine.

5.3.1 O/F ratio

The combustion reaction between kerosene and oxygen can be represented as follows :

$$2C_{12}H_{26}(l) + 37O_2(g) \rightarrow 24CO_2(g) + 26H_2O(g) \tag{5.25}$$

The stoichiometric O/F ratio is equal to 3.7. However, the best operative mixture ratio for high-performance rocket engines ranges between 2.5 to 3.5. To find the best O/F ratio, NASA CEA nested analysis was done considering different performance parameters.

The conditions taken for the analysis are tabulated below:

Parameter	Value
Chamber pressure (bar)	115
Expansion ratio (A_e/A_t)	58.5
Fuel	Kerosene (RP1)
Oxidizer	Oxygen (LOX)
Fuel temperature (K)	298
Oxidizer temperature (K)	90
O/F ratio	2,3,4,5,6,7,8,9

Table 5.22: *Parameters considered for CEA analysis*

Variation of vacuum specific impulse for different O/F ratios

The below fig. 5.14 depicts that maximum vacuum specific impulse is achieved around 2 to 4. Further analysis was carried out and found that at 2.8 O/F ratio, LOX/KEROSENE propellant combination has the highest maximum vacuum specific impulse.

O/F	Vacuum sp.impulse (m/s)
2	3385.8
3	3580.5
4	3410.5
5	3229.9
6	3060.3
7	2906.4
8	2768.8
9	2646.1

Table 5.23: *Vacuum specific impulse values for different O/F ratios*

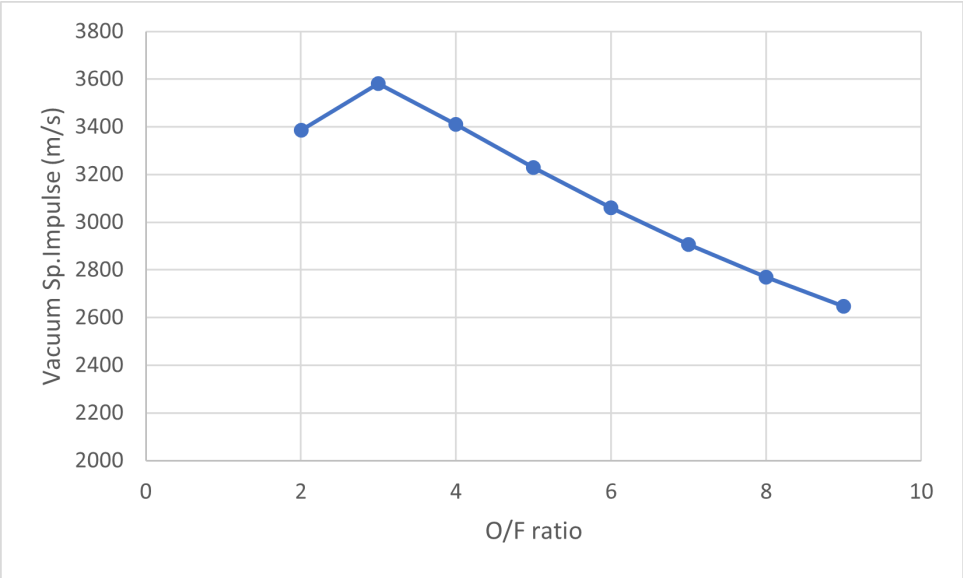

Figure 5.14: *Variation of vacuum specific impulse for different O/F ratios*

Variation of vacuum specific impulse for different chamber pressures at different O/F ratios

Vacuum specific impulse (m/s)								
O/F	P_c 20 bar	P_c 40 bar	P_c 60 bar	P_c 80 bar	P_c 100 bar	P_c 120 bar	P_c 150 bar	P_c 200 bar
2	3380.2	3382.8	3384.1	3384.9	3385.4	3385.9	3386.4	3386.9
3	3528.6	3550.2	3562.3	3570.5	3576.7	3581.6	3587.5	3594.8
4	3359.5	3380.4	3392.2	3400.4	3406.6	3411.6	3417.6	3425.2
5	3196.4	3210.6	3218.4	3223.6	3227.5	3230.7	3234.3	3238.9
6	3040.6	3049.1	3053.6	3056.7	3058.9	3060.7	3062.8	3065.4
7	2894.8	2899.8	2902.5	2904.3	2905.6	2906.6	2907.8	2909.3
8	2762	2765	2766.6	2767.6	2768.3	2768.9	2769.6	2770.5
9	2642.1	2643.9	2644.8	2645.4	2645.8	2646.2	2646.6	2647

Table 5.24: *Vacuum specific impulse values for different chamber pressures at different O/F ratios*

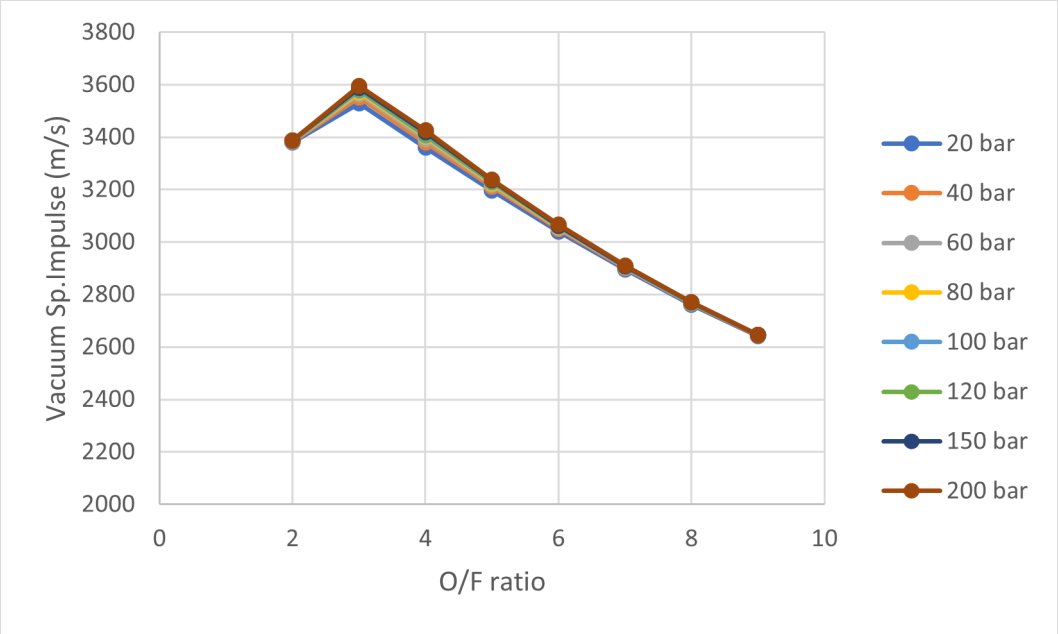

Figure 5.15: *Variation of vacuum specific impulse for different chamber pressures at different O/F ratios*

Analysis was done to determine the effect of mixture ratio on vacuum specific impulse at different chamber pressures (20 bar, 40 bar, 60bar, 80 bar, 100 bar, 120 bar, 150 bar, 200 bar) by keeping the expansion ratio constant at 58.5

The above fig. 5.15 shows that vacuum specific impulse increases slightly with increase in chamber pressure because for higher chamber pressures, combustion temperature increases which is directly proportional to specific impulse.

Variation of vacuum specific impulse for different expansion ratios at different O/F ratios

Vacuum specific impulse (m/s)							
O/F	**ε 20**	**ε 50**	**ε 75**	**ε 100**	**ε 125**	**ε 150**	**ε 200**
2	3234	3366.4	3414.7	3445.9	3468.7	3486.4	3513
3	3355.2	3550.9	3625.1	3673.5	3708.7	3736	3776.8
4	3191.6	3381.4	3454.7	3503.2	3538.9	3566.9	3608.8
5	3036.4	3204.9	3267.6	3308.2	3337.7	3360.5	3394.4
6	2892.6	3038.9	3092.3	3126.6	3151.3	3170.5	3198.7
7	2758.8	2887.7	2934.2	2964	2985.4	3001.9	3026.1
8	2636.4	2752.1	2793.6	2820	2838.9	2853.4	2874.6
9	2525.5	2631	2668.5	2692.3	2709.2	2722.2	2741.2

Table 5.25: *Vacuum specific impulse values for different expansion ratios at different O/F ratios*

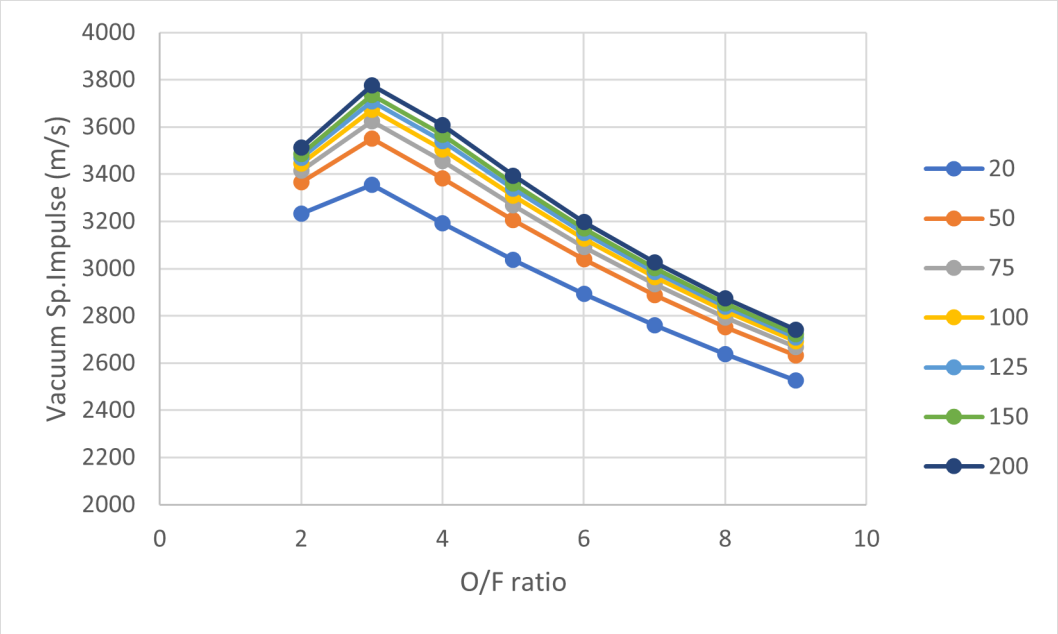

Figure 5.16: *Variation of vacuum specific impulse for different expansion ratios at different O/F ratios*

To understand how the expansion ratio is affecting the vacuum specific impulse vs mixture ratio, analysis was done at different expansion ratios (20,50,75,100,125,150,200) by keeping chamber pressure constant at 115 bar. Similar to LOX/LH_2 case, for higher expansion ratios, a higher vacuum specific impulse is achieved.

Variation of combustion temperature and molar mass for different O/F ratios

As mentioned in the LOX/LH_2 case vacuum specific impulse is not the only criteria for deciding the O/F ratio. Analysis was done to study the variation of combustion temperature and molar mass for different mixture ratios, as shown in the below graphs.

O/F	Combustion temperature (K)
2	3370.3
3	3779.8
4	3703.7
5	3572.1
6	3427.8
7	3278.6
8	3127.1
9	2975.2

Table 5.26: *Combustion temperature values for different O/F ratios*

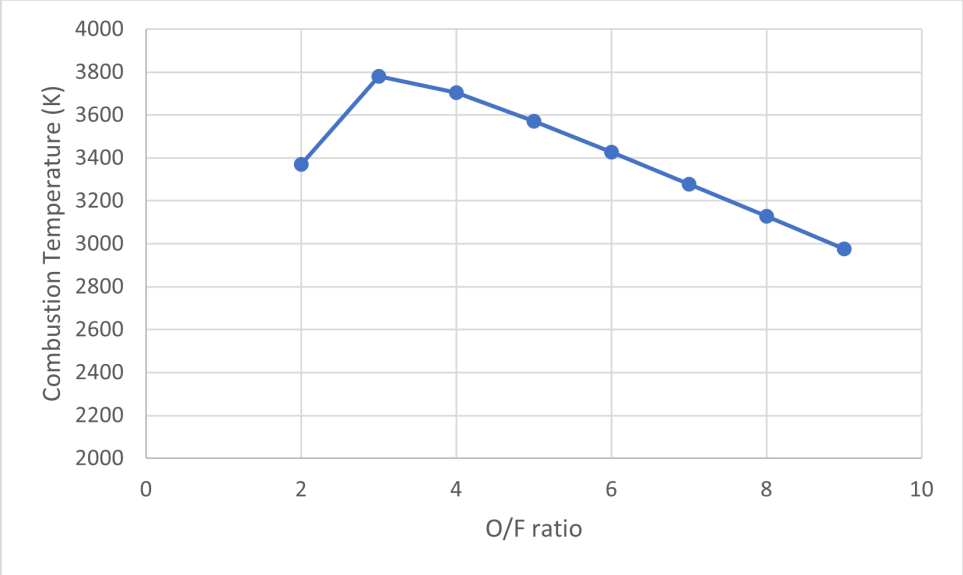

Figure 5.17: *Variation of combustion temperature for different O/F ratios*

Molar mass (kg/kmol)			
O/F	**Chamber**	**Throat**	**Exit**
2	20.894	21.027	21.231
3	24.904	25.265	28.230
4	27.104	27.486	30.851
5	28.566	28.933	31.360
6	29.583	29.916	31.475
7	30.295	30.582	31.541
8	30.790	31.023	31.591
9	31.129	31.306	31.631

Table 5.27: *Molar mass values for different O/F ratios*

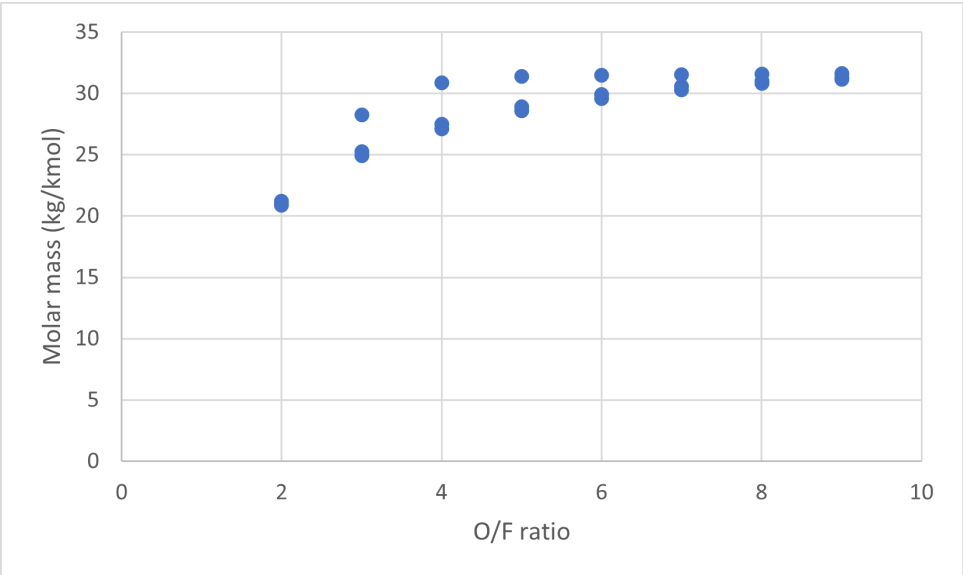

Figure 5.18: *Variation of molar mass for different O/F ratios*

From the fig. 5.17, the maximum combustion temperature is achieved around the stoichiometric value. However, the optimum O/F ratio is not one with the highest combustion temperature. The combustion temperature curve shows a decreasing trend for higher O/F values.

From the fig. 5.18, molar mass shows different values at different sections of the combustion and nozzle for the same O/F ratio. At the nozzle exit section, molar mass increases due to the recombination reactions considered for the shifting equilibrium case. The molar mass shows an increasing trend for O/F ratio variation.

By taking into all the different performance parameters variation with O/F ratio, an optimum O/F value of 2.8 is choose for LOX/KEROSENE engine.

5.3.2 Chamber pressure

The conditions taken for the analysis are tabulated below:

Parameter	Value
Chamber pressure (bar)	20,40,60,80,100,120,140,160,180,200,220,240,260,280,300
Expansion ratio (A_e/A_t)	58.5
Fuel	Kerosene (RP1)
Oxidizer	Oxygen (LOX)
Fuel temperature (K)	298
Oxidizer temperature (K)	90
O/F mixture ratio	2.8

Table 5.28: *Parameters for CEA analysis*

Vacuum specific impulse variation with chamber pressure

Chamber pressure P_c (bar)	Vacuum specific impulse (m/s)
20	3546.8
40	3564.0
60	3573.3
80	3579.5
100	3584.1
120	3587.8
140	3590.8
160	3593.3
180	3595.5
200	3597.4
220	3599.1
240	3600.6
260	3602.0
280	3603.3
300	3604.4

Table 5.29: *Vacuum specific impulse values for different chamber pressures*

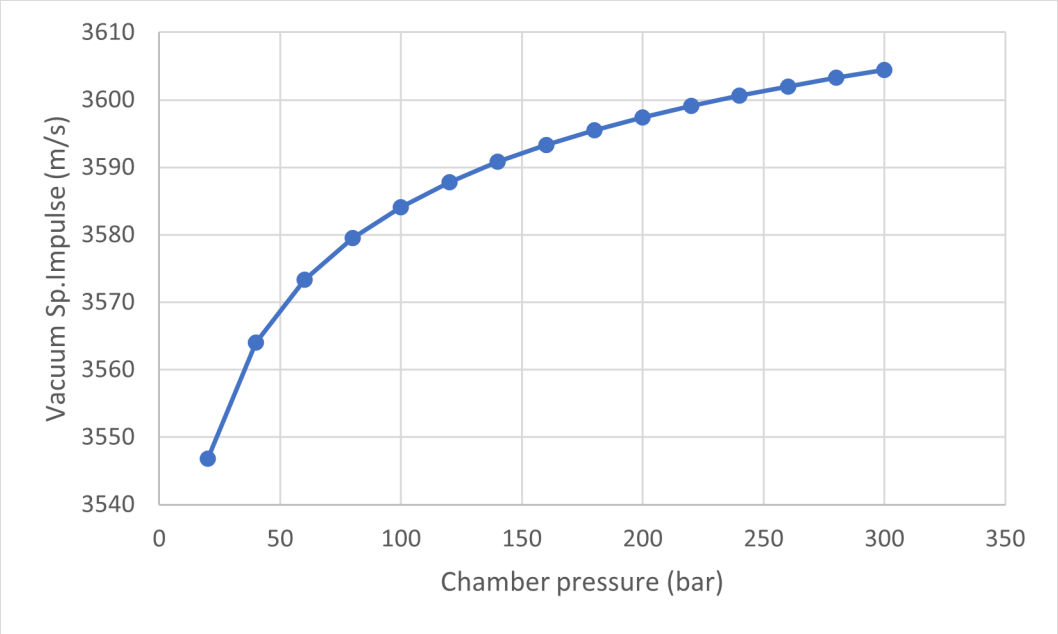

Figure 5.19: *Variation of vacuum specific impulse for different chamber pressures*

The fig. 5.19 shows the effect of chamber pressure on the vacuum specific impulse. It shows an increasing trend, but the effect of chamber pressure seemed less, as also shown in the fig. 5.15, because the specific impulse depends mostly on O/F ratio, combustion temperature and molar mass.

Combustion temperature variation with chamber pressure

Chamber pressure P_c (bar)	**Combustion temperature (K)**
20	3508.7
40	3611.6
60	3672.8
80	3716.4
100	3750.5
120	3778.3
140	3802.0
160	3822.4
180	3840.5
200	3856.7
220	3871.3
240	3884.7
260	3896.9
280	3908.3
300	3918.9

Table 5.30: *Combustion temperature values for different chamber pressures*

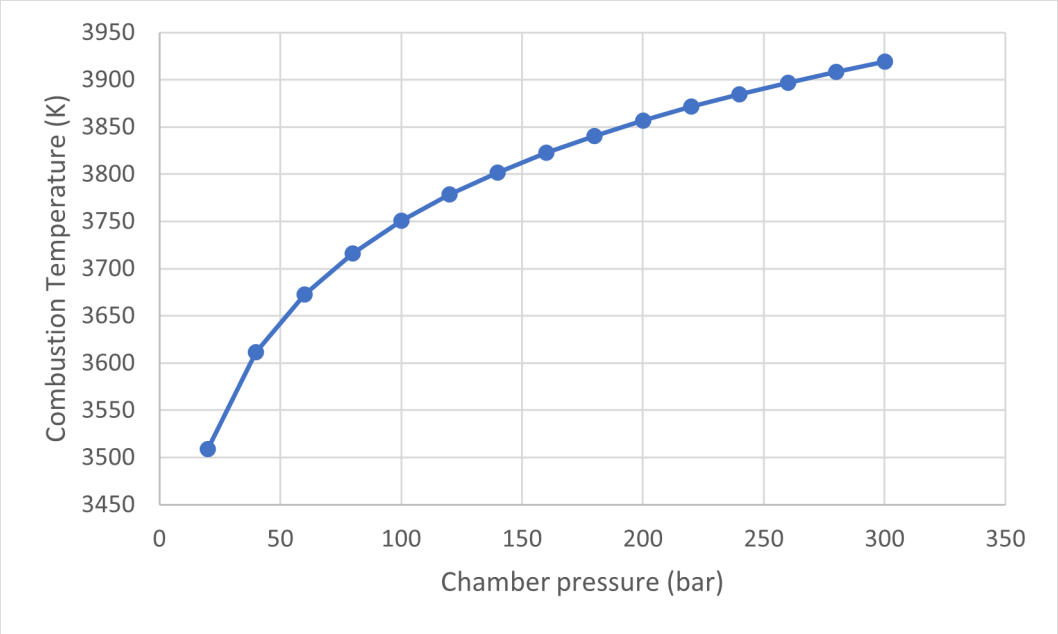

Figure 5.20: *Variation of combustion temperature for different chamber pressures*

The fig. 5.20 shows the combustion temperature variation with the chamber pressure, which is similar to that of a vacuum specific impulse. Combustion temperature increases with increase in chamber pressure because the combustion products behave like an ideal fluid at such high temperatures. It is a characteristic feature of an ideal gas to increase the temperature with an increase in pressure.

Coefficient of thrust variation with chamber pressure

Chamber pressure P_c (bar)	**Coefficient of thrust**
20	1.9237
40	1.9194
60	1.9165
80	1.9144
100	1.9127
120	1.9112
140	1.9100
160	1.9089
180	1.9079
200	1.9070
220	1.9062
240	1.9055
260	1.9048
280	1.9042
300	1.9036

Table 5.31: *Coefficient of thrust values for different chamber pressures*

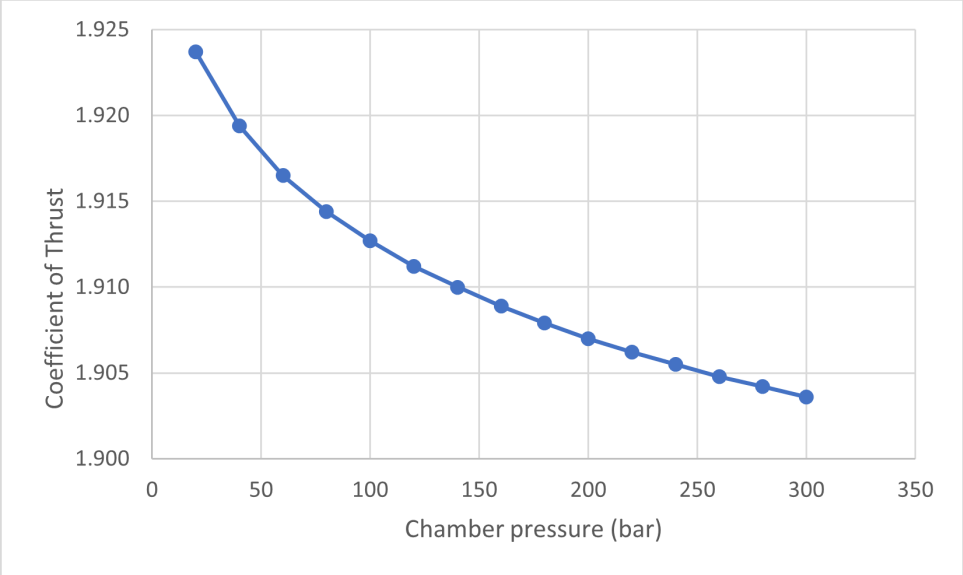

Figure 5.21: *Variation of coefficient of thrust for different chamber pressures*

The fig. 5.21 shows the coefficient of thrust variation with the chamber pressure, which reduces with the increase in chamber pressure. Chamber pressure has a very minimal effect on the coefficient of thrust because it is primarily a parameter of the merit of a nozzle.

Characteristic velocity variation with chamber pressure

Chamber pressure P_c (bar)	**Characteristic velocity (m/s)**
20	1750.3
40	1765.3
60	1774
80	1780
100	1784.7
120	1788.4
140	1791.6
160	1794.3
180	1796.6
200	1798.7
220	1800.6
240	1802.3
260	1803.9
280	1805.4
300	1806.7

Table 5.32: *Characteristic velocity values for different chamber pressures*

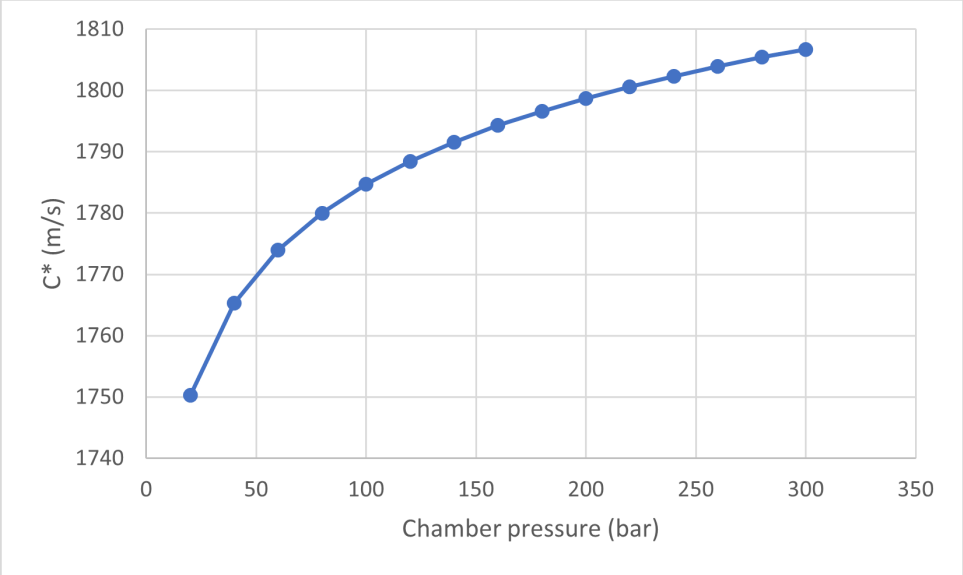

Figure 5.22: *Variation of characteristic velocity for different chamber pressures*

The fig. 5.22 shows the characteristic velocity variation with chamber pressure which increases with an increase in chamber pressure. From the variation in characteristic velocity, we can say it is a weak form of chamber pressure values.

5.3.3 Expansion ratio (A_e/A_t)

The conditions taken for the analysis are tabulated in table 5.33:

Parameter	Value
Chamber pressure (bar)	115
Expansion ratio (A_e/A_t)	10,20,30,40,50,60,70,80,90,100,120,140,160
Fuel	Kerosene (RP1)
Oxidizer	Oxygen (LOX)
Fuel temperature (K)	298
Oxidizer temperature (K)	90
O/F mixture ratio	2.8

Table 5.33: *Parameters considered for CEA analysis*

Vacuum specific impulse variation with expansion ratio

From the fig. 5.23, which shows the variation of vacuum specific impulse for different expansion ratios. Vacuum specific impulse dependence on expansion ratio is like that of chamber pressure. It keeps increasing with an increase in expansion ratio. Therefore, practical limits on expansion ratio limit the maximum performance that can be achieved.Here the possibility of shocks in the nozzle due to over-expansion is not taken into account.

Expansion ratio	Vacuum specific impulse (m/s)
10	3202.10
20	3375.40
30	3462.60
40	3518.90
50	3559.70
60	3591.20
70	3616.70
80	3637.90
90	3656.00
100	3671.80
120	3698.00
140	3719.30
160	3737.00

Table 5.34: *Vacuum specific impulse values for different expansion ratios*

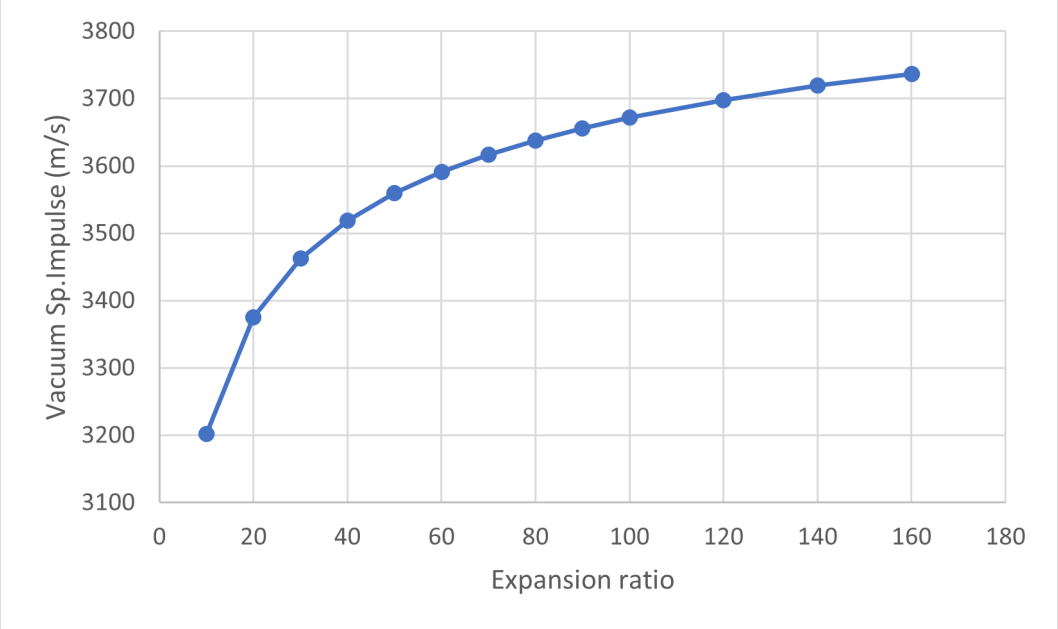

Figure 5.23: *Variation of vacuum specific impulse for different expansion ratios*

Coefficient of thrust variation with expansion ratio

Effect of expansion ratio on coefficient of thrust is shown in the fig. 5.24, it shows that Ct increases with increase in expansion ratio because from the eq. (5.11), it depends on only expansion ratio and gamma value and it is directly proportional to expansion ratio.

Expansion ratio	Coefficient of thrust
10	1.6380
20	1.7611
30	1.8232
40	1.8633
50	1.8922
60	1.9146
70	1.9327
80	1.9477
90	1.9605
100	1.9716
120	1.9901
140	2.0051
160	2.0176

Table 5.35: *Coefficient of thrust values for different expansion ratios*

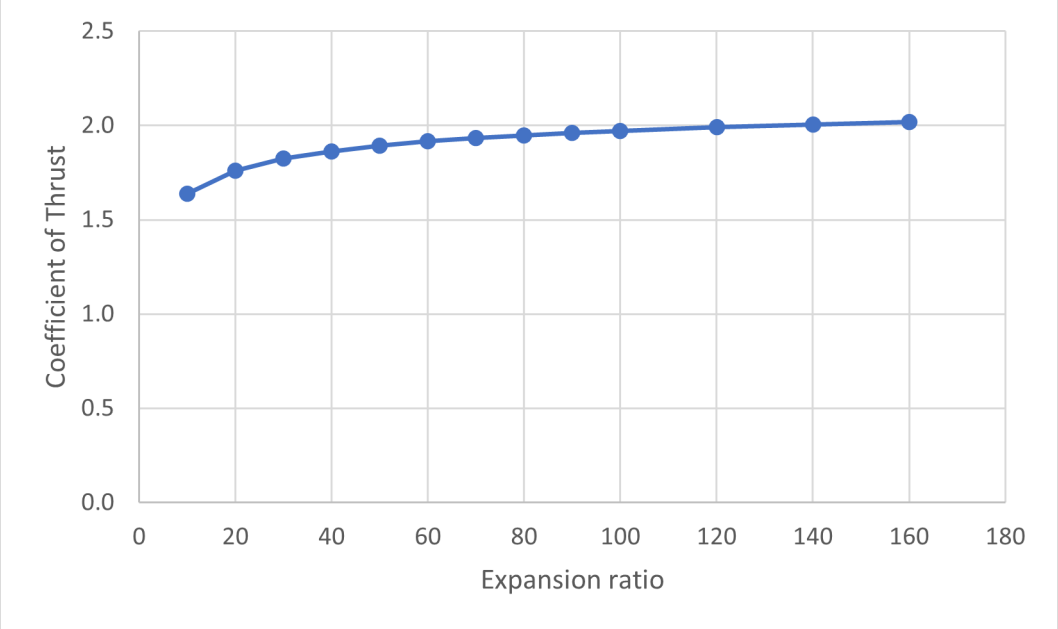

Figure 5.24: *Variation of coefficient of thrust for different expansion ratios*

Characteristic velocity variation with expansion ratio

Characteristic velocity variation with expansion ratio is shown in the fig. 5.25. As it is a parameter of merit of the combustion chamber, the expansion ratio will not have any effect on it,which can be seen by the constant curve.

Expansion ratio	Characteristic velocity
10	1787.60
20	1787.60
30	1787.60
40	1787.60
50	1787.60
60	1787.60
70	1787.60
80	1787.60
90	1787.60
100	1787.60
120	1787.60
140	1787.60
160	1787.60

Table 5.36: *Characteristic velocity values for different expansion ratios*

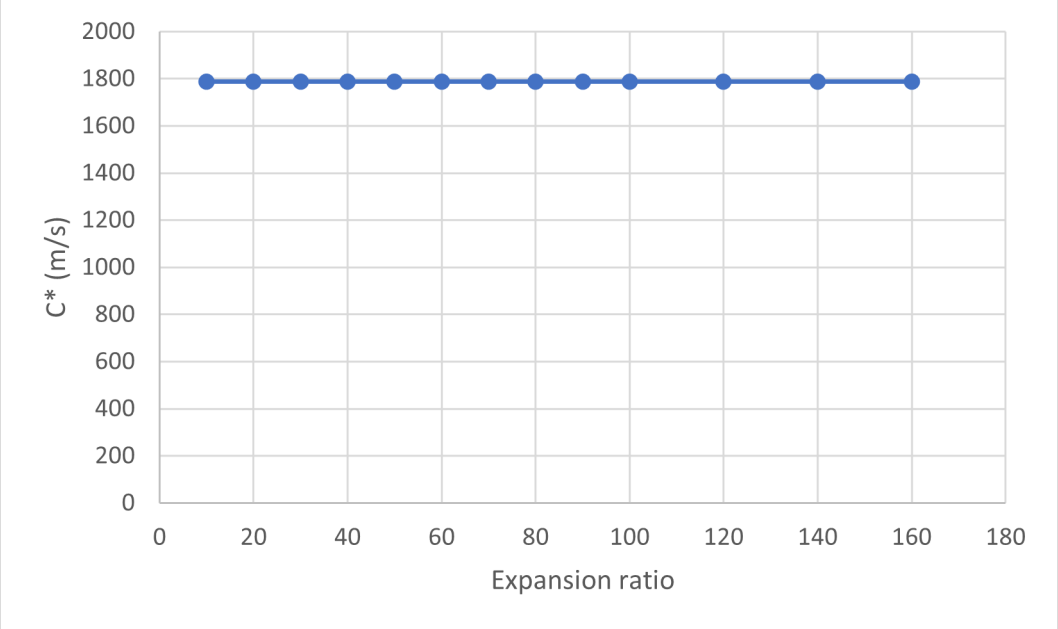

Figure 5.25: *Variation of characteristic velocity for different expansion ratios*

5.3.4 Combustion products

The conditions taken for the analysis are tabulated below:

Parameter	Value
Chamber pressure (bar)	115
Expansion ratio (A_e/A_t)	58.5
Fuel	Kerosene (LH2)
Oxidizer	Oxygen (LOX)
Fuel temperature (K)	298
Oxidizer temperature (K)	90
O/F mixture ratio	2.8

Table 5.37: *Parameters considered for CEA analysis*

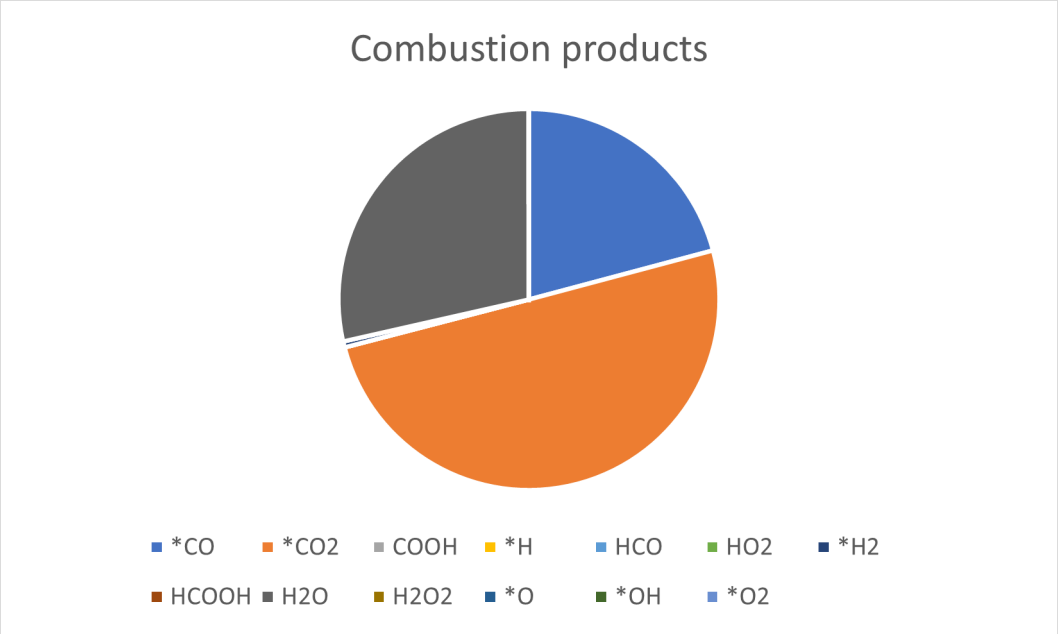

Figure 5.26: *Combustion products of LOX/RP-1*

From the above figure, we can say that RP-1 will mainly produce CO2, water vapour, carbon soot, carbon monoxide, which again mostly becomes CO2 and a few sulfur compounds. So the exhaust products from a LOX/KEROSENE engine it is not that different from what a regular internal combustion car produces, just a whole lot of it at once.

5.3.5 Masses and volumes

Taking the same assumptions made in the case of LOX/LH_2 engine and using the results of LOX/KEROSENE case from CEA analysis which are tabulated below.

Parameters	**Specification values**
Vacuum specific impulse (s)	365.6
Expansion ratio (A_e/A_t)	58.5
Exit diameter (d_e) (m)	2.15
O/F ratio	2.8
Coefficient of thrust (C_t)	1.9116
Chamber pressure (P_c) (bar)	115
Density of fuel (kg/m^3)	820
Density of oxidizer (kg/m^3)	1140

Table 5.38: *Input values from CEA analysis*

Mass and volumes for core stage LOX/KEROSENE engine

Masses and volumes obtained by using the same methodology as in section 5.2.5 are listed below

Parameter	**Value**
Mass of oxidizer(LOX) (kgs)	157261
Mass of fuel (kgs)	56165
Total mass of propellant (kgs)	213425
Volume of oxidizer (m^3)	138
Volume of fuel (m^3)	68
Volume of oxidizer tank (m^3)	152
Volume of fuel tank (m^3)	75
Total volume of tanks (m^3)	227

Table 5.39: *Core mass and volumes of LOX/RP-1*

Mass and volumes for booster stage LOX/KEROSENE engine

Using the same parameters in the table 5.38 and by the same methodology, we get the mass and volumes for the booster stage. Mass and volumes of oxidizer and fuel both are added, and just the total masses and volumes are listed in the below table.

Parameter	Value
Total mass of propellant (kgs)	290188
Total volume of tanks (m^3)	309

Table 5.40: *Booster mass and volumes of LOX/RP-1*

5.4 LOX/LCH_4 ENGINE

LOX/Methane appears to be a good choice for the current Ariane 5 launcher due to its expected good performance. Cooling capacity, low soot production, and reasonable material compatibility. Similar to the above cases, different performance parameters are analysed for LOX/LCH_4 propellant combinations.

5.4.1 O/F ratio

The chemical reaction between methane and oxygen gives us water and carbon dioxide as shown below:

$$CH_4 + 2O_2 \rightarrow CO_2 + 2H_2O \tag{5.26}$$

From the above combustion reaction, given the molecular weight of CH_4 is 16 and that of O_2 is 32, we have a stoichiometric mixture ratio of about 4. The optimum mixture ratio typically delivers the highest engine performance (measured by specific impulse). Investigation of different parameters for various mixture ratios is done. Taking the following conditions:

Parameter	**Value**
Chamber pressure (bar)	115
Expansion ratio (A_e/A_t)	58.5
Fuel	Methane (LCH4)
Oxidizer	Oxygen (LOX)
Fuel temperature (K)	112
Oxidizer temperature (K)	90
O/F ratio	2,3,4,5,6,7,8,9

Table 5.41: *Parameters considered for CEA analysis*

Variation of vacuum specific impulse for different O/F ratios

O/F	**Vacuum specific impulse (m/s)**
2	3281.9
3	3646.4
4	3644.1
5	3446.1
6	3259.8
7	3094.3
8	2948.0
9	2818.2

Table 5.42: *Vacuum specific impulse values for different O/F ratios*

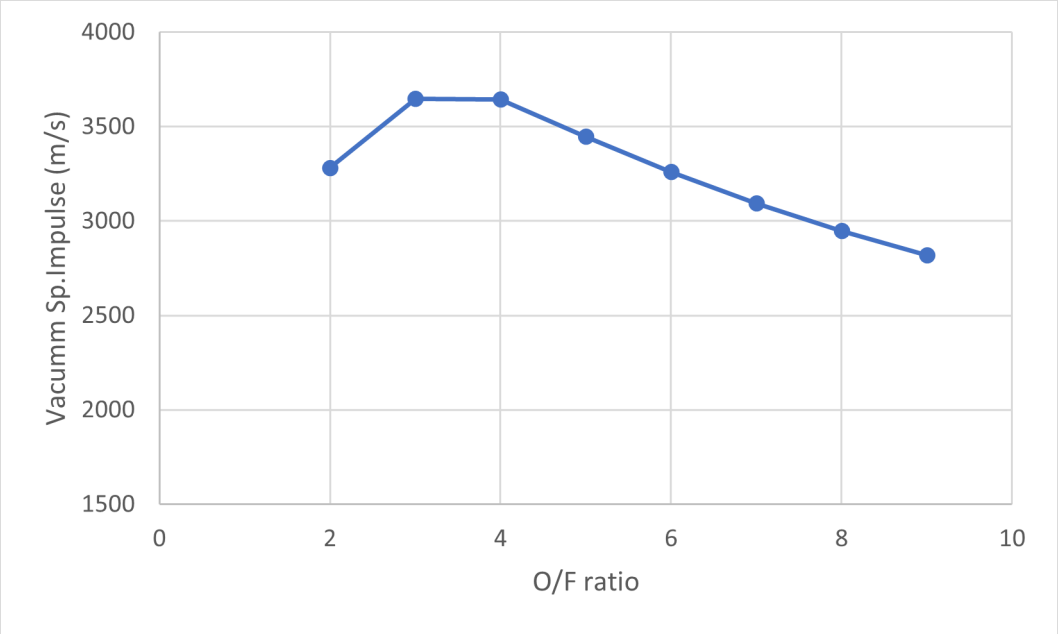

Figure 5.27: *Variation of vacuum specific impulse for different O/F ratios*

The above fig. 5.27 illustrates the effect of different mixture ratios on vacuum specific impulse. The maximum vacuum specific impulse values were found in the range of 2.5 to 4. Further CEA analysis was done for these mixture ratios and found at a mixture ratio of 3.5 vacuum specific impulse is maximum.

Variation of vacuum specific impulse for different chamber pressures at different O/F ratios

Analysis was done to determine the effect of mixture ratio on vacuum specific impulse at different chamber pressures (20 bar, 40 bar, 60bar, 80 bar, 100 bar, 120 bar, 150 bar, 200 bar) by keeping expansion ratio constant at 58.5

As seen before the at a higher chamber pressure, a more vacuum specific impulse is achieved at that particular mixture ratio. However, the effect of chamber pressure was too small on vacuum specific impulse.

Vacuum specific impulse (m/s)								
O/F	**P_c 20 bar**	**P_c 40 bar**	**P_c 60 bar**	**P_c 80 bar**	**P_c 100 bar**	**P_c 120 bar**	**P_c 150 bar**	**P_c 200 bar**
2	3273	3275.9	3277.9	3279.6	3281	3282.2	3283.8	3286.1
3	3631	3637.8	3641.4	3643.7	3645.3	3646.7	3648.2	3650
4	3593.2	3614.1	3625.9	3634.1	3640.3	3645.3	3651.3	3658.9
5	3410.4	3425.5	3433.8	3439.4	3443.5	3446.9	3450.8	3455.6
6	3237.7	3247.2	3252.3	3255.7	3258.3	3260.3	3262.6	3265.5
7	3080.6	3086.5	3089.7	3091.8	3093.4	3094.6	3096	3097.8
8	2939.4	2943.2	2945.2	2946.5	2947.4	2948.2	2949.1	2950.1
9	2812.8	2815.2	2816.5	2817.3	2817.9	2818.3	2818.9	2819.5

Table 5.43: *Vacuum specific impulse values for different chamber pressures at different O/F ratios*

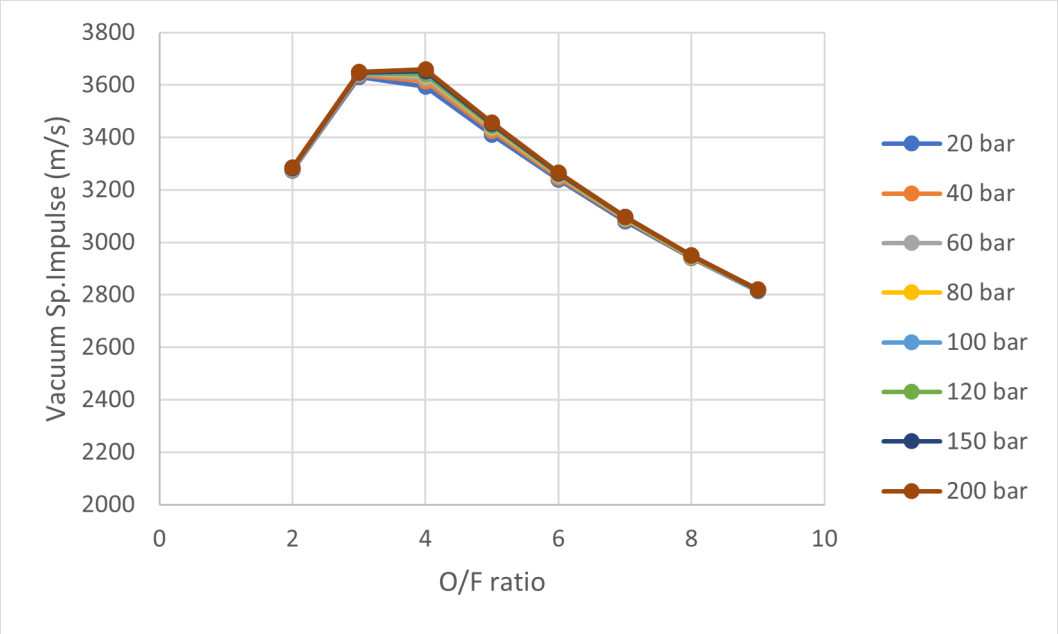

Figure 5.28: *Variation of vacuum specific impulse for different chamber pressures at different O/F ratios*

Variation of vacuum specific impulse for different expansion ratios at different O/F ratios

The below fig. 5.29 demonstrates the effect of expansion ratio on vacuum specific impulse at different mixture ratios. Analysis was done at different expansion ratios (20,50,75,100,125,150,200) by keeping chamber pressure constant at 115 bar and other parameters mentioned in table 5.41 constant. Vacuum specific impulse higher at a certain mixture ratio for higher expansion ratios. Higher expansion ratios extract higher performance from the exhaust gases. However, at the same time, if the expansion ratio is too high, the exhaust pressure goes below the ambient pressure, and atmospheric air can push back into the nozzle, causing flow separation along the nozzle walls.

Vacuum specific impulse (m/s)							
O/F	**ε 20**	**ε 50**	**ε 75**	**ε 100**	**ε 125**	**ε 150**	**ε 200**
2	3130.2	3261.7	3312.7	3346.7	3372	3392.1	3422.6
3	3461.4	3622.8	3681.6	3719.6	3747.1	3768.4	3800
4	3410.9	3613.1	3691.3	3743	3781.2	3811.1	3856.2
5	3237.6	3419	3486.8	3530.7	3562.7	3587.4	3624.1
6	3077.3	3236.5	3294.7	3332.2	3359.3	3380.1	3411
7	2932.7	3073.8	3124.9	3157.6	3181.1	3199.2	3225.9
8	2802.7	2929.7	2975.3	3004.3	3025.1	3041.1	3064.6
9	2685.8	2801.6	2842.9	2869	2887.8	2902.1	2923

Table 5.44: *Vacuum specific impulse values for different expansion ratios at different O/F ratios*

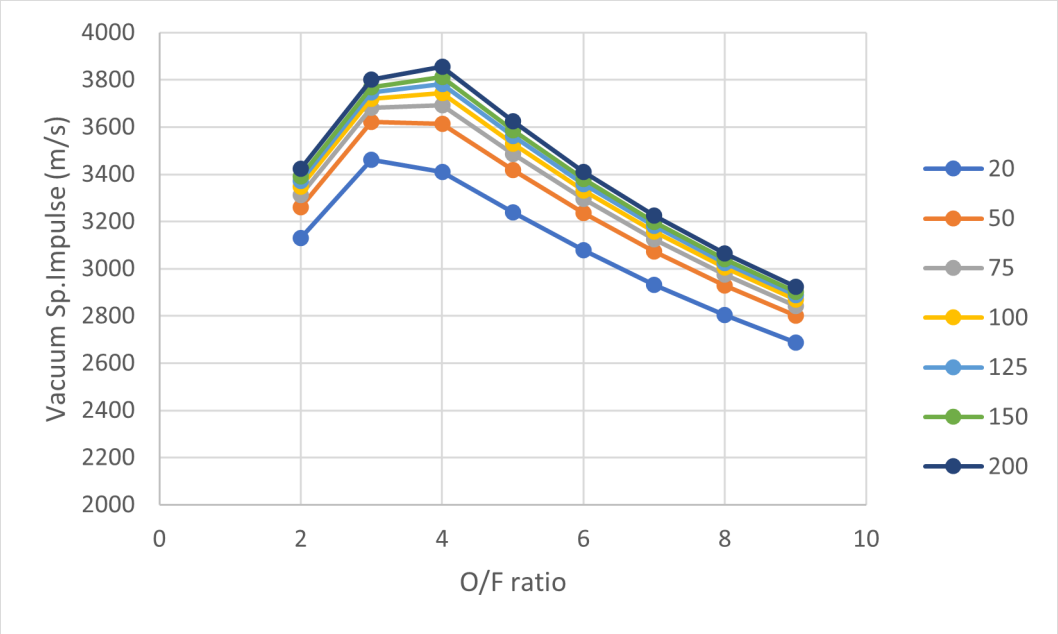

Figure 5.29: *Variation of vacuum specific impulse for different expansion ratios at different O/F ratios*

Variation of combustion temperature and molar mass for different O/F ratios

The fig. 5.30 depicts the behaviour of combustion temperature for different mixture ratios. The maximum combustion temperature is achieved around the stoichiometric value. However, it is not the optimum mixture ratio. The optimum mixture ratio is often chosen towards more fuel-rich mixture ratio conditions because off-stoichiometric mixtures burn cooler than stoichiometric mixtures, making engine cooling easier.

O/F	Combustion temperature (K)
2	2555.5
3	3521.8
4	3628.3
5	3542.4
6	3422.7
7	3293.7
8	3161.8
9	3029.5

Table 5.45: *Combustion temperature values for different O/F ratios*

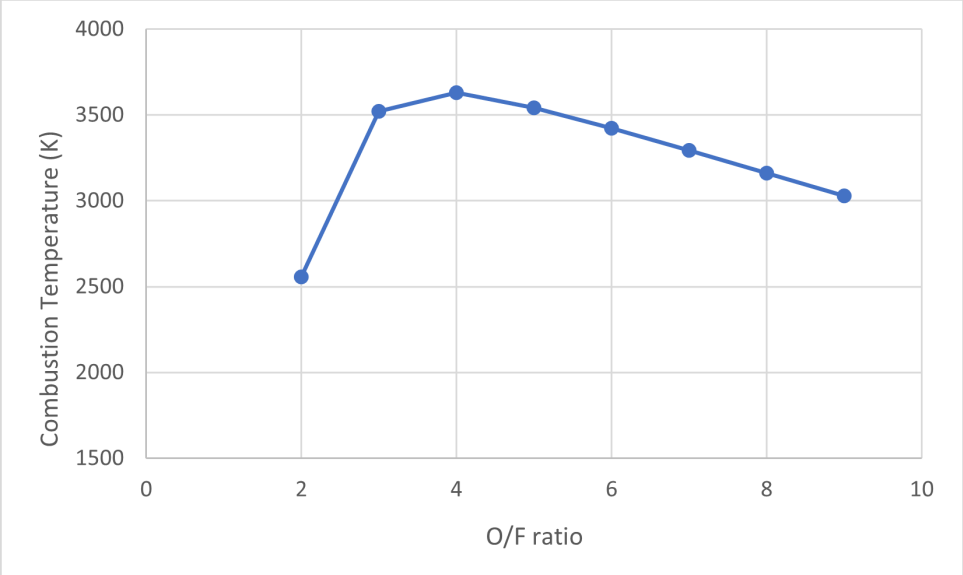

Figure 5.30: *Variation of combustion temperature for different O/F ratios*

Molar mass (kg/kmol)			
O/F	**Chamber**	**Throat**	**Exit**
2	16.025	16.036	16.895
3	16.025	16.036	16.895
4	23.251	23.559	26.256
5	25.004	25.313	27.416
6	26.277	26.567	28.015
7	27.233	27.493	28.460
8	27.961	28.183	28.814
9	28.520	28.701	29.104

Table 5.46: *Molar mass values for different O/F ratios*

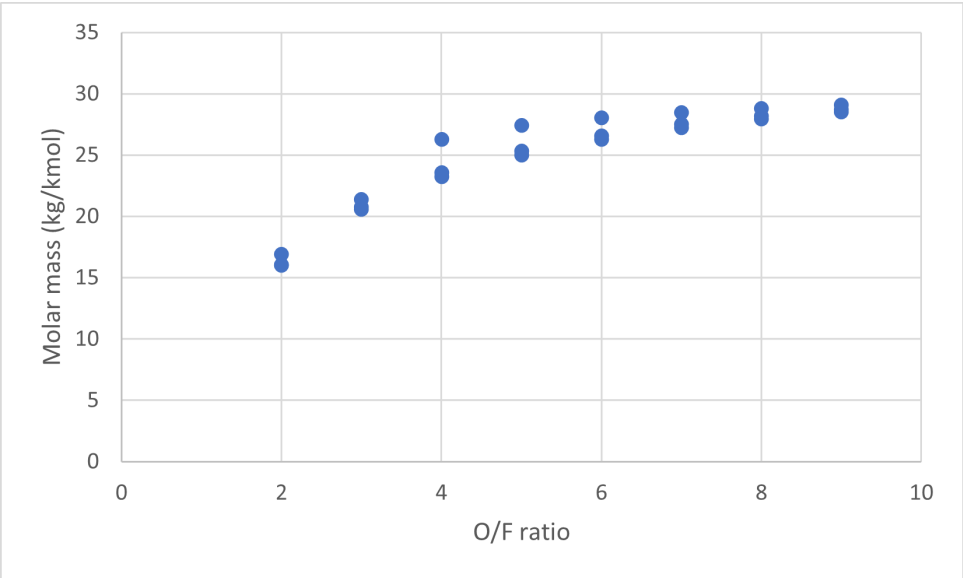

Figure 5.31: *Variation of molar mass for different O/F ratios*

The fig. 5.31 demonstrates the nature of molar mass variation for different mixture ratios at different sections of the combustion process. Because of shifting equilibrium, the molar mass increases at the nozzle exit section due to recombination reactions.

By considering the effect of all the parameters on the performance, an optimum mixture ratio of 3.5 choose for LOX/METHANE engine

5.4.2 Chamber pressure

The conditions taken for the analysis are tabulated below:

Parameter	Value
Chamber pressure (bar)	20,40,60,80,100,120,140,160,180,200,220,240,260,280,300
Expansion ratio (A_e/A_t)	58.5
Fuel	Methane (LCH4)
Oxidizer	Oxygen (LOX)
Fuel temperature (K)	112
Oxidizer temperature (K)	90
O/F mixture ratio	3.5

Table 5.47: *Parameters for CEA analysis*

Vacuum specific impulse variation with chamber pressure

The fig. 5.32 shows the effect of chamber pressure on the vacuum specific impulse. It shows an increasing trend, but the effect of chamber pressure seemed value less as also shown in fig. 5.28, because the specific impulse depends mostly on O/F ratio, combustion temperature and molar mass.

Chamber pressure P_c(bar)	Vacuum specific impulse (m/s)
20	3657.2
40	3672.3
60	3680.4
80	3685.8
100	3689.9
120	3693.1
140	3695.7
160	3697.9
180	3699.8
200	3701.5
220	3702.9
240	3704.3
260	3705.5
280	3706.5
300	3707.6

Table 5.48: *Vacuum specific impulse values for different chamber pressures*

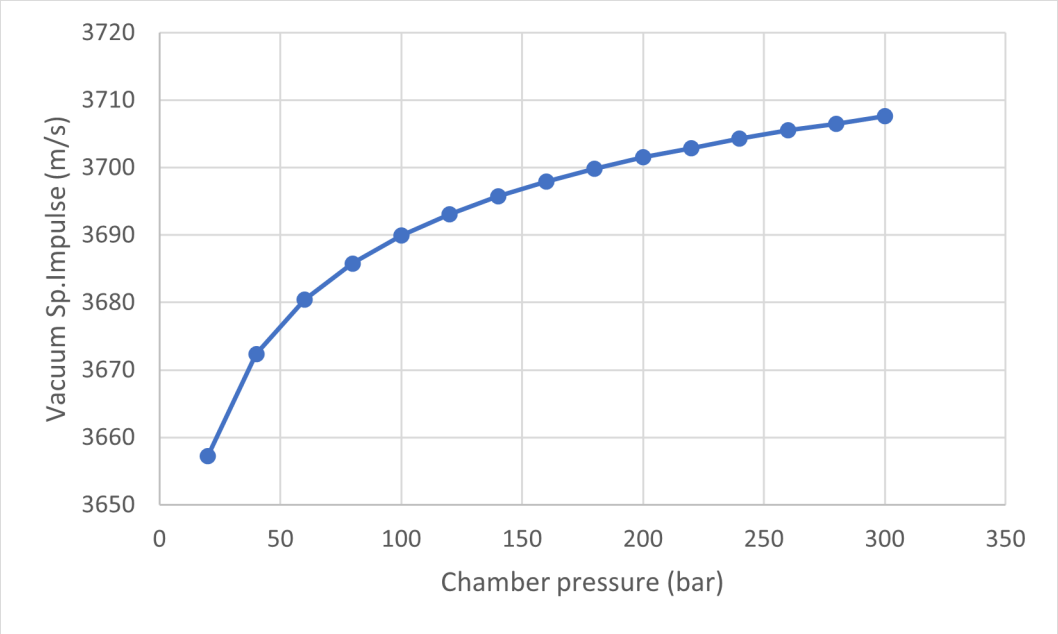

Figure 5.32: *Variation of vacuum specific impulse for different chamber pressures*

Combustion temperature variation with chamber pressure

The fig. 5.33 shows an increasing trend of combustion temperature with the chamber pressure. The increase in chamber pressure reduces the dissociation of species, thus yielding an increase in combustion temperature.

Chamber pressure P_c (bar)	**Combustion temperature (K)**
20	3391.4
40	3483.9
60	3538.4
80	3577.1
100	3607.2
120	3631.7
140	3652.5
160	3670.4
180	3686.2
200	3700.4
220	3713.1
240	3724.8
260	3735.4
280	3745.3
300	3754.5

Table 5.49: *Combustion temperature values for different chamber pressures*

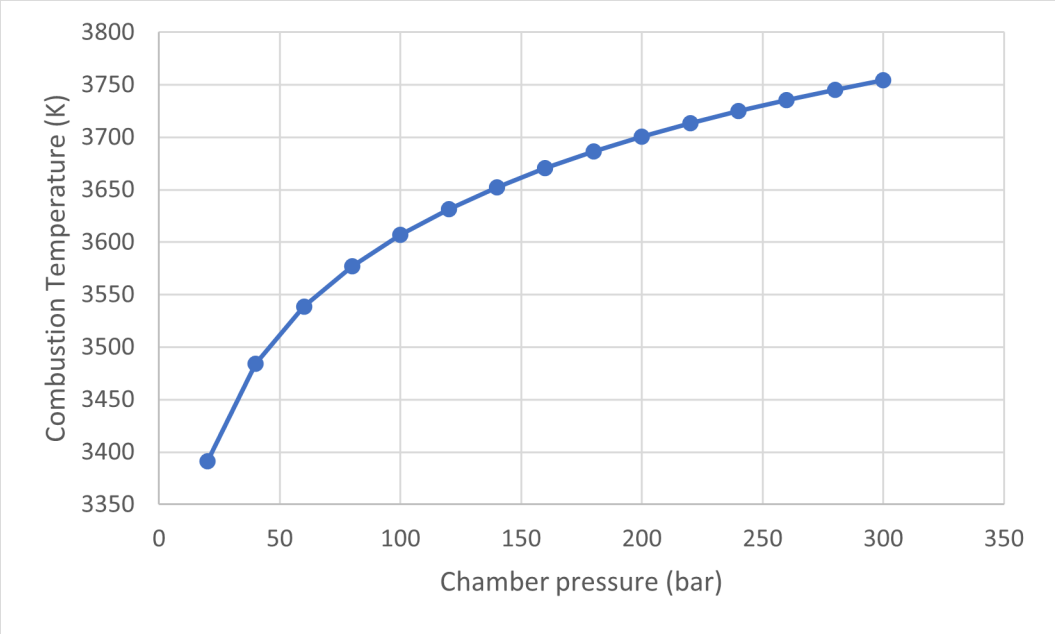

Figure 5.33: *Variation of combustion temperature for different chamber pressures*

Coefficient of thrust variation with chamber pressure

The fig. 5.34 shows the coefficient of thrust variation with the chamber pressure, which reduces with the increase in chamber pressure. Chamber pressure has a very minimal effect on the coefficient of thrust because it is mostly a parameter of the merit of a nozzle.

Chamber pressure P_c (bar)	**Coefficient of thrust**
20	1.9241
40	1.9194
60	1.9164
80	1.9142
100	1.9124
120	1.9109
140	1.9097
160	1.9086
180	1.9076
200	1.9067
220	1.9059
240	1.9052
260	1.9045
280	1.9039
300	1.9033

Table 5.50: *Coefficient of thrust values for different chamber pressures*

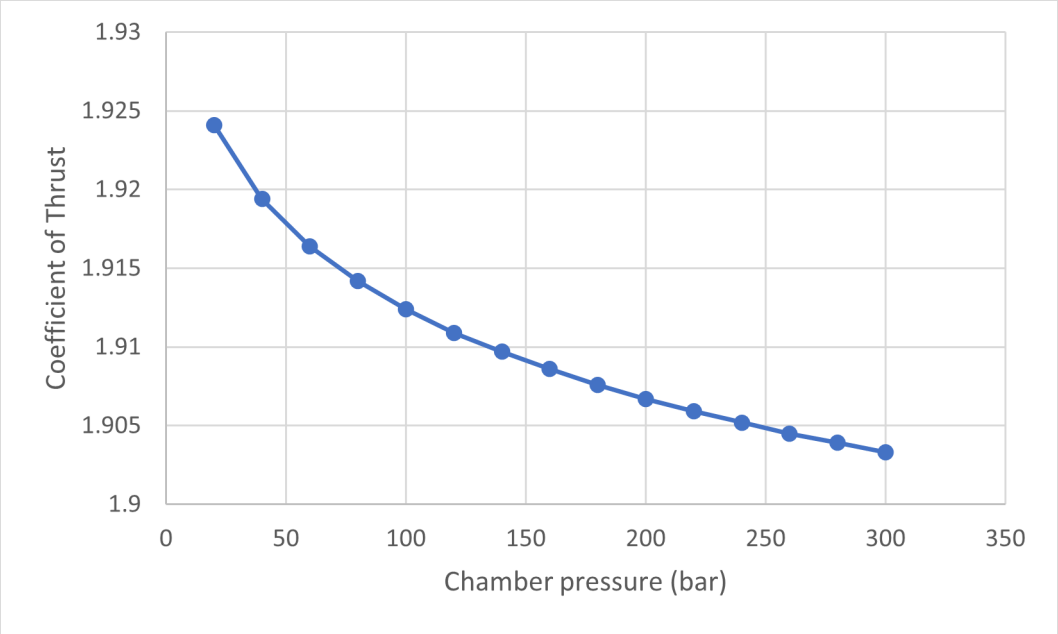

Figure 5.34: *Variation of coefficient of thrust for different chamber pressures*

Characteristic velocity variation with chamber pressure

The fig. 5.35 shows the characteristic velocity variation with chamber pressure which increases with an increase in chamber pressure. From the variation in characteristic velocity, we can say it is a weak form of chamber pressure values.

Chamber pressure P_c(bar)	**Characteristic velocity (m/s)**
20	1806.1
40	1820.4
60	1828.6
80	1834.3
100	1838.7
120	1842.2
140	1845.1
160	1847.7
180	1849.9
200	1851.8
220	1853.6
240	1855.2
260	1856.6
280	1858
300	1859.2

Table 5.51: *Characteristic velocity values for different chamber pressures*

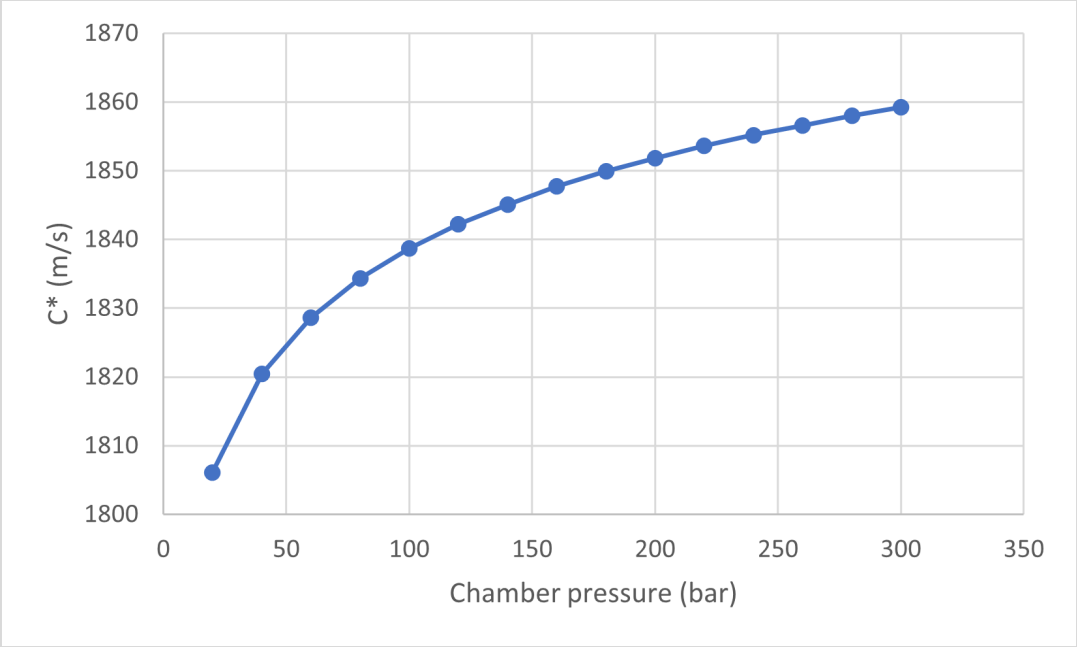

Figure 5.35: *Variation of characteristic velocity for different chamber pressures*

5.4.3 Expansion ratio (A_e/A_t)

The conditions taken for the analysis are tabulated in table 5.52:

Parameter	Value
Chamber pressure (bar)	115
Expansion ratio (A_e/A_t)	10,20,30,40,50,60,70,80,90,100,120,140,160
Fuel	METHANE (LCH4)
Oxidizer	Oxygen (LOX)
Fuel temperature (K)	112
Oxidizer temperature (K)	90
O/F mixture ratio	2.8

Table 5.52: *Parameters considered for CEA analysis*

Vacuum specific impulse variation with expansion ratio

The fig. 5.36 shows an increasing trend of vacuum specific impulse for an increase in expansion ratio. However, the maximum vacuum specific impulse that can be achieved is limited by the practical expansion ratio feasible. Here the possibility of shocks in the nozzle due to over-expansion is not taken into account.

Expansion ratio	Vacuum specific impulse (m/s)
10	3299.20
20	3476.70
30	3565.70
40	3623.10
50	3664.60
60	3696.70
70	3722.60
80	3744.30
90	3762.70
100	3778.70
120	3805.40
140	3827.00
160	3845.10

Table 5.53: *Vacuum specific impulse values for different expansion ratios*

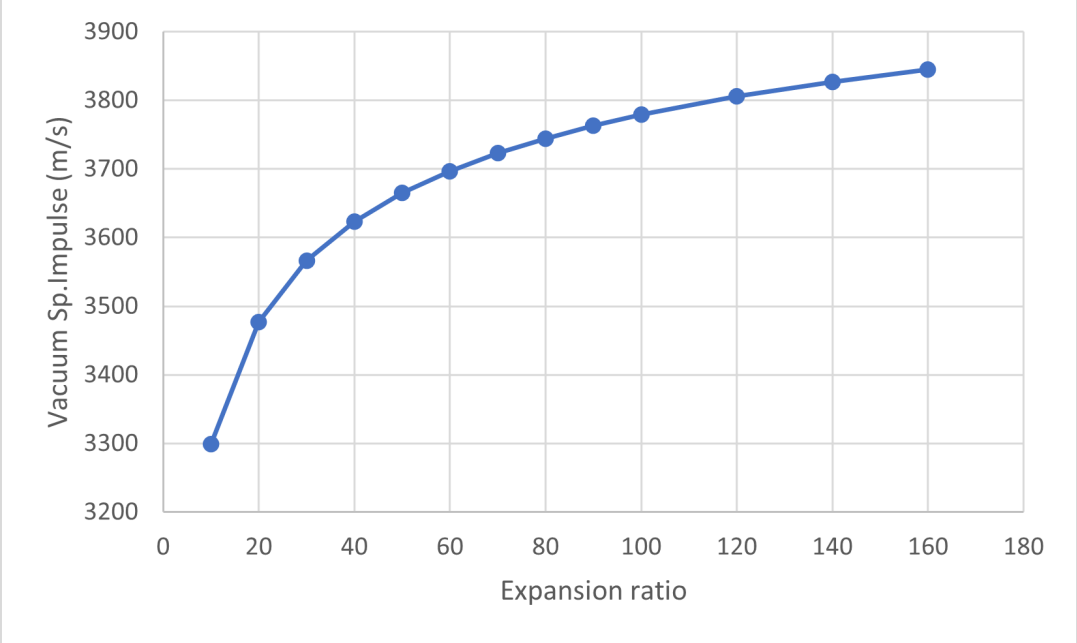

Figure 5.36: *Variation of vacuum specific impulse for different expansion ratios*

Coefficient of thrust variation with expansion ratio

The coefficient of thrust is a parameter of the merit of the nozzle. It increases with an increase in expansion ratio as shown in the fig. 5.37

Expansion ratio	Coefficient of thrust
10	1.6387
20	1.7620
30	1.8238
40	1.8635
50	1.8922
60	1.9143
70	1.9322
80	1.9470
90	1.9597
100	1.9707
120	1.9890
140	2.0038
160	2.0161

Table 5.54: *Coefficient of thrust values for different expansion ratios*

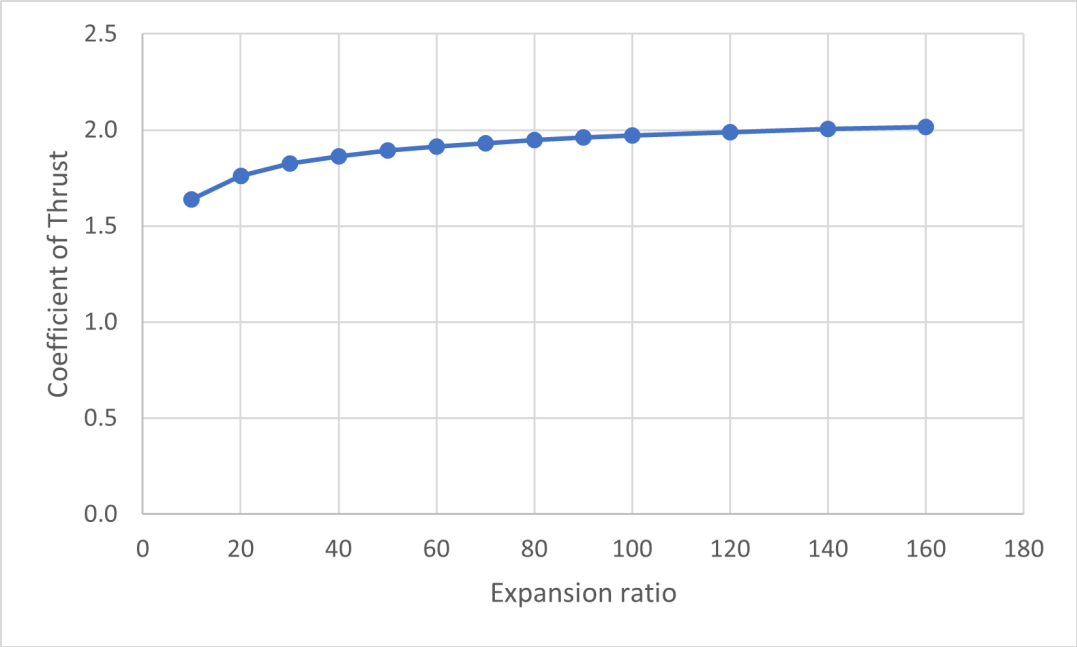

Figure 5.37: *Variation of coefficient of thrust for different expansion ratios*

Characteristic velocity variation with expansion ratio

Characteristic velocity is independent of nozzle parameter, which is shown in the fig. 5.38 by a constant value of characteristic velocity for different expansion ratios.

Expansion ratio	Characteristic velocity (m/s)
10	1841.40
20	1841.40
30	1841.40
40	1841.40
50	1841.40
60	1841.40
70	1841.40
80	1841.40
90	1841.40
100	1841.40
120	1841.40
140	1841.40
160	1841.40

Table 5.55: *Characteristic velocity values for different expansion ratios*

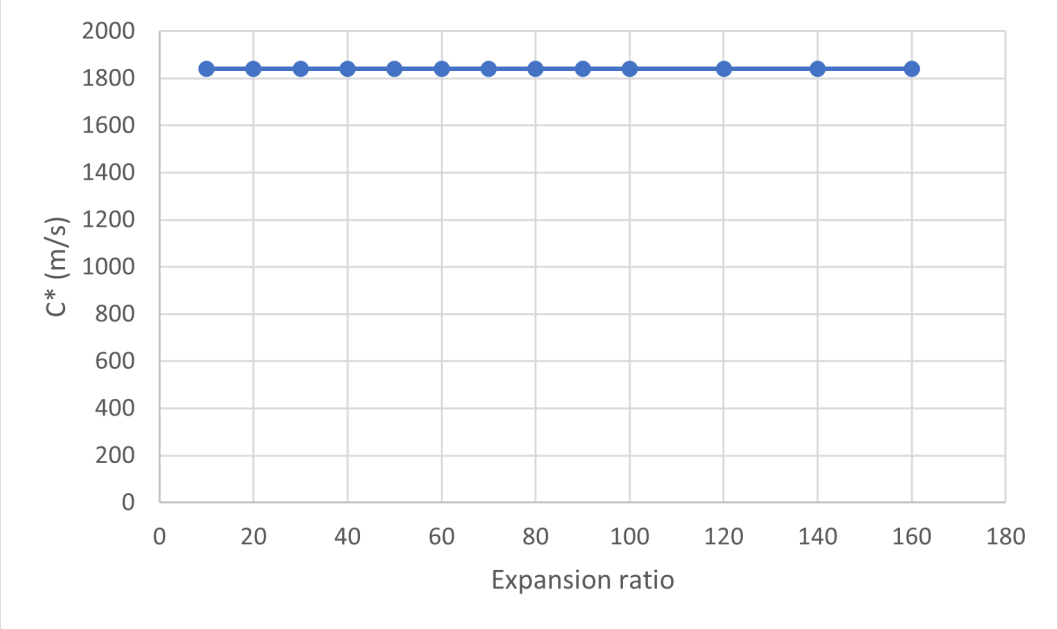

Figure 5.38: *Variation of characteristic velocity for different expansion ratios*

5.4.4 Combustion products

The conditions taken for the analysis are tabulated below:

Parameter	Value
Chamber pressure (bar)	115
Expansion ratio (A_e/A_t)	58.5
Fuel	METHANE (LCH4)
Oxidizer	Oxygen (LOX)
Fuel temperature (K)	298
Oxidizer temperature (K)	90
O/F mixture ratio	2.8

Table 5.56: *Parameters considered for CEA analysis*

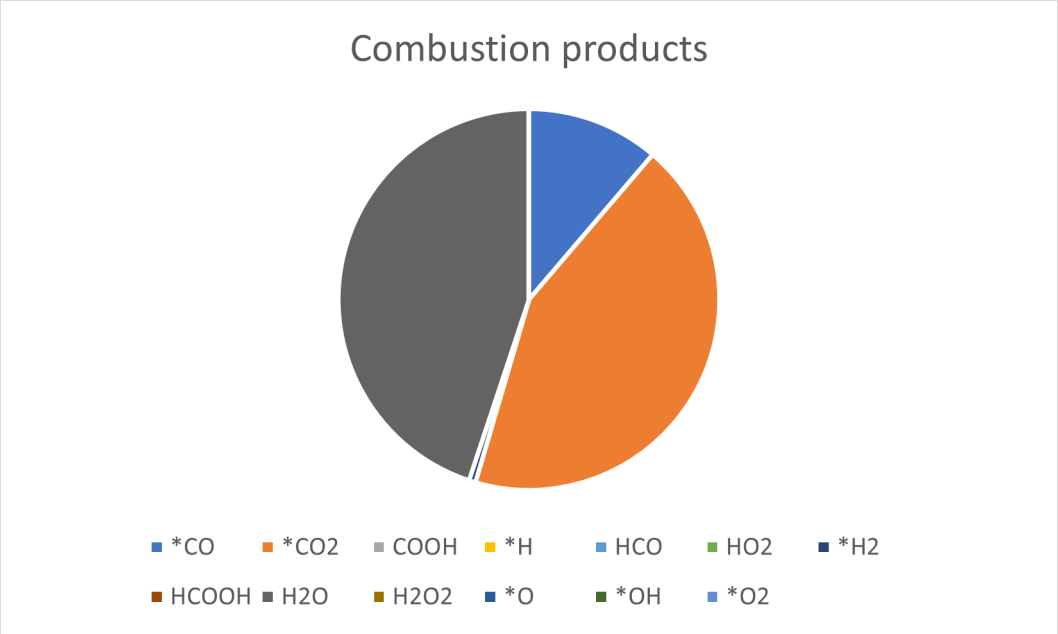

Figure 5.39: *Combustion products of LOX/LCH_4*

Combustion of LOX/Methane is probably the next most clean after LOX/hydrogen. When burnt, methane becomes CO_2, water vapour and a bit of carbon monoxide and some other ions, as shown in the above figure. Methane in the atmosphere is a natural potent greenhouse gas. Therefore it is better when it is burned and split into CO_2 and H_2O, as far as greenhouse gases go.

5.4.5 Masses and volumes

Following the same methodology and assumptions made to calculate mass and volumes of Hydrogen and Kerosene engines, mass and volumes of LOX/METHANE propellant combination.

Input data used for these calculations are taken from the CEA analysis results and from the reference engine are mentioned in the below table:

Parameters	Specification values
Vacuum specific Impulse (s)	376.38
Expansion ratio (A_e/A_t)	58.5
Exit diameter (d_e) (m)	2.15
O/F ratio	3.5
Coefficient of thrust (C_t)	1.9113
Chamber pressure (P_c) (bar)	115
Density of fuel (kg/m^3)	423
Density of oxidizer (kg/m^3)	1140

Table 5.57: *Input values from CEA analysis*

Mass and volumes for core stage LOX/METHANE engine

Masses and volumes obtained by using the same methodology as in section 5.2.5 are listed below

Parameter	Value
Mass of oxidizer(LOX) (kgs)	161245
Mass of fuel (kgs)	46070
Total mass of propellant (kgs)	207315
Volume of oxidizer (m^3)	141
Volume of fuel (m^3)	109
Volume of oxidizer tank (m^3)	156
Volume of fuel tank (m^3)	120
Total volume of tanks (m^3)	275

Table 5.58: *Core mass and volumes of LOX/LCH$_4$*

Mass and volumes for booster stage LOX/METHANE engine

Using the same parameters in the table 5.57 and by the same methodology, we get the mass and volumes for the booster stage. Mass and volumes of oxidizer and fuel both are added, and just the total masses and volumes are listed in the below table.

Parameter	Value
Total mass of propellant (kgs)	281880
Total volume of tanks (m^3)	374

Table 5.59: *Booster mass and volumes of LOX/LCH$_4$*

5.5 Performance Comparison

Various theoretical performance parameters obtained from NASA CEA analysis for the three different propellant combination is compared in this section to find the best propellant combination. Liquid oxygen is the common oxidizer for the three propellant combinations, so for different sections, propellant combinations are referred to as HYDROGEN, KEROSENE and METHANE.

5.5.1 Combustion temperature

Variation with O/F ratio

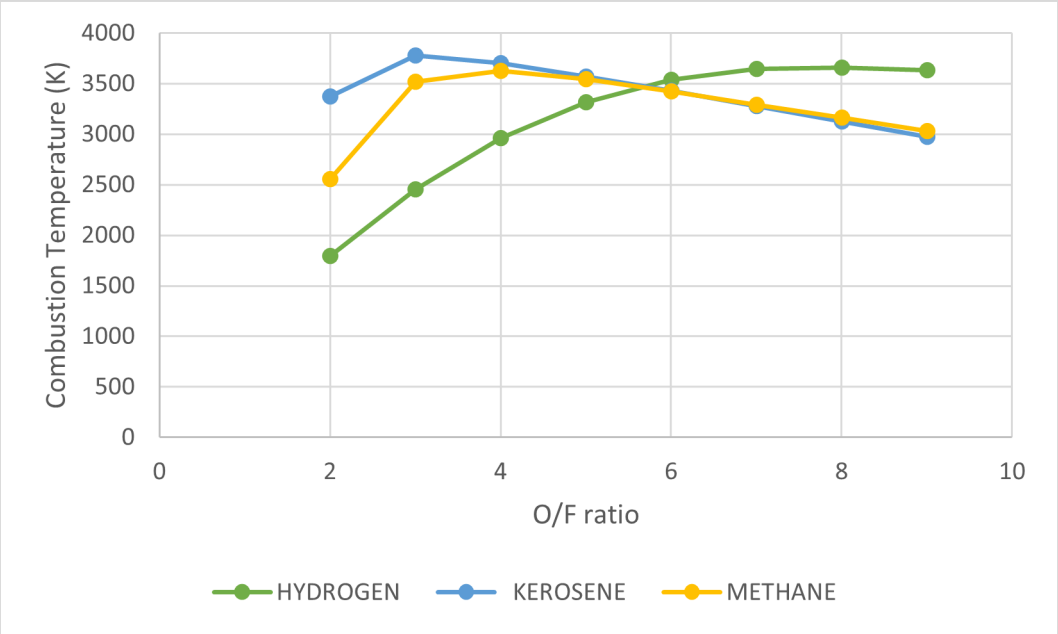

Figure 5.40: *Variation of combustion temperature for three fuels at various O/F ratios*

The fig. 5.40 shows the effect of oxidizer to fuel ratio on combustion temperature for three different fuels (Hydrogen, Kerosene, Methane) at a fixed chamber pressure of 115 bar and expansion ratio of 58.5. Firstly, it is observed that the combustion temperature increased significantly till the stoichiometric ratio and then started decreasing gradually for all three fuels. Maximum combustion temperature is achieved at a stoichiometric ratio of around 8,3 and 4 for hydrogen, kerosene and methane, respectively. Kerosene has a maximum combustion temperature of about 3779.8 K at an O/F ratio of 3 because of its higher molecular weight and negative enthalpy. For the most part, methane has a lower combustion temperature than kerosene which can be an advantage for reusable engines.

Variation with chamber pressure

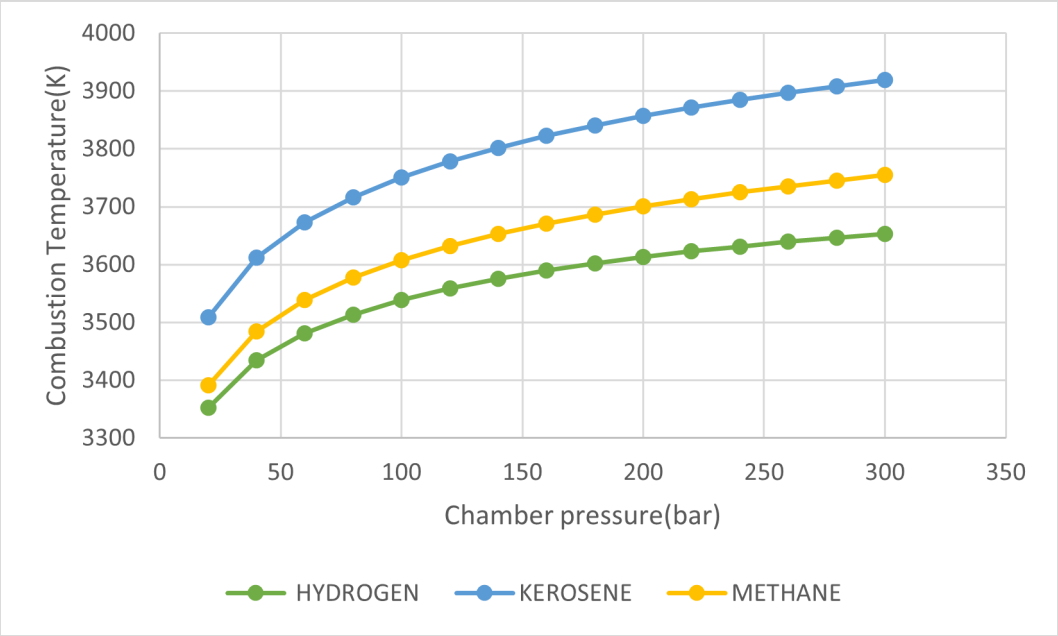

Figure 5.41: *Variation of combustion temperature for three fuels at various chamber pressures*

The above fig. 5.7 shows the behaviour of combustion temperature of hydrogen, kerosene and methane at various chamber pressures. Combustion temperature increases with an increase in chamber pressure for all three cases, with kerosene having the highest combustion temperature at all pressures, followed by methane and hydrogen.

5.5.2 Molar mass for different O/F ratios

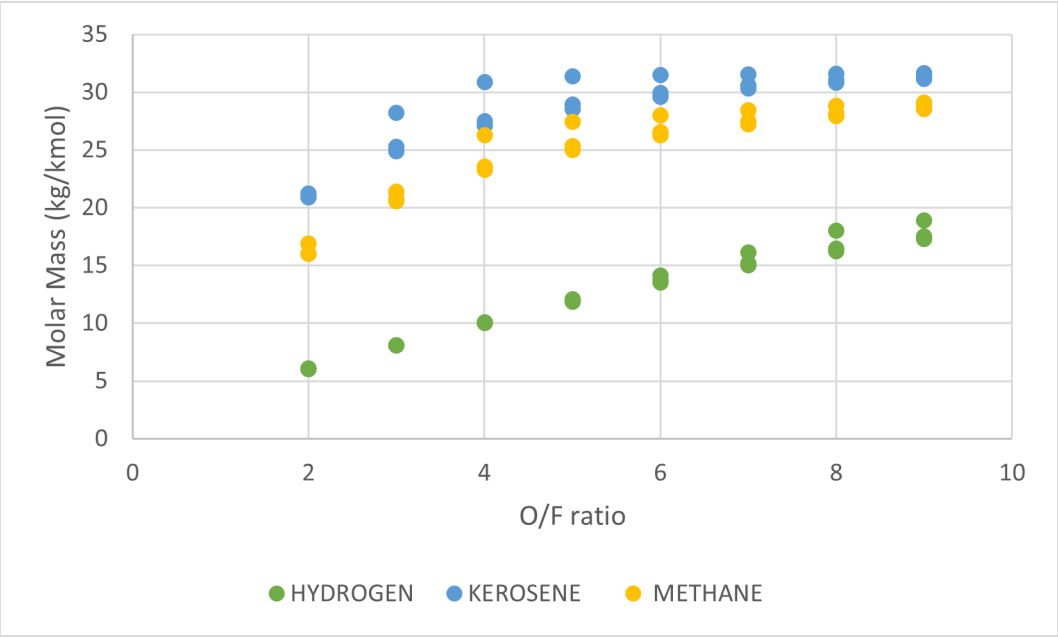

Figure 5.42: *Variation of molar mass for three fuels at various O/F ratios*

This fig. 5.42 compares the molar masses of hydrogen, kerosene and methane at different O/F ratios. Hydrogen has the lowest molar mass for all the mixture ratios, which means higher specific impulse from eq. (5.7).

5.5.3 Vacuum specific impulse

Variation with O/F ratio

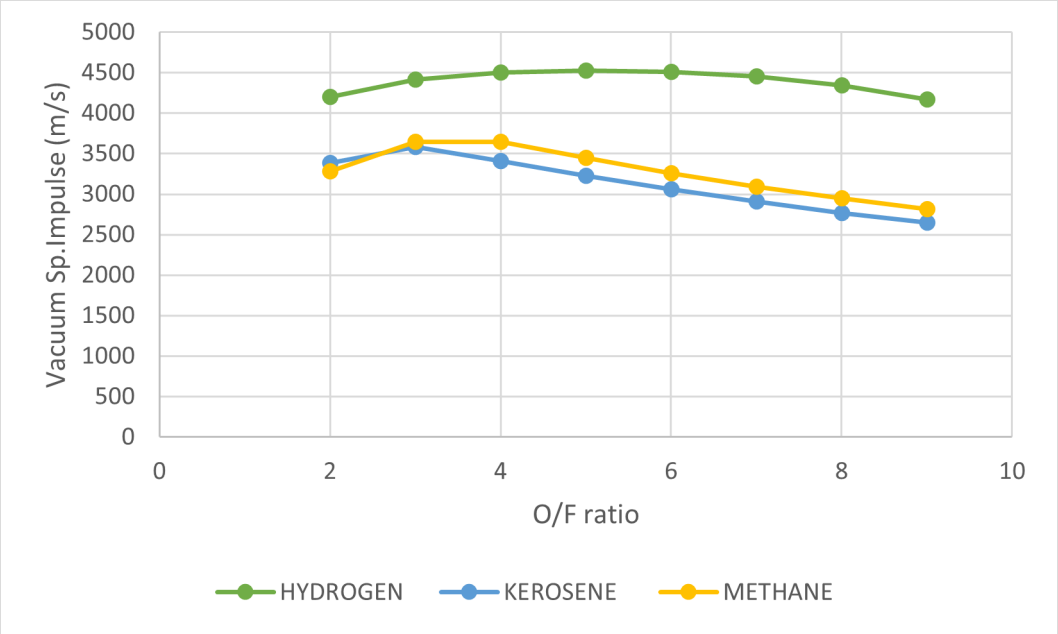

Figure 5.43: *Variation of vacuum specific impulse for three fuels at various O/F ratios*

The above fig. 5.43 explains the nature of vacuum specific impulse of hydrogen, kerosene and methane for various O/F ratios. Hydrogen shows the highest vacuum specific impulse out of the three even though its lower combustion temperature from the fig. 5.40, this is because of its lower molar mass shown in fig. 5.42. On the other hand, methane has a lower vacuum specific impulse than hydrogen but slightly higher than kerosene. Compared to hydrogen, methane will have a better density specific impulse due to this; fuel tank sizes can be reduced a lot, which is proven in the later sections.

Variation with chamber pressure

The above fig. 5.44 shows the variation of vacuum specific impulse of three different fuels, namely hydrogen, kerosene and methane, for different chamber pressures. Like the above case, hydrogen shows the highest vacuum specific impulse, followed by methane and kerosene. The effect of chamber pressure is insignificant, as explained in previous sections.

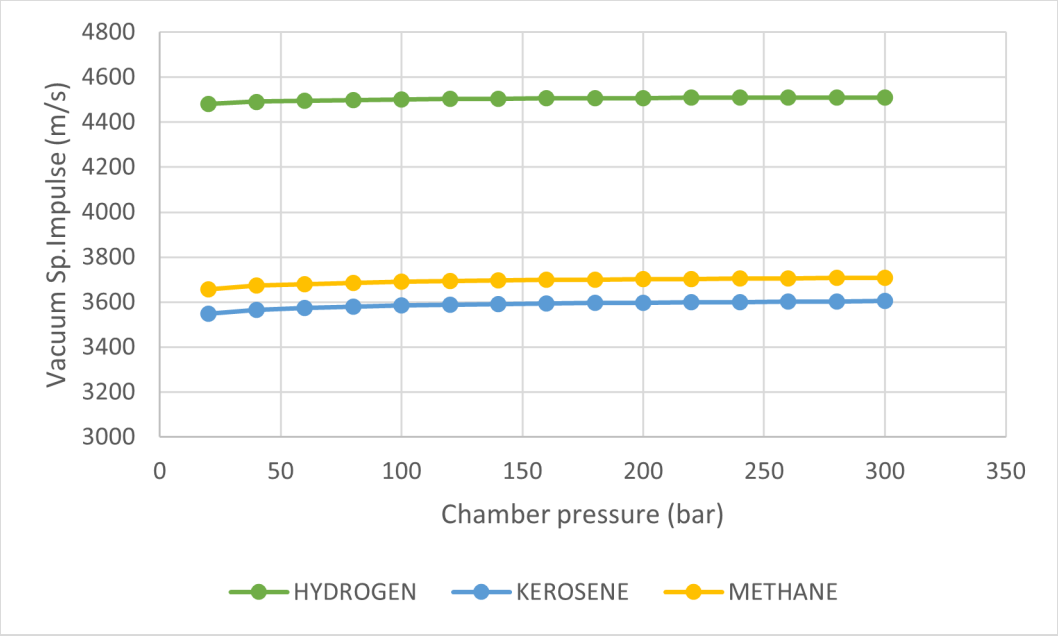

Figure 5.44: *Variation of vacuum specific impulse for three fuels at various chamber pressures*

Variation with expansion ratio

The effect of expansion ratio on vacuum specific impulse for hydrogen, kerosene and methane is shown in the fig. 5.45.

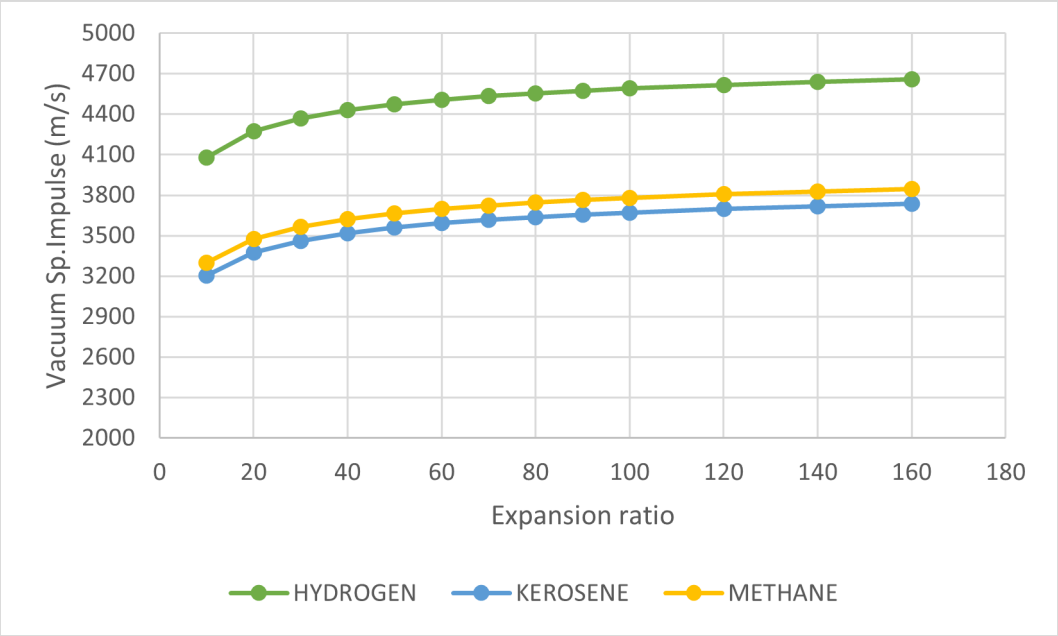

Figure 5.45: *Variation of vacuum specific impulse for three fuels at various expansion ratios*

All three fuel show an increasing trend with hydrogen having the highest vacuum specific impulse of the three.

5.5.4 Coefficient of thrust

Variation with chamber pressure

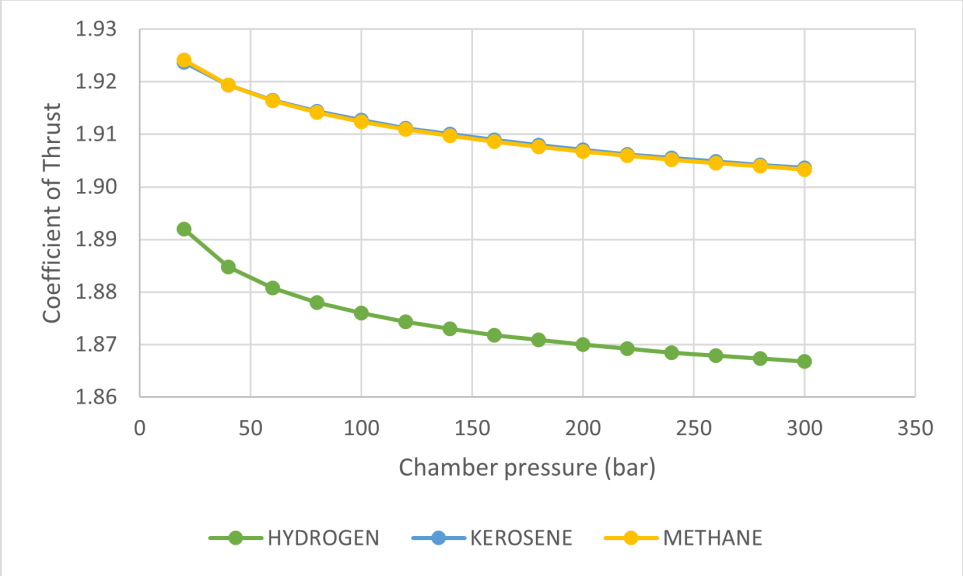

Figure 5.46: *Variation of coefficient of thrust for three fuels at various chamber pressures*

The fig. 5.46 compares the coefficient of thrust variation of hydrogen, kerosene and methane for different chamber pressures. It shows a decreasing trend for the three cases with, hydrogen having the least and kerosene and methane coefficient of thrust values are almost identical.

Variation with expansion ratio

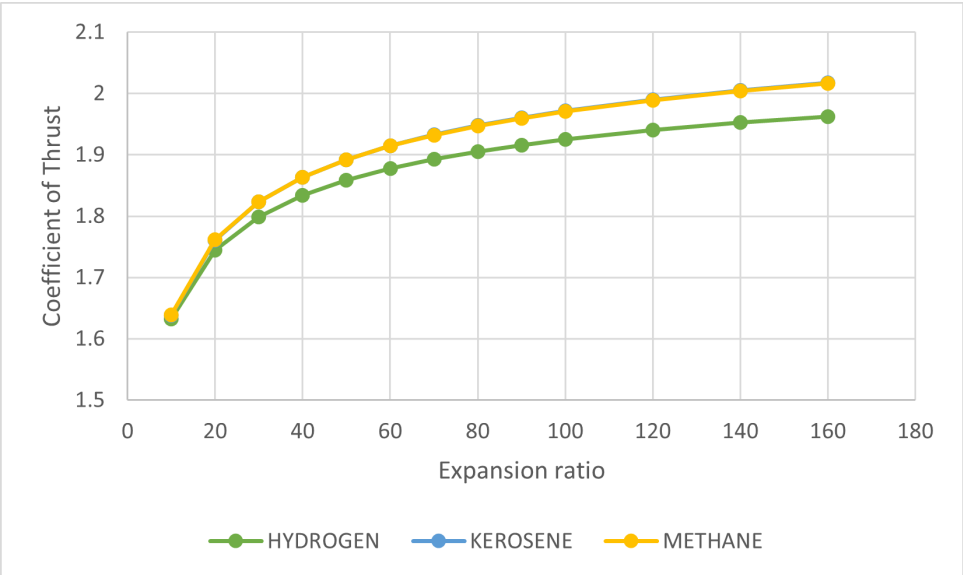

Figure 5.47: *Variation of coefficient of thrust for three fuels at various expansion ratios*

The fig. 5.47 shows the variation of coefficient of thrust for different expansion ratios. All three fuels show an increase in the coefficient of thrust for an increase in expansion ratio. Kerosene and methane have almost identical curves, while hydrogen has the least coefficient of the thrust of all three. Kerosene and methane have higher values of coefficient of thrust due to their lower gamma values because in vacuum conditions, coefficient of thrust is only a function of gamma and expansion ratio.

5.5.5 Characteristic velocity

Variation with chamber pressure

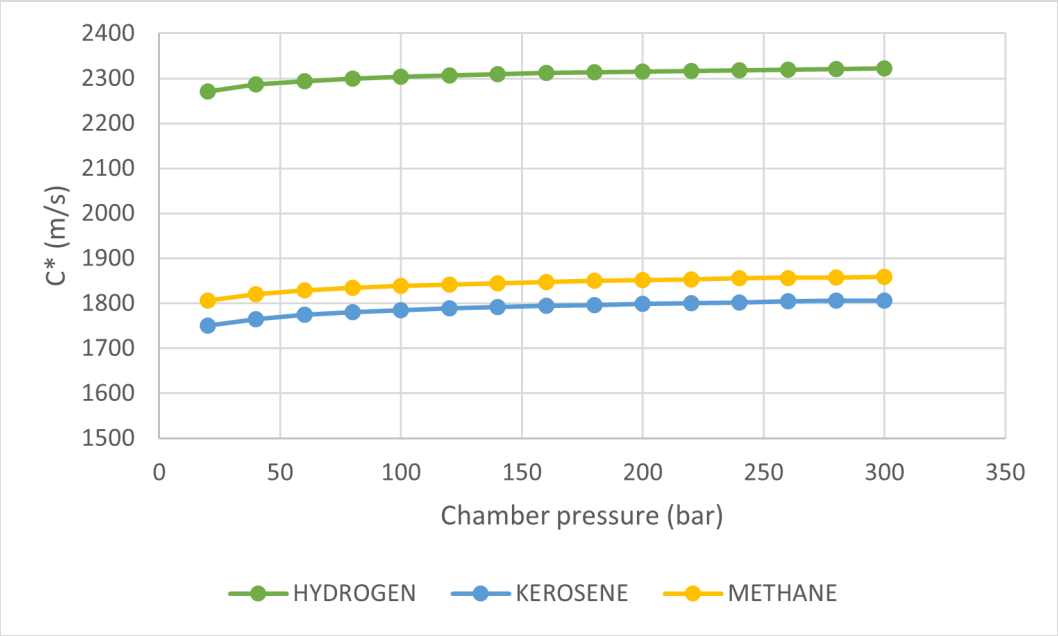

Figure 5.48: *Variation of characteristic velocity for three fuels at various chamber pressures*

This fig. 5.48 explains the effect of chamber pressure on characteristic velocity (C*) for hydrogen, kerosene and methane. It shows a minimal change in the characteristic velocity for different chamber pressures in all three cases. Hydrogen has the highest followed by methane ad kerosene because propellants with lower molecular weight gives higher characteristic velocities from the eq. (5.9).

Variation with expansion ratio

The fig. 5.49 shows the effect of expansion ratio on the characteristic velocity for hydrogen, kerosene and methane. Characteristic velocity shows no change for the three cases because, as explained before, it is a parameter of the combustion chamber. So the expansion ratio variation will not affect it. Similar to the above case, hydrogen has the highest values, followed by methane and kerosene.

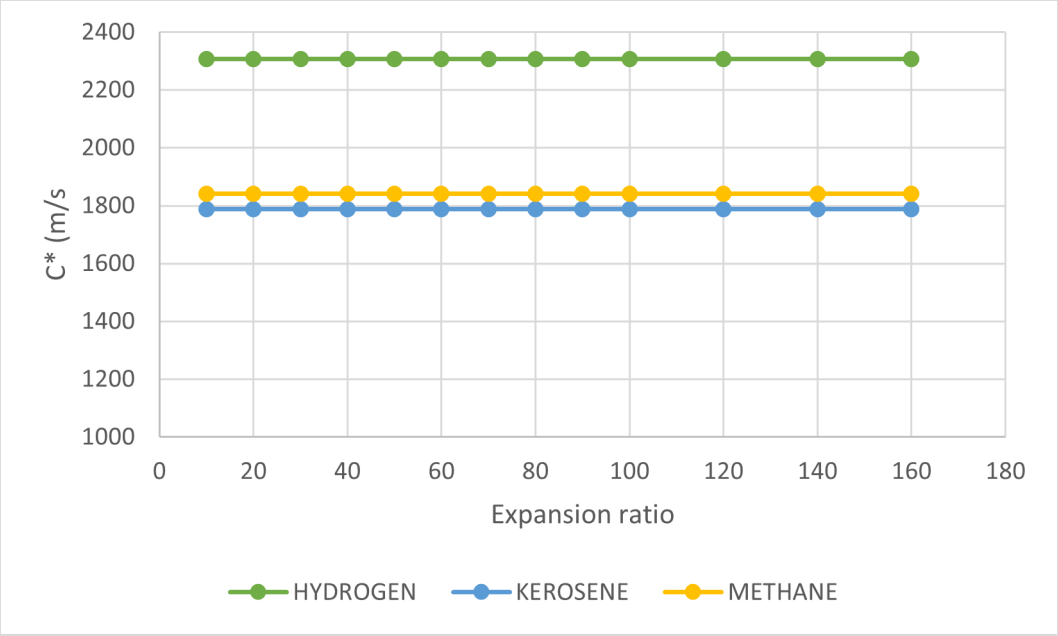

Figure 5.49: *Variation of characteristic velocity for three fuels at various expansion ratios*

5.5.6 Masses and volumes

For core stage masses comparison

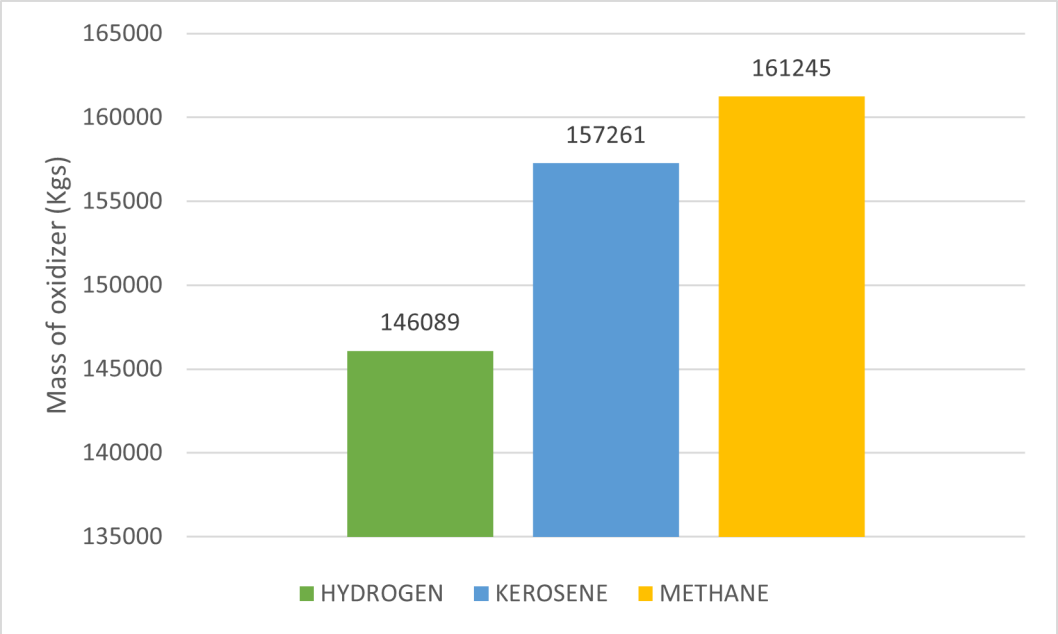

Figure 5.50: *Comparison of oxidizer masses*

The above diagram shows the amount of oxidizer (LOX) required in each case. Methane case required the highest amount of oxidizer, almost 15000 kgs of more oxidizer mass than hydrogen.

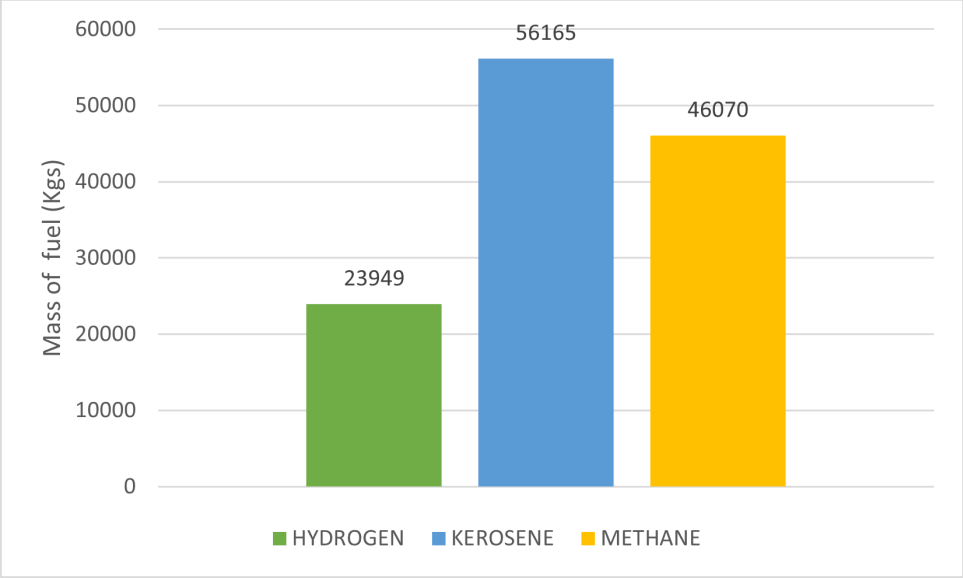

Figure 5.51: *Comparison of fuel masses*

The above diagram shows the amount of fuel required in each case. Kerosene case required the highest amount of fuel, around 32000 kgs of more fuel mass compared to hydrogen. Masses of fuels are much less compared to oxidizers in all the three cases because of choosing oxygen rich conditions to get higher performances.

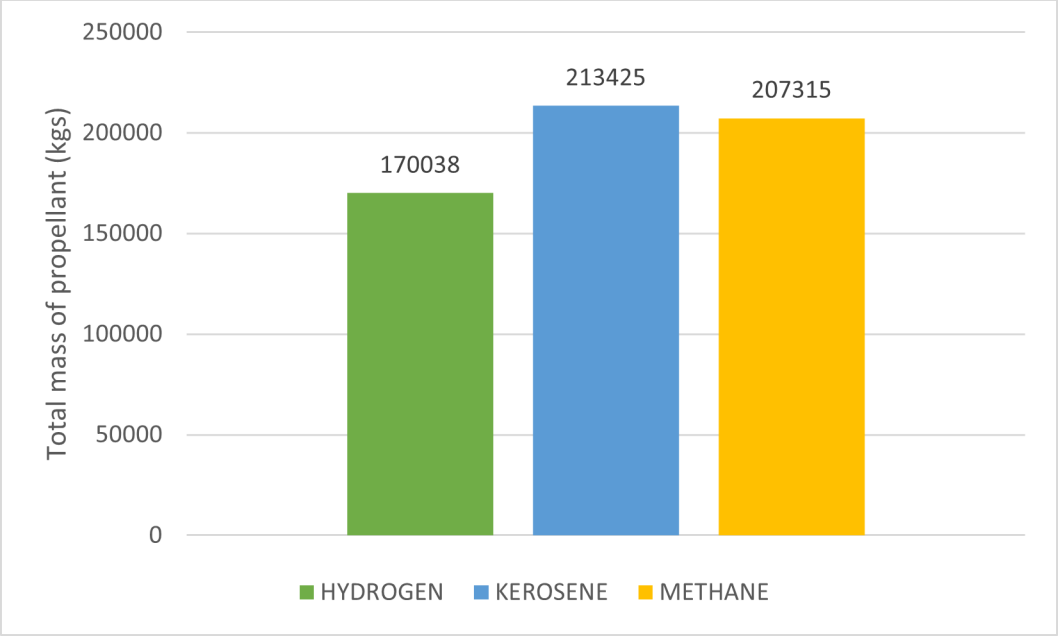

Figure 5.52: *Comparison of total propellant masses*

This chart compares the total mass required for each propellant combination. Hydrogen has the least amount of mass required because of its high specific impulse. High Specific impulse means less amount of fuel required to do the same work. Methane has the second-highest specific impulse, so the total mass of methane is less compared to kerosene which has the least specific impulse of the three.

For core stage tank volumes comparison

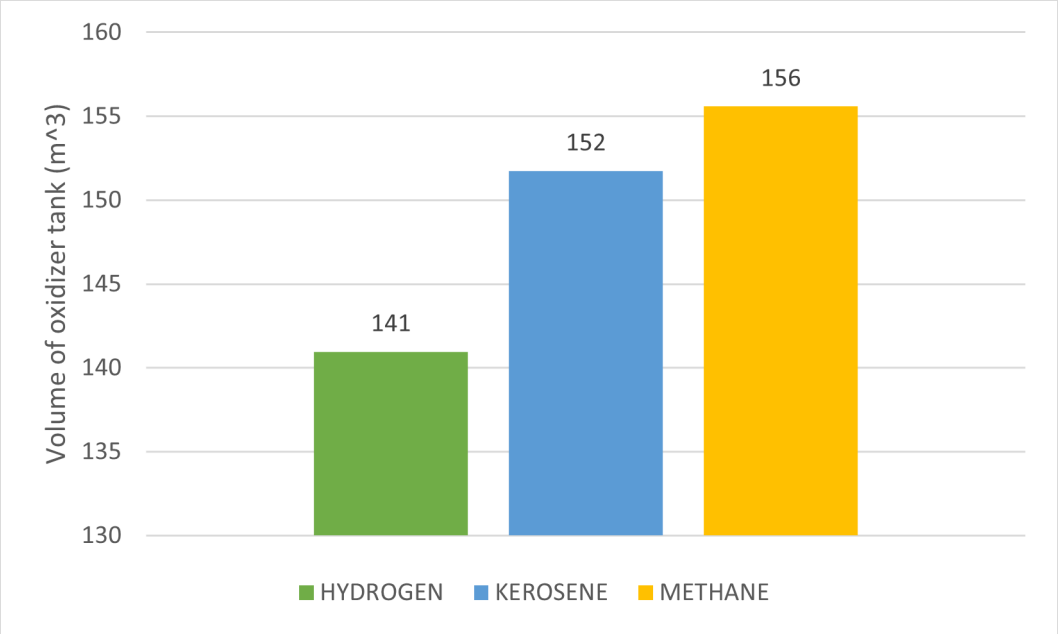

Figure 5.53: *Comparison of oxidizer tank volumes*

This fig. 5.53 compares the oxidizer tank volumes for the three cases. Since the oxidizer (LOX) is the same in all the propellants, the chart follows the same trend as that of the mass of oxidizers.

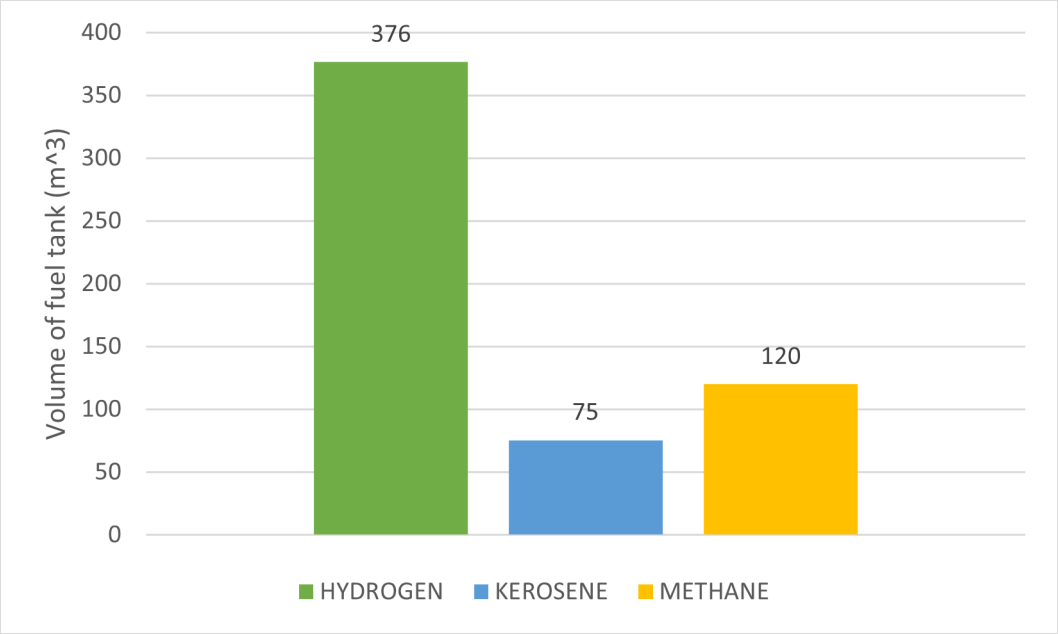

Figure 5.54: *Comparison of fuel tank volumes*

This fig. 5.54 compares the volumes of fuel tanks of hydrogen, kerosene and methane. Hydrogen fuel tank volumes are more than two times that of methane and even more for kerosene cases. This is due to the low density of hydrogen.

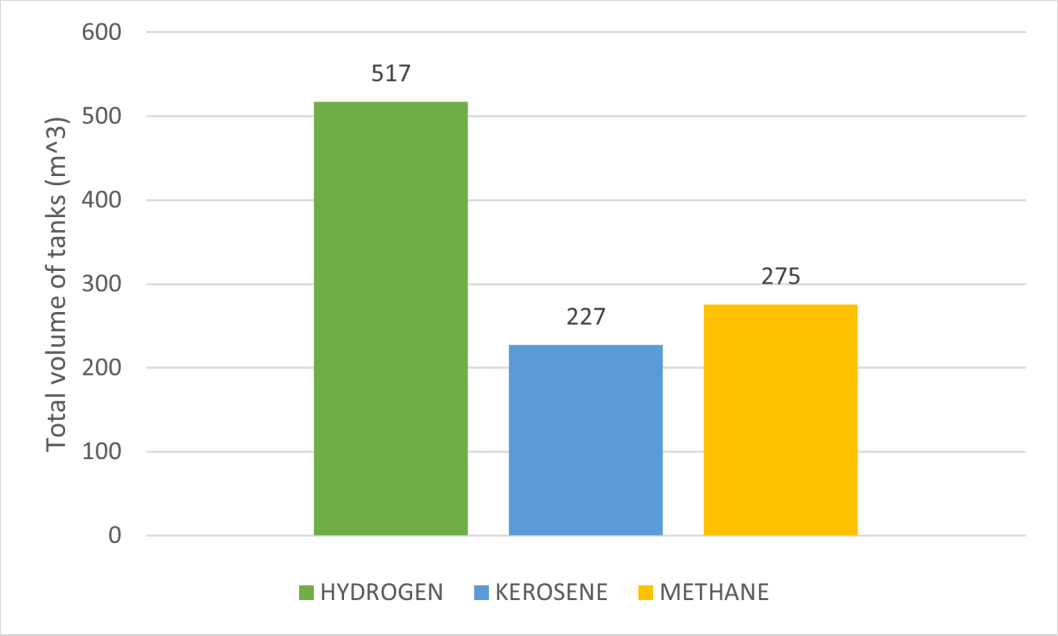

Figure 5.55: *Comparison of total tank volumes*

From the above chart comparing total volumes of propellant tanks, hydrogen has the largest tank volumes, followed by methane and kerosene. This large tank volume of hydrogen will nullify the low propellant mass advantage because large tanks result in high aerodynamic drag, larger and heavier vehicle structure and also larger tanks needs more insulation which increases the tank mass on the other hand methane having slightly higher tank volume than kerosene can be benefited by its low propellant mass and higher specific impulse compared to kerosene.

For booster stage masses comparison

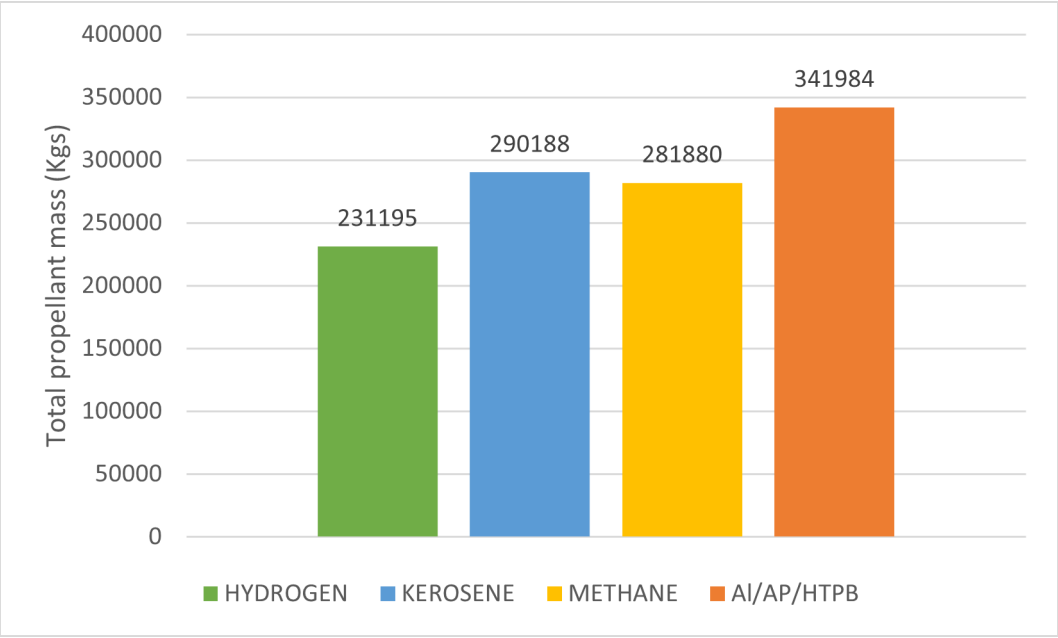

Figure 5.56: *Comparison of booster total propellant masses*

This fig. 5.56 shows the total propellant mass required for the booster stage for hydrogen, kerosene, methane and the solid propellant (AI/Al/HTPB). Compared to solid propellant, all three show lesser masses, almost 60000 kgs less in the methane case. The reduction in propellant mass means an increase in the payload.

For booster stage tank volumes comparison

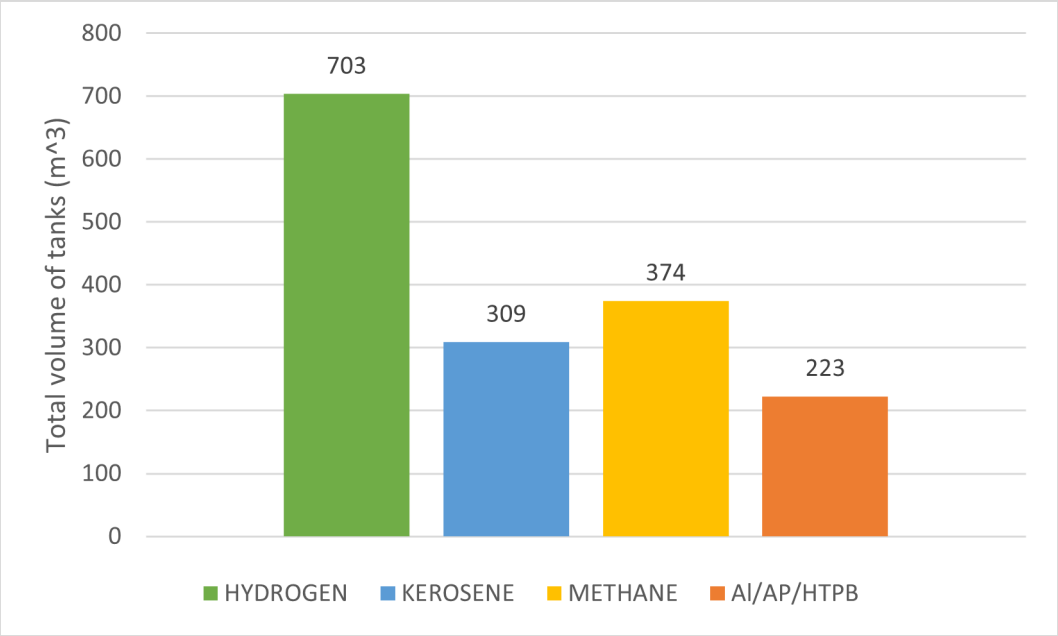

Figure 5.57: *Comparison of booster total tank volumes*

In the case of tank volumes, solid propellant has the least volume as shown in the fig. 5.57. The difference in tank volumes between the solid propellant case and the methane case is very small compared to that of hydrogen.

6 Chapter

Conclusion and Future Work

6.1 Conclusion

The current work presented a detailed study of liquid propellant pairs propulsive parameters using the chemical equilibrium software NASA CEA. Three fuels, namely HYDROGEN, KEROSENE and METHANE reacting with the liquid oxidizer, have been simulated considering shifting equilibrium conditions.

Firstly, the vacuum specific impulse, combustion temperature and molar mass over a range of O/F from 2 to 9 for a chamber pressure of 115 bar and expansion ratio of 58.5 have been obtained and analyzed. In the following, the most relevant results are summarized:

- In terms of vacuum specific impulse, LOX/LH_2 pair proven to be the best option of three followed by LOX/LCH_4 and LOX/RP-1.
- In terms of combustion temperature LOX/LCH_4 and LOX/RP-1.
- In terms of combustion temperature showed lower values which can be an advantage for reusable purposes.
- In terms of molar mass, LOX/LH_2 showed the lowest values for all O/F ratios, due to which the pair showed the highest vacuum specific impulse values.

Secondly, the vacuum specific impulse, combustion temperature, coefficient of thrust and characteristic velocity over a range of chamber pressures have been investigated. Here are the significant findings:

- The effect of chamber pressure on vacuum specific impulse seemed insignificant for all three fuel pairs. Again LOX/LH_2 pair showed the maximum values for all chamber pressures.
- For all three fuels investigated, combustion temperature showed an increasing trend for different chamber pressures.

- Coefficient of the thrust of LOX/RP-1 and LOX/LCH_4 and LOX/RP-1.
- In terms of combustion temperature had almost identical curves. Moreover, all three fuel pairs have decreasing trends for different chamber pressures.
- LOX/LH_2 pair has the highest combustion efficiency due to their greater characteristic values followed by LOX/LCH_4 and LOX/RP-1.
- In terms of combustion temperature and LOX/RP-1.

Thirdly, the vacuum specific impulse, coefficient of thrust and characteristic velocity over a range of expansion ratios have been studied. Some of the major findings:

- The effect of expansion ratio was similar for all the three-fuel pairs, with LOX/LH_2 pair having the higher values.
- LOX/Rp1 and LOX/LCH_4 has almost identical and higher values than LOX/LH_2 due to their lower gamma values.
- Characteristic velocity is a parameter of merit of the combustion chamber. So, all the three fuel characteristic velocities showed a constant curve for different expansion ratios.

The combustion products of the three fuel pairs at their respective optimum mixture ratios were compared, and hydrogen is proven to be the cleanest propellant pair, followed by methane and kerosene. Furthermore, compared to solid propellant exhaust products from the [methane03], both LOX/LCH_4 and LOX/RP-1 reduce the total generated exhaust mass and eliminate the harmful species like chlorides and AL2O3 but slightly increase the sum of CO and CO_2, which means less depletion of the ozone layer and less acid deposition.

Finally, the core stage of Ariane 5 launcher LOX/LCH_4 requires a total propellant mass of about 10 per cent more compared to the LOX/LH_2 case. The total tank volume for LOX/LCH_4 is 30 per cent less than LOX/LCH_4, which means less aerodynamic drag and a reduction in insulation material mass. LOX/LCH_4 engine is about 10s higher than for a LOX/RP-1 engine. An increased tank size counterbalanced this advantage of the higher energetic content of methane over kerosene. For the Booster case, similar conclusions can be drawn between the three liquid propellants. For a reusable liquid booster, one can expect lower operational and maintenance expenses and more environmentally friendly than a solid booster.

6.2 Future Development

The present work can be improved in many directions: Total inert mass can be calculated using mass estimation relations. The chamber pressure and expansion ratio for each case can be optimized.

References

[1] T.Neill et al. "Practical Uses of Liquid Methane in Rocket Engine Applications". In: *57th International Astronautical Congress*. DOI: 10.2514/6.IAC-06-C4.1.01. eprint: https://arc.aiaa.org/doi/pdf/10.2514/6.IAC-06-C4.1.01. URL: https://arc.aiaa.org/doi/abs/10.2514/6.IAC-06-C4.1.01 (cit. on p. 1).

[2] J.P.Dutheil and Y.Boue. "Highly reusable LOX/LCH4 ACE rocket engine designed for SpacePlane Technical Maturation progress via key system demonstrators results". In: *7th EUROPEAN CONFERENCE FOR AERONAUTICS AND SPACE SCIENCE (EUCASS)*. DOI: 10.13009/EUCASS2017-552. URL: https://www.eucass.eu/doi/EUCASS2017-552.pdf (cit. on p. 1).

[3] H.Burkhardt et al. "Kerosene vs. Methane: A Propellant Tradeoff for Reusable Liquid Booster Stages". In: *Journal of Spacecraft and Rockets* 41.5 (2004), pp. 762–769. DOI: 10.2514/1.2672. eprint: https://doi.org/10.2514/1.2672. URL: https://doi.org/10.2514/1.2672 (cit. on p. 1).

[4] D. Haeseler et al. "Green Propellant Propulsion Concepts for Space Transportation and Technology Development Needs". In: *ESA Special Publication*. Ed. by A. Wilson. Vol. 557. ESA Special Publication. Oct. 2004, p. 4.1 (cit. on pp. 4, 5).

[5] I. A. Klepikov, B. I. Katorgin, and V. K. Chvanov. "The new generation of rocket engines, operating by ecologically safe propellant "liquid oxygen and liquefied natural gas(methane)"". In: *Acta Astronautica* 41.4 (Jan. 1997), pp. 209–217. DOI: 10.1016/S0094-5765(98)00076-9 (cit. on pp. 7, 14).

[6] IHI Corporation SAKAGUCHI Hiroyuki Space Development Department. "Methane Engine Just for Future Space Transportation". In: eprint: https://www.ihi.co.jp/var/ezwebin_site/storage/original/application/c947f865f960ed20f82895dcaa4bbbb1.pdf (cit. on p. 7).

[7] G. P. Sutton and O. Biblarz. "Rocket Propulsion Elements Seventh Edition". In: 2007 (cit. on p. 9).

[8] M.Martinez-Sanchez. "Lecture 25: Basic Turbomachine Performance". In: eprint: https://ocw.mit.edu/courses/aeronautics-and-astronautics/16-512-rocket-propulsion-fall-2005/lecture-notes/lecture_25.pdf (cit. on pp. 9, 10).

[9] F. Maggi. "LRE Technology,Space Propulsion Lecture". In: 2019-2020 (cit. on pp. 11, 12).

[10] A.J. Giovanetti, Lewis Research Center., and United Technologies Corporation. *Deposit formation and heat transfer in hydrocarbon rocket fuels [microform] : [final progress report] / Anthony J. Giovanetti, Louis J. Spadaccini, [Eugene L. Szetela]*. English. NASA Lewis Research Center Cleveland, OH, 1983, p. 1 v. (Cit. on p. 16).

[11] R. Cook and R. J. Quentmeyer. "Advanced cooling techniques for high-pressure, hydrocarbon-fueled rocket engines". In: 1980 (cit. on p. 17).

[12] P.Pempie, T.Froehlich, and H.Vernin. "LOX/methane and LOX/kerosene high thrust engine trade-off". In: *37th Joint Propulsion Conference and Exhibit*. DOI: 10.2514/6.2001-3542. eprint: https://arc.aiaa.org/doi/pdf/10.2514/6.2001-3542. URL: https://arc.aiaa.org/doi/abs/10.2514/6.2001-3542 (cit. on pp. 18, 23).

[13] P.Pascal and H.Gorecki. "A-01V HIGH THRUST LOX-CH4 ENGINE HIGH THRUST LOX-CH4 ENGINE". In: May 2000 (cit. on pp. 20, 22).

[14] DON WARREN and C. LANGER. "History in the making - The mighty F-1 rocket engine". In: *25th Joint Propulsion Conference*. DOI: 10.2514/6.1989-2387. eprint: https://arc.aiaa.org/doi/pdf/10.2514/6.1989-2387. URL: https://arc.aiaa.org/doi/abs/10.2514/6.1989-2387 (cit. on p. 22).

[15] Paris D. Coulon Directorate of Launchers ESA. "Vulcain-2 Cryogenic Engine Passes First Test with New Nozzle Extension". In: eprint: https://www.esa.int/esapub/bulletin/bullet102/Coulon102.pdf (cit. on p. 24).

[16] D. Haeseler, A. Goetz, and A. Froehlich. "Non-toxic propellants for future advanced launcher propulsion systems". In: *36th AIAA/ASME/SAE/ASEE Joint Propulsion Conference and Exhibit*. DOI: 10.2514/6.2000-3687. eprint: https://arc.aiaa.org/doi/pdf/10.2514/6.2000-3687. URL: https://arc.aiaa.org/doi/abs/10.2514/6.2000-3687.